Electronic Supplementary Material (ESI) for Environmental Science: Atmospheres.

Supplementary Materials for

Deposited particles and human lung lining fluid are major, dynamic reservoirs of thirdhand tobacco smoke exposure

Roger Sheu, Tori Hass-Mitchell, Akima Ringsdorf, Thomas Berkemeier, Jo Machesky, Achim Edtbauer, Thomas Klüpfel, Alexander Filippi, Benjamin A. Musa Bandowe, Marco Wietzoreck, Petr Kukučka, Haijie Tong, Gerhard Lammel, Ulrich Pöschl, Jonathan Williams, Drew R. Gentner*

*Corresponding author. Email: drew.gentner@yale.edu

Table of Contents

S1. Sample and data collection

S1.1 Secondhand smoke sample collection

In addition to the methods details provided in the main text, Figure S26 summarizes the experiment and Table S1 provides details on online PTR-TOF data and adsorbent tubes samples for the five experimental trials. In each trial, pairs of common, popular cigarettes were burned together to generate an average SHS profile over the two cigarettes. The 1 m^3 chamber was constructed using an aluminum frame (80/20 Inc.) and polycarbonate (Makrolon) sheets, and the chamber interior was supplied with purified air balanced against outlet flows (e.g., 30 SLPM) (Figure S26). Continuous purified air flow throughout the chamber during the cigarette burning enabled combustion and promoted SHS mixing. In addition to the polycarbonate walls and aluminum base/frame, two new cotton shirts were placed in the chamber during cigarette combustion for most experiments, though their presence is not expected to markedly affect the airborne SHS chemical composition during the initial period when data and samples were collected. Specifically, the SHS measurements, the collection of particulate matter (PM) samples for off-gassing, and the exposure of lung lining fluid (LLF) occurred over the initial ~10–15 minutes of each experimental trial when deposition to the shirts is not expected to substantially alter the airborne particle-phase or gas-phase chemical composition. Nor should it affect the comparative analysis of SHS versus THS off-gassing from PM/LLF derived from that SHS, which is the focus of this study. Flow measurements/control were carried out with mass flow controllers and meters (Alicat).

For SHS measurements, the Vocus PTR-TOF was connected to the chamber via a short segment of Teflon (FEP) tubing, with a PTFE filter included in the flow-path to remove PM, prevent PTR-TOF contamination, and focus on gas-phase measurements. Flow through this sampling line was set at 10 SLPM to reduce losses. The PTR-TOF inlet flow rate was ~100 sccm, though this value fluctuated and was monitored over the course of the multi-week experiment. To avoid saturating the mass spectrometer's detector while also ensuring sufficient signal for minor masses, the incoming gas flow was sub-sampled and diluted with a known flow of purified air, adjusted based on PTR-TOF responses between SHS and THS measurements (Figure S26). In between experiments, the chamber was flushed with purified air, and gas-phase concentrations in the chamber were measured prior to each experiment to determine and correct for background levels.

It should be noted that for this experiment, the cigarettes were lit and placed in the chamber without forced air flow through the cigarette. Thus, entirely sidestream smoke (representative of SHS) was directly emitted without intending to mimic exhaled mainstream smoke. This design represents a slight difference from other studies that use a smoking machine to generate both mainstream and sidestream smoke. This experiment was focused on the behaviors of THS off-gassing and as such, only sidestream SHS was used. While this difference may have resulted in lower combustion temperatures with lower air/fuel ratios and overall greater incomplete combustion, the study does not aim to provide emission factors on a per cigarette basis so any bias is minimal in the context of the study objectives.

S1.2 PM sample collection and off-gassing

Concurrent with online measurements of SHS, gas and particle samples were collected for offline SHS analysis (details below), including PM samples on baked out quartz filters (Whatman Qm-A) for offline GC analysis via thermal desorption (e.g., Figure S2). PM samples for subsequent online and offline analysis of THS off-gassing from PM were collected on new PTFE filters (Pall) in a dedicated, passivated stainless steel filter holder[1] attached directly to the side of the 1 m^3 chamber. For PTR-TOF measurements of PM off-gassing, the previously-collected PTFE filters were placed in a separate, pre-cleaned PFA filter holder with background checks prior to adding the PM sample. An active flow of purified air at 220 sccm near atmospheric pressure was flowed through the filter samples and sub-sampled (similar to SHS measurements) to measure real-time PM off-gassing emissions with the PTR-TOF.

Between collection and the various analysis periods, PM samples were continuously "aged" throughout each experiment with a flow of purified air at 220 sccm through the polytetrafluoroethylene (PTFE) filter and periodic measurements using the PTR-TOF or offline sample collection as indicated in Table S1. Vocus analysis of PM off-gassing from the same trial but at different time points indicates the use of the same filter, aged for longer periods between measurements. As discussed in the manuscript, this advection at 10 m s^{-1} through the filter was slightly accelerated compared to real-world indoor vertical transport via diffusion (~1–5 m s^{-1}).

S1.3 LLF sample collection and off-gassing

Surrogate lung (or epithelial) lining fluid (LLF) was made following protocols set initially by Charrier et al.[2] and updated in Tong et al.[3] A phosphate buffered solution containing various salts

— 114 mM NaCl, 7.8 mM Na_2HPO_4, and 2.2 mM KH_2PO_4, led to a pH between 7.2 and 7.4. Antioxidants were included via the addition of 200 μM ascorbic acid sodium salt, 300 μM citric acid, 100 μM reduced L-glutathione, and 100 μM uric acid sodium salt. Chelex 100 resin, mentioned in Charrier et al., was not included.

For LLF off-gassing measurements, particle-filtered air from the chamber during SHS generation (7–14 minutes, Table S1) was pulled at 500 sccm through a solvent-cleaned and baked-out glass bubbler filled with ~25 mL of room temperature (24–25°C) surrogate lung lining fluid (LLF). This surrogate lung lining fluid contained phosphate-buffered HPLC-grade water solution (2.2 KH_2PO_4 and 7.8 mM Na_2HPO_4), 114 mM NaCl, and 4 antioxidants (via the addition of 200 μM ascorbic acid sodium salt, 300 μM citric acid, 100 μM reduced L-glutathione, and 100 μM uric acid sodium salt).[2] A blank for the LLF was run on the PTR-TOF prior to pulling SHS into the LLF. Afterwards, aqueous-phase (LLF) off-gassing measurements were collected by flowing 220–240 sccm of purified air to the bottom of the bubbler and taking a subsample of the headspace outflow for PTR-TOF measurement following dilution. A filter was included between the bubbler outflow and the PTR-TOF to prevent any generated aerosols (i.e., water, salts) from reaching the PTR-TOF, with background checks prior to LLF off-gassing.

Given the elevated concentrations found in SHS (Table S3), concentrations of major known SHS organic compounds likely approached saturation in the aqueous-phase. Minimal time was taken between collection of SHS VOCs in the surrogate lung lining fluid and subsequent connection of the bubbler to the Vocus PTR-TOF to minimize losses from the fluid to the headspace. The brief amount of elapsed time also helped to minimize reactions of the organic compounds with the aqueous-phase contents, including the antioxidants or with water itself.

The combination of these interactions, including partitioning out of the aqueous phase and potential aqueous phase chemistry with either antioxidants or water, may influence the absolute/relative concentrations of THS measured via gas-phase methods. Other physical considerations for the LLF off-gassing measurements—including (a) the effect of SHS exposure flow rate on the dissolution and saturation of these VOCs into the aqueous phase, (b) the effect of available bubble surface area is on the rate of partitioning, (c) the rate of diffusion of these gases throughout the fluid and other potential bodily reservoirs (e.g., adipose tissue), and (d) additional multiphase partitioning interactions that must be considered with the addition of SHS

particles to LLF—warrant consideration through future studies and modeling of these physical and chemical phenomena.

S1.4 Vocus instrument details

Molecules to be analyzed by the Vocus ionize in a 50 cm long focusing ion-molecular reactor (FIMR), which was run at a temperature of 373K, a pressure of 1.8 mbar, and a voltage differential of 475V (500V front, 25V back), leading to an E/N of ~135 Td. At this E/N, ionization efficiency should be elevated, though the high E/N also leads to an increase in water cluster abundance. Two calibration gases, one with 12 components and one with 79 components, were run. The 12 component calibration gas was used repeatedly (at least daily) throughout the experiments, while the 79 component mix was used once in the middle of the sampling. Compound details for calibration gases can be found in Table S2.

For PTR-TOF measurements, the SHS or THS off-gassing flow was subsampled and diluted to properly adjust the flow rates for optimal instrument sensitivity and to avoid saturation. The flow rate into the PTR-TOF fluctuated (82.9–102.2 sccm) across the campaign with possible effects from high sample loading and was routinely measured at least daily to monitor and adjust for changes. If minor changes occurred between flow checks, it would not have affected the observed relative chemical profile of SHS or THS. Data processing accounted for the recorded subsampling and dilution flows along with the most recent Vocus inlet flow measurement. In the case of extremely concentrated conditions (i.e., SHS), the dilution ratio was high, with the dilution flow being closer to the total Vocus flow. Thus, flow measurements of the PTR-TOF flow were typically taken shortly before beginning an experiment to reduce the potential for drift, though we note that absolute concentrations (not relative chemical profiles) in the on-line data may be sensitive to the flow rate drift. We note that Trial 3 did not have a PTR-TOF flow rate measurement immediately prior to cigarette combustion, as a flow check was conducted earlier in the day prior to Trial 2.

S1.5 Collection of gas-phase organic compounds via adsorbent tubes

Custom-packed adsorbent tubes containing quartz wool, glass beads, Tenax TA, and Carbopack X for gas-phase sampling and quartz or PTFE filters for aerosol-phase sampling were placed in a modified 316L stainless steel filter housing (Pall) to sample SHS directly from the chamber. Following initial measurements via PTR-TOF to examine off-gassing dynamics at high-time resolution, adsorbent tubes were also used to collect emissions at a flow rate of 150 sccm from

both the PM and the LLF samples immediately downstream of the filter or bubbler, respectively. Because PM and LLF off-gassing were first measured on the PTR-TOF, to examine high time resolution off-gassing dynamics, prior to sampling on the adsorbent tubes, these samples were collected following a brief period of aging, ranging 10–80 minutes (Table S1). Adsorbent tubes and filters were stored in a freezer at ≤ -30°C and then shipped to Yale University for analysis.

Adsorbent tubes were desorbed using a thermal desorption unit and cooled injection system (GERSTEL TD 3.5+/CIS) and were injected into a gas chromatograph (GC; Agilent 7890B) containing a DB-5MS-UI column (30m x 250µm x 0.25µm; Agilent) for chromatographic separation. Two different detectors were used to measure these compounds: a vacuum electron impact mass spectrometer (GC-EIMS; Agilent 5977A) and an atmospheric pressure chemical ionization time of flight mass spectrometer (GC-TOF; Agilent 6550).

S1.6 Collection of particulate matter via polytetrafluoroethylene (PTFE) filters

PTFE (Tisch, 47mm) filters were collected at ~26 SLPM (with supplemental filters at 10 SLPM), stored at ≤ –30 °C, and shipped prior to analysis following published methods.[4] To extract the PM, they were sonicated in 1.5mL methanol for 60 minutes. For analysis, 5µL of the sample was injected into a high-performance liquid chromatograph (HPLC; Agilent, 1260 Infinity with Thermo Scientific Hypercarb porous graphitic carbon reverse-phase column, 30mm x 2.1mm x 3µm), ionized using electrospray ionization (ESI), and detected using the same TOF as in GC-TOF (Agilent 6550). The filter LC-TOF analysis was run on both positive and negative mode. Due to differences in ionization efficiencies, positive mode ESI detects less functionalized compounds (i.e., fewer nitrogen and oxygen atoms, mostly $CHN_{0\text{-}2}O_{0\text{-}2}$ compounds), while negative mode ESI is more amenable to detecting highly functionalized compounds (i.e., $CHO_{2\text{-}6}$ and $CHN_{1\text{-}2}O_{1\text{-}5}$). Quartz filters were collected using the same methodology as PTFE filters. Filter punches from the quartz filters were inserted into empty glass tubes, thermally desorbed with a split flow to avoid saturating the detector, and run via GC-TOF, then analyzed using the soft ionization methods described for the adsorbent tubes.

S1.7 Polycyclic Aromatic Compound collection via polyurethane samplers

Polyurethane foam (PUF) samples were collected and analyzed using a separate setup to quantify levels of various polycyclic aromatic compounds (PACs) containing nitrogen/oxygen (Figure S4A). For separate supporting measurements of select individual polycyclic aromatic compounds

(PACs) containing oxygen/nitrogen molecular functionality (e.g., naphthoquinones), THS off-gassing from previously collected PM (i.e., PTFE filters that sampled SHS from the main chamber) were collected on polyurethane foam (PUF), transferred into pre-cleaned thimbles, spiked with a mixture of deuterated PACs, and extracted on a Soxhlet apparatus with dichloromethane (DCM) as the extraction solvent. PUFs were placed downstream and in line with recently-exposed PTFE filters in filter holders that use flow rates of 17–30 SLPM of forced purified air flow passing through them for 18-48 hours. The extracts were then concentrated to 500 µL on a TurboVap concentrator (Biotage, Sweden). Each extract was transferred into a 3 mL SPE column containing 500 mg SiOH (Macherey-Nagel, Germany) for clean-up. The target compounds were eluted from the SPE columns with a hexane:DCM mixture (4:1 v/v), followed by DCM. Eluates from each sample were collected together and further concentrated on a TurboVap before being transferred into a GC-vial for GC-MS/MS measurements. Targeted analyses for select PACs were performed using a Trace 1310 gas chromatograph (GC) coupled with a TSQ8000 Evo triple quadrupole mass selective detector (MS/MS; Thermo Scientific, Waltham, USA). The MS was operated with negative chemical ionization (with CH_4 as the ionizing gas), monitoring selected ions specific to each compound. Each compound in the extract was identified by a comparison of their mass spectra (masses of ions and their relative ratio) and GC retention times to known calibration standards. The concentrations of the target compounds were determined using corrections via internal standards. Further details of the analytical procedure can be found elsewhere.[5] See Table S1 for a summary of observations. Additional exploratory analysis of the extracts for polychlorinated biphenyls (PCBs) and polychlorinated dibenzo-dioxins/furans (PCDD/Fs) was also conducted following the method in Degrendele et al., excluding surrogate internal standards.[6]

S1.8 PCB and PCDD/F analysis using polyurethane samples

Dioxin-like PCBs (12 target compounds evaluated) were found in off-gassing PM samples collected on the PUF samples and analyzed as part of an exploratory analysis of PCBs and PCDD/Fs (Figure S4B). Observed concentrations varied across the 3 PM off-gassing samples tested and between target PCBs. As the extracts were spiked with internal standard, but not the PUF material itself, the off-gassing reported here may represent a lower estimate. While some PCDD/Fs were detected in the semi-quantitative analysis, none of the PCDD/Fs (7 PCDDs and 10 PCDFs were targeted) were confirmed in PM off-gassing and are presented as upper limits

(e.g., <2.2 pg per sample), and losses during the sample extraction were similarly not quantifiable.

S2. Vocus data processing and analysis

S2.1 Targeting masses important to SHS and THS

The following details are intended to supplement the description in the main text Methods section and the associated methods details above. Compounds violating the nitrogen rule were discarded, and these masses were compared to the PTR-TOF's *m/z* values. A tolerance of up to 0.005 *m/z* was used, but further manual processing confirmed these assignments. The masses were then filtered according to their contribution to the total signal and whether they correlated well with other known tobacco smoke emissions. This step ensured the filtering of unwanted signals, including water clusters and contaminants.

Code was written in Igor Pro to analyze the PTR-TOF data from this project. Slight variations in mass calibration over the long measurement period meant that *m/z* values had to be matched across the four main data files generated from Tofware (Tofwerk) while accounting for any slight shifts. This was done using a maximum interval for mass shifts between files, defined by the mass resolution of the instrument (i.e., $M/\Delta M = 10{,}000$) or fixed at 0.01 *m/z* for larger compounds. To correct for mass shifts across the entire data set, masses that fell within this interval were assigned to each other, and the daily use of the 12 compound calibration gas ensured that these *m/z* would not change substantially from file to file.

Then, a list of possible compounds with the formulas $C_{1\text{-}42}H_{3\text{-}86}O_{0\text{-}8}N_{0\text{-}2}$ was generated and their expected masses were calculated. The closest viable formula to the observed *m/z* (within the mass resolution of the instrument) was selected, except for compounds that do not follow the supposed formulas (e.g., siloxanes). For some masses with known contributions from tobacco smoke[7,8] and biomass burning,[9] tentative compound identifications were made (e.g., Table S3), and some were further confirmed using GC-EIMS data. The data started with 3362 available signals at masses ranging from *m/z* = 15.0191 to *m/z* 525.1202. It is worth noting that the Vocus uses a low-pass filter at lower *m/z* values to avoid saturation of the detector from the hydronium ion (H_3O^+, m/z = 19.0178).

Generating a list of important masses became paramount to providing focus to our online analyses because the initial Vocus data of 3362 potential compounds included all detected

masses. We started with the list of the 150 largest signals observed in a secondhand smoke sample. We also included compounds that stood out compared to its closest *m/z* neighbors, which essentially acted as a low-pass filter. This search was done using the local median factor, which is similar to the median absolute deviation. For each *m/z*, its abundance was compared to the median abundance for its 15 nearest neighbors (7 below, 7 above, and itself). Other compounds with fairly simple formulas (low counts of oxygen and nitrogen) and sufficient abundance were also included. In addition, we evaluated the correlation of candidate *m/z*'s in secondhand smoke to 2,5-dimethylfuran and/or nicotine for potential inclusion. Through this process, the list of 3362 available masses was narrowed down to 417, approximately half of which had putative chemical identifications.

S2.2 Sensitivity calculations to convert ion abundances to concentrations

We can use previously determined compound properties to calculate sensitivity [cps/ppb] by compound. k is $k_{capture}$ from ADO theory, which can be calculated for a compound using polarizability (α) and dipole moment (μ). Methods in Sekimoto et al. provide estimates for polarizability and dipole moment based on each compound's molecular weight and elemental composition/functional group, respectively.[10] Code graciously provided by Jordan Krechmer and Kanaki Sekimoto greatly expedited these calculations and estimations.

$$Sens_{meas} = k \times A \times F_{VOC \cdot H^+} \times T \qquad [S1]$$

A – Product of analyte reaction time and molecule count in the drift tube.

$F_{VOC \cdot H^+}$ – Proportion of the parent compound that fragments.

T – Transmission factor.

For masses that were not present in the calibration gas, which included a wide range of compounds across the complex mixture, fragmentation estimates were not included at the time of processing. The lack of sufficient data on fragmentation patterns for many of the detected compounds necessitated that most compounds were evaluated on their parent ion without corrections for fragmentation. Thus, data for most of the masses were either potential underestimates due to lower abundances of the expected parent ion of $[M+H]^+$ or, in some cases, overestimates if a fragment of a larger compound contributed extra signal to the target mass. The potential for fragmentation is influenced by molecular structure. Compounds such as isoprene and monoterpenes are known to fragment, while others, such as most aromatics, are known to

not fragment. This fragmentation also prevents the quantification of alkanes with PTR-TOF in H_3O^+ mode, though such measurements could be made in with other reagents (e.g., NO^+).

In order to determine *T* as a function of *m/z*, calculated sensitivities for calibration gas compounds in the 79 component calibration gas (Table S2) were determined by fitting the regression of measured sensitivities to their $k_{capture}$ (i.e., their k_{ADO}). The sensitivity measured by the Vocus for calibration compounds was compared with a calculated sensitivity for these same calibration compounds derived from Vocus parameters, as detailed in previous literature.[10,11] For this particular data set, a slope of 1360 was found for this regression when forced through the origin (Figure S27, top). Then, the ratio $\frac{Sens_{meas}}{Sens_{calc}}$ was plotted against *m/z* and fit with a sigmoidal distribution to determine the *m/z*-dependent transmission factor (Figure S27 bottom, green). The sigmoid function provides the best fit based on the current state of experimental data for compounds commonly included in calibration gases. An explicit representation of the sigmoidal distribution can be found in equation [S2].

$$T(mz) = \frac{1}{1 + e^{-\frac{(44.49 - mz)}{2.89}}} \qquad [S2]$$

This function reaches near unity (within 1%) for transmission efficiency for m/z > 58, similar to transmission curves seen in previous literature.[11] A different treatment for transmission efficiency can be found in Section S2.3.

$Sens_{calc}$ were determined via the earlier regression between $Sens_{meas}$ and $k_{capture}$ and the transmission factor in equation [S2].

$$Sens_{calc} = 1363.1 * k * T(mz) \qquad [S3]$$

The time series data were resampled from having one data point every 1 second to one data point every 10 or 15 seconds, then divided by the compound-dependent sensitivity [cps/ppb] to arrive at time series in terms of parts per billion (ppb).

Subsections of experiments were analyzed for representative concentrations as detailed in the methods section in the main text. To reiterate, for SHS runs, the representative concentration was the average concentration of the target compound for the whole 7–14 minute period. For PM off-

gassing, the representative stabilized concentration was taken as the average concentration of the 5–20 minute period after the start of off-gassing. For LLF off-gassing, the representative concentration was the average concentration of the 0.5–20 minute interval. These endpoints were set since Vocus sample collection periods were non-uniform, and including portions later than 20 minutes would skew comparisons. We note that Trial 3's PM off-gassing test at 18 hours of aging had a run time of 18 minutes and lasted just less than the requisite 20 minutes, but the signal equilibrated rapidly to stable concentrations because of its prior (and ongoing) aging and its 5–18 minute period was deemed to be sufficiently close to a representative average. For each experimental run, background levels (averaged over a 2–4 minute period) in either the SHS chamber, off-gassing setups, or newly-prepared surrogate LLF were determined, preceding each SHS/THS experiment or sample off-gassing time point.

S2.3 Determination of a hybrid sigmoidal/log-normal transmission function to constrain uncertainty

We also considered that the transmission efficiency in the PTR-TOF is unlikely to indefinitely remain at unity for high m/z ions. The filtering via ion transfer optics through the big segmented quadrupole (BSQ) of the PTR-TOF and the effect of losses to inlet walls leads to a theorized, and previously observed, reduction in transmission efficiency. Thus, a sensitivity analysis of SHS, PM off-gassing, and LLF off-gassing concentrations using the purely sigmoidal fit and a piecewise fit are described below and shown in Table S7, where the piecewise function results in slightly higher concentrations of the SVOCs and larger IVOCs observed in THS. The more conservative estimates of PTR-TOF concentrations via the sigmoidal fit are presented elsewhere throughout the manuscript, and we emphasize that the transmission function used does not affect the conclusions on the relationship between THS and SHS.

This comparison and transmission functions are informed by prior work. Previous papers using chemical ionization have noted a drop-off at higher m/z values (upwards of m/z 500).[12] However, those chemical ionization setups also have a rising edge in transmission efficiency occurring at larger m/z values, since they are usually more interested in lower volatility, highly oxidized organic compounds. By contrast, the PTR-TOF used in this study should have a rising edge occurring around m/z 45, since the optics are used as a high-pass filter to prevent hydronium ions (nominal mass 19) from saturating the detector. In Heinritzi et al.,[12] a "2 fold Gaussian" distribution was used to fit the relative transmission curve determined from the

relative depletion method. The relative depletion method was also used with perfluorinated acids in Riva et al.[13] to determine a relative transmission fit, though in that paper, the authors were testing an acetate chemical ionization, atmospheric pressure ionization, time of flight mass spectrometer (CI-APi-TOF) and used a log-normal fit for the transmission efficiency. In Holzinger et al.,[14] a piecewise function consisting of two sigmoid distributions (one for m/z < 59 and one for m/z > 122) on either side of a power curve (m/z 59 to 122) was used to algorithmically calculate a "retrieved transmission" curve. A potential compromise for the lack of available fitting algorithms for these distributions is to use a single log-normal distribution, though we note that the log-normal distribution is concave up throughout the higher mass range, while the m/z > 122 sigmoid used in Holzinger et al. starts concave down, then becomes concave up after some inflection m/z.

It is currently unclear exactly what distribution best fits measured compound transmission efficiencies for the wide molecular weight range observed by Vocus PTR-TOF, and the choice of fit could increase the actual concentrations of these larger compounds by up to a factor of 2 or more. Thus, future work should aim to calibrate across a wider range of I/SVOCs. Some compounds larger than monoterpenes used in Holzinger et al. included D3/D4/D5 siloxanes and trichlorobenzene,[14] but finding more candidate compounds that are stable in the gas-phase under ambient conditions. In Holzinger et al., trichlorobenzene (and trifluorobenzene) had low empirical transmission efficiencies (< 0.1) in the Vocus, so only the siloxanes were relevant for modeling transmission efficiency for m/z > 137. Determining a fit for transmission efficiency for a varied collection of larger, lower volatility compounds may be an important refinement for future Vocus PTR-TOF measurements.

To constrain this uncertainty, for our study, we also calculated PTR-TOF concentrations using a log-normal distribution (as calculated by Igor Pro) and applied it as a piecewise function. Subsequent independent testing on the same Vocus found a sensitivity of 3205 cps/ppb for m/z 107 (xylenes) and a sensitivity of 4549 cps/ppb for m/z 371 (D5 siloxane). A k of 3.515 was determined for D5 siloxane, using literature values of 39.2E-24 cm^3 and 1.35D for the polarizability and dipole moment, respectively. The D5 siloxane $Sens_{actual}$ was estimated by scaling the sensitivity by the experimental data in our study for m/z 107 to m/z 371. Then the $Sens_{actual}/Sens_{expected}$ for D5 siloxane, estimated to be 0.635, was included in the log-normal fit as

seen in Figure S27 bottom (red). To better fit the low m/z compounds, a piecewise function was selected, using the sigmoidal distribution for m/z < 111.6 and log-normal otherwise.

This log-normal distribution had the equation:

$$T = e^{-\left(\frac{\ln\left(\frac{m/z}{x_0}\right)}{width}\right)^2} \qquad [S4]$$

The values of x_o and *width* were determined to be 111.59, and 1.65, respectively.

S2.4 Timescale analysis for LLF experiments

Over the course of the nearly two hours of Vocus run-time for Trial 5's LLF off-gassing, most compounds exhibited an exponential decay trend. An exponential fit was done on the LLF off-gassing data, starting at the data maximum, because some compounds take longer to equilibrate. This behavior may be attributable to either matrix effects with respect to the tubing leading to or inner surfaces of the Vocus. Alternatively, it is possible some compounds take more time to efficiently off-gas from the surrogate LLF. From these exponential fits, the pre-exponential constant and residence time (τ) were recorded. The pre-exponential constant indicates the intercept, which relates to the maximum concentration observed.

The residence time, also known as the e-folding time, was plotted as an independent variable compared to the LLF off-gassing over smoke ratio ($Conc_{LLF}/Conc_{Smoke}$) and also against the Min/Max concentration ratio (Figure S22). In the comparison to the former metric, we note some very interesting bands of behavior. The trends of (i) dark blue and purple, (ii) cyan, and (iii) sea blue can be linear. More data points would reveal whether these trends are consistent throughout a larger collection of compounds. However, for this simplified surrogate LLF system, given a compound with a fairly low Henry's law constant (i.e., affinity for air), we may be able to predict an expected LLF/smoke concentration based on its e-folding time in surrogate LLF.

As for the min/max ratio vs. e-folding time graph, the data appear to have an exponential trend. These two metrics are related, so the minimal deviation from the trend is not too surprising. We would expect the min/max ratio for the two hours of PTR-TOF data to remain low until an e-folding time of approximately an hour. A few compounds have unexpected locations on the plot, though these can be attributed to locally drastic changes near the minimum or maximum that get smoothed out by an exponential fit.

S2.5 Note on 3-ethenylpyridine and the effect of pH of nitrogen-containing compounds

We note that 3-Ethenylpyridine (i.e., 3-Vinylpyridine), a common SHS component, was found to off-gas from LLF at a relatively constant concentration for at least 30 minutes. A possible explanation for this behavior may be 3-ethenylpyridine's pKa. Its pKa of 4.8 means it will primarily be in its un-protonated form, considering aqueous-phase cigarette smoke's pH of 5.3–6.5.

S2.6 Note on Figure 5D, rate constants and maximum saturated quantity

For the uptake and off-gassing analysis presented in Figure 5D (top half), the rate constants are determined via a simple box modeling of the LLF off-gassing, and maximum saturated quantities were calculated directly from Henry's law calculations and the amount of LLF present (25 mL).

S2.7 Determining representative concentrations for SHS, PM off-gassing, and LLF off-gassing

To calculate representative concentrations of PM off-gassing, we used the average of the first 20 minutes excluding a 5 minute lag during the initial portion of the PM off-gassing measurements to avoid bias in the comparisons of THS to SHS. For SHS, we averaged over the whole 7–14 minute period of smoking. This selection enabled measurements of well-mixed SHS in the chamber at the most representative concentrations, and for PM off-gassing it focused on stabilized off-gassing concentrations and avoided brief/occasional spikes in the first moments after the filter flow began that were not representative for the purposes of analyses associated with Figures 3-5. For LLF off-gassing concentrations, the average value for the first 20 minutes of data was determined after excluding the first 30 seconds of data to ensure sufficient flushing of any residual SHS from the bubbler headspace. In Figure 5C, maximum concentrations following 1 hour of off-gassing were calculated for comparison.

Variations in the relative compound abundances in these figures for SHS, PM off-gassing, or LLF off-gassing may be attributed to variations in emissions, collected PM loadings, mixing or flow dynamics within the chamber of off-gassing setups, or dilution variations resulting from the sampling flowrate of the PTR-TOF, which was confirmed at least daily. When observed in select instances, these variations in concentrations tended to be fairly consistent across compounds, meaning that the relative chemical composition of emissions remained similar with slight shifts in absolute concentrations that do not affect the conclusions of this study.

S3. Offline analysis of gas-phase and particle-phase samples

S3.1 GC-TOF analysis of gas and particle samples

The adsorbent tube sampling and analysis approaches are presented in prior work,[1,15] with relevant supplemental information following here. For GC-TOF, code developed in-house (MSDataView and APCI Integration[15–17]) was used to target and integrate compounds based on their elemental composition (e.g., CH, $CHO_{1\&2}$, $CHN_{1\&2}$, $CHN_{1\&2}O_1$). Thereafter, the relative average composition across samples were aggregated once they were observed to be sufficiently similar. Further code written in Igor Pro 8 was used to generate the figures. Given the wide range of analytes without available standards or calibration procedures for GC-TOF, composition is presented as ion abundances, but based on prior work, we note that the contributions of aliphatic hydrocarbons are likely lower limits due to relatively lower response factors.[15] In the process of obtaining sufficient signal across the complex mixture of THS emissions to speciate all compound classes shown in Figure 2, the abundant levels of nicotine in PM off-gassing and SHS led to GC-TOF saturation for nicotine. So, to ensure the appropriate representation of nicotine in Figure 2 (and related data in Figure 1 and Table 1), the ion abundance of nicotine was corrected based on the relative ratio of nicotine to other prominent alkaloids also observed via PTR-TOF.

Tube and filter samples were collected at a variety of sample volumes, which reflect the expected mass loadings in the SHS vs. THS sampled. Compound formulas were determined by starting with the fully saturated compound, e.g., $C_nH_{2n+2+i}N_iO_j$ for the $[C_nH_{2n+3+i}N_iO_j]^+$ ion. Other formulas with the same number of carbons were obtained by subtracting 2 hydrogen atoms at a time, which is akin to a double bond equivalent (DBE) used in other work.[15,18]

Due to the unique nature of tobacco smoke compared to petroleum-related certified reference materials used previously for calibration,[15–17,19,20] abundances were not converted to mass concentrations for the purposes of this manuscript. For example, a greater prevalence of alkenes and the overlap of alkanes, alkenes, and cyclic alkanes (along with other combinations of rings and double bonds observed with GC-EIMS) throughout low DBE chemical formulas (DBE 0 to 3), would lead to larger uncertainties in response factors resulting from variations in chemical structure. Though, we note that response factors (in units of μg $abund^{-1}$) tend to be larger for lower DBEs in the 0 to 3 range, implying that we may expect to see less signal for the same amount of mass. Also, it is worth noting that for hydrocarbons (i.e., CH compounds), the selection of ions is different than might be expected for DBE 0, 1, 2, and 3 compounds. For

these, the ion selected is $[M\text{-}H]^+$ for DBE 0–2 and $[M]^+$ for DBE 3. The selection of $[M\text{-}H]^+$ is necessary because of ionization patterns of alkanes in the Agilent APCI interface.[15] While this was less of a problem in previous analyses of fossil fuel-related mixtures, which are generally low in alkene levels, greater contributions from alkenes in this manuscript introduce some uncertainty in differentiating the identities of these compounds, since alkenes, along with terpenes, ionize as $[M+H]^+$, similar to terpenes, and mono/poly-cyclic aromatic compounds at DBE 4 and greater. For these reasons, hydrocarbons observed via GC-TOF are reported in ion abundances throughout the manuscript.

S3.2 GC-EIMS analysis of adsorbent tubes

For this manuscript, GC-EIMS data were primarily used to verify identifications for compound formulas found in the other gas-phase methods. The NIST database was used to identify compounds based on their peak spectra. Given the complexity of the tobacco smoke compound mixture, as seen in the TICs and EICs in Figure S5, high chemical resolution mass spectrometry with soft ionization was used to provide a detailed speciation within compound classes further separated by DBEs for the SHS, PM, LLF off-gassing and PM off-gassing (Figures 2, S2, Table 1).

S3.3 LC-TOF analysis of PTFE filters

Non-targeted analysis of the LC-TOF data was done via Agilent MassHunter Qualitative software that extracts analyte peaks (i.e., Find by Molecular Feature) and generates molecular formulas (i.e., Generate Formulas). The software uses spectral patterns expected by isotopes and their *m/z* discrepancies to predict these formulas at high-mass accuracy (<1–2 parts per million). These identifications were further processed for QA/QC by in-house code written in Igor Pro 8 (TOF Analysis Code) containing procedures and restrictions described by Ditto et al.[4] that applied strict exclusion criteria for LC peak quality and for molecular formula assignments.[21] The parameterization presented in Li et al. was used to assign a volatility to these compounds.[22] Refer to Ditto et al. for more detail on filter sampling, analysis, and data processing.[4]

S3.4 Nicotine correction for GC-TOF analysis

Nicotine is one of the largest components, by mass, in tobacco smoke. In the process of obtaining sufficient signal for all the ions across the complex mixture of compound classes in Figure 2 (and associated data in Figures 1, S7, and Table 1) to achieve the breadth of desired

speciation for these offline analyses, the nicotine signal was saturated in the GC-TOF measurements, producing a relatively lower nicotine ion abundance. No similar issues with saturation were observed in PTR-TOF data. To resolve any potential misinterpretation by viewers of the nicotine-related GC-TOF data on SHS or PM off-gassing (e.g Figure 1C, 2A/E; Table 1), PTR-TOF data from the Vocus were used to correct for this discrepancy as follows. The ratio between nicotine ($C_{10}H_{14}N_2$) and $C_{10}H_{12}N_2$ compounds (e.g., Anatabine, Anabaseine) was found in the Vocus data and we used the following relation to normalize the nicotine concentration expected in the GC-TOF data.

$$Conc_{Nicotine,\,GC-TOF} = Conc_{C_{10}H_{12}N_2,\,GC-TOF} * \left(\frac{Conc_{Nicotine,Vocus}}{Conc_{C_{10}H_{12}N_2,Vocus}}\right) \qquad [S5]$$

We found that the ratio of Nicotine to $C_{10}H_{12}N_2$ in the Vocus was approximately 24.6 for both PM off-gassing and SHS data. Using such a correction on the PM, SHS and PM off-gassing samples (LLF off-gassing nicotine levels were sufficiently low to avoid requiring this correction) resolved the misrepresentation and increased the nicotine abundance by a factor of 2-3 in the GC-TOF data on average and resulted in nicotine representing 15% of PM off-gassing by ion abundance. We emphasize that ion abundance is not intended to be equivalent to mass concentrations in this study given known differences in GC-TOF response factors, and thus the reported concentrations throughout the study are derived from PTR-TOF. We acknowledge that future work should continue to expand the detailed quantitative speciation of THS, though point to limitations in the availability of calibration standards for GC-TOF and highlight that the conclusions of this study are not impacted by this GC-TOF nicotine correction.

S4. Equilibrium timescale modeling (PM)

S4.1 Equilibrium timescale calculations

Equilibrium timescales for deposited PM were calculated for the purposes of contextualizing the results to real-world conditions and are shown in Figure S19 and mentioned in the *Discussion* section. While Weschler & Nazaroff primarily apply partitioning theory to SVOCs in their 2008 paper, the fundamental physics behind partitioning behavior can be applied to organic compounds of any volatility.[23] These physical principles form the foundation for our physical understanding of the flux and equilibria of VOCs between gas, particle, and liquid phases. The separation between these phases can be described by equilibrium constants, which include

effective saturation concentration (C*) for gas/particle partitioning and Henry's law coefficients (H^{cp}) for gas/aqueous partitioning.

Mass transfer fluxes are expressed as pseudo-reactions and can be limited by three different processes: gas-phase diffusion, interfacial transport, and bulk diffusion [24]. For PM equilibrium partitioning timescales, we calculated potential bulk diffusion timescales for a characteristic length range from 0.1–1000 nm and a bulk diffusivity (related to viscosity) between 10^{-19}–10^{-12} $m^2\ s^{-1}$ using its timescale equations from previous literature.[24–26] The characteristic length range represents two extremes in PM off-gassing, with the smaller end representing initial surface film growth and the other end equivalent to a layer of sizable particles on the filter. The bulk diffusivity range extends down to viscosities previously modeled for highly viscous organic (e.g., α-pinene SOA) mixtures, while the upper limit approaches water's diffusion coefficient at 298K. Substrate properties also play a role in the film thickness and diffusivity, so a thicker layer, analogous to a painted surface (40–240 μm), was considered as in Algrim et al.[27] Generally, bulk diffusion timescales are longer than gas-phase diffusion for these highly viscous bulk reservoirs; interfacial transport was also considered separately, when assumed to be the limiting process.

Normally, the evaluation of these three diffusive processes in search of a limiting step involves the uptake of a molecule toward a bulk particle or surface. In this study, the PM experiment involves flowing purified air through the filter, which would be the opposite mechanism of previously done equilibrium timescale modeling.[26] However, these calculations can be reversed without issue, since the same principles guide the physical processes being studied. In brief, bulk diffusion was assumed to be the limiting factor. The timescale for bulk diffusion (τ_b) can be calculated from the following equation.

$$\tau_b = \frac{4L^2}{\pi^2 D_b} \qquad [S6]$$

L – Characteristic length [m] (e.g., thickness of a layer or radius of a sphere)
D_b – Bulk diffusion coefficient [$cm^2\ s^{-1}$]

Bulk diffusion coefficients, directly related to viscosity, can vary widely based on aerosol composition. Recent work has modeled and predicted bulk diffusion coefficients for α-pinene

SOA to be between 2.5–8.5 x 10^{-15} cm^2 s^{-1}. Meanwhile, an upper bound of 10^{-8} was chosen to ensure that aerosols with liquid behavior were included.

We modeled timescales for a range of characteristic lengths (5 nm–250 μm) and bulk diffusion coefficients (10^{-15}–10^{-8} cm^2 s^{-1}) (Figure S19). Note that the timescale for bulk diffusion is volatility-independent, reducing a factor for consideration. These characteristic lengths range in applicability from surface films (8nm–15nm)[28] to particles, with size designations ranging from ultrafine (<100nm) to coarse mode (>1μm), and to thick porous surfaces (e.g., paints).[27]

4.2 Factors affecting equilibrium timescales and compound fates

The rate and composition of THS off-gassing will be impacted by the chemical composition and physical-chemical properties of both the deposited PM and that of the surrounding environment, such as phase state, viscosity, pH, and toxicity.[29–32] For example, pH may affect both the off-gassing of reduced nitrogen-containing species and their uptake to other surfaces and aerosols. Also, sorptive interactions of THS with materials/furnishings will be compound dependent and potentially more retentive than PM or aqueous THS reservoirs.

In indoor spaces with THS, the thickness of the deposited particle layer will influence internal diffusion length scales and thus fluxes, similar to the experimental setup, where a compound's off-gassing lifetime from the collected PM on filters would also depend on the thickness of the PM layers accumulated on the filter fibers. When PM penetrates porous surfaces such as previously mentioned paints, the PM would have less surface area exposed to the surrounding air, and a layer of deposited particles would result in partitioning behavior more similar to an organic film, further extending the lifetime of the THS contaminants (Figure S19). Also, the presence of water (as bulk aqueous-phase water or relative humidity) can affect the partitioning and emission of organic compounds from both PM and surfaces.

The composition of indoor non-tobacco-related aerosols will also impact in-building transport, as acidic and aqueous aerosols have been shown to irreversibly uptake reduced nitrogen species through protonation,[33,34] which would pull them out of equilibrium into the particles and facilitate off-gassing from contaminated surfaces. Thus, the presence of aerosols and their dynamically-changing indoor aerosol mass concentrations and composition may influence both THS off-gassing timescales and concentrations of airborne THS particle-bound compounds (and human exposure) by enhancing off-gassing from plentiful THS reservoirs (i.e., deposited PM).[33]

With chemical transformation lifetimes that are competitive with ventilation, the gas-phase oxidation of reactive compounds like alkenes, aromatics, and terpenes (e.g., limonene) can lead to production of gas-phase oxidation products, some of which lead to the generation of indoor SOA. Similarly, large THS fluxes may lead to the formation of secondary ultrafine particles (dia. < 100 nm), similar to prior observations of SHS oxidation.[35]

S5. Multi-compartment body model

S5.1 Kinetic multi-compartment model calculations

The kinetic multi-compartment model used to study aqueous phase uptake and THS off-gassing consists of four compartments (Figure S23) and was evaluated over time using the following differential equations. The model explicitly treats inhalation and exhalation gas flow, air-liquid partitioning to the lung lining fluid, as well as transport between the three condensed phase compartments. For simplicity, only aqueous-phase partitioning according to Henry's law is considered in the model. The model simulations were divided into alternating smoking and non-smoking periods, which differ in the boundary conditions of the differential equations. A smoking event consisted of 10 cigarette puffs of 5 s length each, during which inhaled breath had the organic compound concentration of mainstream smoke. A puff was assumed to occur once every 30 seconds. In non-smoking periods, the inhaled breath was assumed to be free of smoke components.

The descriptive set of differential equations was solved in MATLAB (ode23tb). Descriptions of symbols and values for the model input parameters included in these differential equations can be found in Table S6. For convenience, they have also been included below the equations.

$$\frac{dc_{lung}}{dt} = \frac{(c_{air} - c_{lung}) * \frac{V_{tidal}}{V_{lung}}}{t_{breath}} + \alpha * \frac{W}{4} * \left(\frac{c_{LLF}}{K_{air,LLF}} - c_{lung}\right) * \frac{A_{LLF}}{V_{lung}} \quad [S7]$$

$$\frac{dc_{LLF}}{dt} = \alpha * \frac{W}{4} * \left(c_{lung} - \frac{c_{LLF}}{K_{air,LLF}}\right) * \frac{A_{LLF}}{V_{LLF}} + k_{LLF,blood} * \left(c_{blood} - \frac{c_{LLF}}{K_{LLF,blood}}\right) \quad [S8]$$

$$\frac{dc_{blood}}{dt} = k_{LLF,blood} * \left(\frac{c_{LLF}}{K_{LLF},blood} - c_{blood}\right) * \frac{V_{LLF}}{V_{blood}} + k_{blood,tissue} * \left(c_{tissue} - \frac{c_{blood}}{K_{blood,tissue}}\right) \quad [S9]$$

$$\frac{dc_{tissue}}{dt} = k_{blood,tissue} * \left(\frac{c_{blood}}{K_{blood,tissue}} - c_{tissue}\right) * \frac{V_{blood}}{V_{tissue}} \quad [S10]$$

$\frac{dc_{lung}}{dt}, \frac{dc_{LLF}}{dt}, \frac{dc_{blood}}{dt}, \frac{dc_{tissue}}{dt}$ - Change in concentration of a compound in each layer over time [cm^{-3} s^{-1}].

c_{air}, c_{lung}, c_{LLF}, c_{blood}, c_{tissue} – Concentration of target compound in inhaled breath, lung gas-phase, LLF, blood, tissue, respectively [cm^{-3}].

V_{tidal}, V_{lung}, V_{blood}, V_{tissue} – Lung tidal, lung average, blood, and tissue volume, respectively [m^3].

t_{breath} – Puff/breath duration [s].

α – Mass accommodation coefficient, i.e., fraction of airborne molecules that adsorb to a surface upon contact [unitless]

W – Mean thermal velocity [cm s^{-1}].

A_{LLF} – Surface area of lung lining fluid [cm^2].

$K_{air,LLF}$, $K_{LLF,blood}$, $K_{blood,tissue}$ – Equilibrium constant for the target compound between air/LLF (Henry's law constant), LLF/blood, and blood/tissue [unitless], assumed to be unity.

$k_{LLF,blood}$, $k_{blood,tissue}$ – Rate coefficient of transport for LLF/blood and blood/tissue [s^{-1}].

In the model, partitioning coefficients between LLF, blood and tissue are assumed unity. Transport between LLF and blood is assumed to be fast at rate of 1 min^{-1}. The transport rate between blood and tissues was checked against experimental data on exhaled breath concentration from Jordan et al.[36] and determined to 0.33 h^{-1}, which is typical for moderately-perfused tissues.[37] All model input parameters (e.g., breathing parameters, compartment sizes) can be found in Table S6.

S5.2 Further THS LLF considerations

This section is an addendum to Section 4.1.3 in the main text discussing differences between our results and real-world conditions. First, there may be differences between the properties of surrogate LLF and real LLF, including possible variations in pH, the inclusion of lipids and proteins, chemical interactions of THS compounds with human LLF components not included here, and increased viscosity that may affect relevant physical processes in the respiratory tract, and potentially in blood.[38]

Second, other tissues in the respiratory tract or throughout the body will engage in non-aqueous partitioning, especially for compounds with low Henry's law constants. Both short-term off-gassing and peak concentrations can be affected due to interactions with tissues directly exposed to smoke, and more persistent uptake can occur to other less-perfused or adipose tissues, especially with heavy and long-term smoking. In both cases, this is key for lipophilic THS

compounds that could interact with lipids in LLF/blood or fats and lipids throughout the body.[37,39] In a real world context, lipophilic substances will more readily partition into body compartments, depending on the compartment's lipid content. The multi-compartment model results are similar to the limited literature data on smokers' breath, with faster decays in lower H' compounds studied[36,37,40] and greater persistence for the one available compound in the moderate H' range (i.e., acetonitrile[36,41]). However, the slightly slower decay and persistence of lower H' compounds in breath following smoking at elevated levels of up to 10's of ppb seen in prior research (e.g., benzene, acetylene, 2,5-dimethylfuran, 2-methylfuran[37,42,43]) may suggest non-aqueous uptake to tissues (along with particle deposition) playing a role in extending the off-gassing timescales of lower H' THS components.

Third, within these multi-compartment bodily reservoirs, the metabolism of tobacco smoke contaminants (e.g., the conversion of nicotine to cotinine) also needs to be considered as a loss process for the complex mixture of THS compounds and their metabolites, for many of which we only have limited toxicokinetic data. Some of the prominent precursors to these metabolites have been previously identified as potential biomarkers for SHS/THS exposure (i.e., detection in urine), including nicotine, cotinine,[44] PAHs, TSNAs, nicotelline,[44] and 3-ethenylpyridine,[45] among others.[46] Additionally, their cycling through and departure from the body further complicate their lifetimes from the various aqueous-phase reservoirs. The temporal evolution, lifetimes, and cycling of these and other THS components across the various aqueous-phase bodily reservoirs may be impacted by in vivo processing and potentially protein-facilitated diffusion, as previously hypothesized for acetonitrile.[38]

Fourth, with real-world smoking, large concentrations of particles from mainstream smoke will deposit on airway surfaces or dissolve into LLF.[47] While the dissolution or suspension of PM into the body's aqueous-phase has been theorized,[48] this interaction has not been previously studied in high chemical detail or for THS. While particles were intentionally filtered in this study to independently focus on gas-phase uptake into LLF (with the intentional exception of one experiment, Figures S16, S20), this particle deposition would provide an additional in-lung THS reservoir similar to the off-gassing PM reservoir described in this work and likely extend the persistence of THS compounds in smokers' breath.

References

1. Sheu R, Marcotte A, Khare P, Charan S, Ditto JC, Gentner DR. Advances in offline approaches for chemically speciated measurements of trace gas-phase organic compounds via adsorbent tubes in an integrated sampling-to-analysis system. *J Chromatogr A*. 2018;1575:80–90. November 2018. https://linkinghub.elsevier.com/retrieve/pii/S0021967318311610.

2. Charrier JG, McFall AS, Richards-Henderson NK, Anastasio C. Hydrogen peroxide formation in a surrogate lung fluid by transition metals and quinones present in particulate matter. *Environ Sci Technol*. 2014.

3. Tong H, Lakey PSJ, Arangio AM, et al. Reactive Oxygen Species Formed by Secondary Organic Aerosols in Water and Surrogate Lung Fluid. *Environ Sci Technol*. 2018;52:11642–11651. October 16, 2018. https://pubs.acs.org/doi/abs/10.1021/acs.est.8b03695. Accessed September 30, 2021.

4. Ditto JC, Barnes EB, Khare P, et al. An omnipresent diversity and variability in the chemical composition of atmospheric functionalized organic aerosol. *Commun Chem*. 2018;1:1–13. December 2, 2018. http://www.nature.com/articles/s42004-018-0074-3. Accessed April 21, 2021.

5. Kitanovski Z, Shahpoury P, Samara C, Voliotis A, Lammel G. Composition and mass size distribution of nitrated and oxygenated aromatic compounds in ambient particulate matter from southern and central Europe-implications for the origin. *Atmos Chem Phys*. 2020;20:2471–2487.

6. Degrendele C, Fiedler H, Kočan A, et al. Multiyear levels of PCDD/Fs, dl-PCBs and PAHs in background air in central Europe and implications for deposition. *Chemosphere*. 2020;240:124852.

7. Sleiman M, Logue JM, Luo W, Pankow JF, Gundel LA, Destaillats H. Inhalable constituents of thirdhand tobacco smoke: Chemical characterization and health impact considerations. *Environ Sci Technol*. 2014;48:13093–13101.

8. Sheu R, Stönner C, Ditto JC, Klüpfel T, Williams J, Gentner DR. Human transport of thirdhand tobacco smoke: A prominent source of hazardous air pollutants into indoor nonsmoking environments. *Sci Adv*. 2020;6:eaay4109. March 4, 2020. https://advances.sciencemag.org/content/6/10/eaay4109/tab-article-info.

9. Koss AR, Sekimoto K, Gilman JB, et al. Non-methane organic gas emissions from biomass burning: identification, quantification, and emission factors from PTR-ToF during the FIREX 2016 laboratory experiment. *Atmos Chem Phys*. 2018;18:3299–3319. March 7, 2018. https://doi.org/10.5194/acp-18-3299-2018. Accessed May 22, 2021.

10. Sekimoto K, Li SM, Yuan B, et al. Calculation of the sensitivity of proton-transfer-reaction mass spectrometry (PTR-MS) for organic trace gases using molecular properties. *Int J Mass Spectrom*. 2017;421:71–94. 2017. https://doi.org/10.1016/j.ijms.2017.04.006.

11. Krechmer J, Lopez-Hilfiker F, Koss A, et al. Evaluation of a New Reagent-Ion Source and Focusing Ion-Molecule Reactor for Use in Proton-Transfer-Reaction Mass Spectrometry.

Anal Chem. 2018.

12. Heinritzi M, Simon M, Steiner G, et al. Characterization of the mass-dependent transmission efficiency of a CIMS. *Atmos Meas Tech*. 2016;9:1449–1460.

13. Riva M, Brüggemann M, Li D, et al. Capability of CI-Orbitrap for Gas-Phase Analysis in Atmospheric Chemistry: A Comparison with the CI-APi-TOF Technique. *Anal Chem*. 2020;92:8142–8150. June 16, 2020. https://pubs.acs.org/doi/full/10.1021/acs.analchem.0c00111. Accessed October 12, 2021.

14. Holzinger R, Joe Acton WF, Bloss WW, et al. Validity and limitations of simple reaction kinetics to calculate concentrations of organic compounds from ion counts in PTR-MS. *Atmos Meas Tech*. 2019;12:6193–6208.

15. Khare P, Marcotte A, Sheu R, Walsh AN, Ditto JC, Gentner DR. Advances in offline approaches for trace measurements of complex organic compound mixtures via soft ionization and high-resolution tandem mass spectrometry. *J Chromatogr A*. 2019;1598:163–174. August 2019. https://linkinghub.elsevier.com/retrieve/pii/S0021967319302882.

16. Sheu R, Fortenberry CF, Walker MJ, et al. Evaluating Indoor Air Chemical Diversity, Indoor-to-Outdoor Emissions, and Surface Reservoirs Using High-Resolution Mass Spectrometry. *Environ Sci Technol*. 2021;55:10255–10267. August 3, 2021. https://pubs.acs.org/doi/pdf/10.1021/acs.est.1c01337. Accessed July 22, 2021.

17. Khare P, Machesky J, Soto R, He M, Presto AA, Gentner DR. Asphalt-related emissions are a major missing nontraditional source of secondary organic aerosol precursors. *Sci Adv*. 2020;6:eabb9785.

18. Gentner D, Isaacman G. Elucidating secondary organic aerosol from diesel and gasoline vehicles through detailed characterization of organic carbon emissions. *Proc Natl Acad Sci*. 2012;109:18318–18323. 2012. http://www.pnas.org/content/109/45/18318.short. Accessed October 13, 2014.

19. Worton DR, Zhang H, Isaacman-Vanwertz G, Chan AWH, Wilson KR, Goldstein AH. Comprehensive Chemical Characterization of Hydrocarbons in NIST Standard Reference Material 2779 Gulf of Mexico Crude Oil. *Environ Sci Technol*. 2015;49:13130–13138.

20. Reddy CM, Arey JS, Seewald JS, et al. Composition and fate of gas and oil released to the water column during the Deepwater Horizon oil spill. *Proc Natl Acad Sci U S A*. 2012.

21. Kind T, Fiehn O. Seven Golden Rules for heuristic filtering of molecular formulas obtained by accurate mass spectrometry. *BMC Bioinformatics*. 2007;8:1–20.

22. Li Y, Pöschl U, Shiraiwa M. Molecular corridors and parameterizations of volatility in the chemical evolution of organic aerosols. *Atmos Chem Phys*. 2016;16:3327–3344.

23. Weschler CJ, Nazaroff WW. Semivolatile organic compounds in indoor environments. *Atmos Environ*. 2008;42:9018–9040. December 2008. https://linkinghub.elsevier.com/retrieve/pii/S1352231008008480.

24. Mai H, Shiraiwa M, Flagan RC, Seinfeld JH. Under What Conditions Can Equilibrium

Gas–Particle Partitioning Be Expected to Hold in the Atmosphere? *Environ Sci Technol*. 2015;49:11485–11491. October 6, 2015. https://pubs.acs.org/doi/10.1021/acs.est.5b02587.

25. Seinfeld JH, Pandis SN. *Atmospheric Chemistry and Physics: From Air Pollution to Climate Change*. Vol 2nd.; 2006. 2006. http://www.knovel.com/knovel2/Toc.jsp?BookID=2126.

26. Shiraiwa M, Seinfeld JH. Equilibration timescale of atmospheric secondary organic aerosol partitioning. *Geophys Res Lett*. 2012;39:1–6.

27. Algrim LB, Pagonis D, de Gouw JA, Jimenez JL, Ziemann PJ. Measurements and modeling of absorptive partitioning of volatile organic compounds to painted surfaces. *Indoor Air*. 2020;30:745–756.

28. Weschler CJ, Nazaroff WW. Growth of organic films on indoor surfaces. *Indoor Air*. 2017;27:1101–1112.

29. Ditto JC, Joo T, Khare P, et al. Effects of Molecular-Level Compositional Variability in Organic Aerosol on Phase State and Thermodynamic Mixing Behavior. *Environ Sci Technol*. 2019;53:13009–13018. November 19, 2019. https://pubs.acs.org/doi/abs/10.1021/acs.est.9b02664.

30. DeRieux W-SW, Li Y, Lin P, et al. Predicting the glass transition temperature and viscosity of secondary organic material using molecular composition. *Atmos Chem Phys*. 2018;18:6331–6351. May 4, 2018. https://acp.copernicus.org/articles/18/6331/2018/.

31. Shiraiwa M, Li Y, Tsimpidi AP, et al. Global distribution of particle phase state in atmospheric secondary organic aerosols. *Nat Commun*. 2017;8:1–7.

32. Weber RJ, Guo H, Russell AG, Nenes A. High aerosol acidity despite declining atmospheric sulfate concentrations over the past 15 years. *Nat Geosci*. 2016;9:282–285. April 22, 2016. http://www.nature.com/articles/ngeo2665.

33. DeCarlo PF, Avery AM, Waring MS. Thirdhand smoke uptake to aerosol particles in the indoor environment. *Sci Adv*. 2018;4:eaap8368. May 9, 2018. https://advances.sciencemag.org/lookup/doi/10.1126/sciadv.aap8368.

34. Collins DB, Wang C, Abbatt JPD. Selective Uptake of Third-Hand Tobacco Smoke Components to Inorganic and Organic Aerosol Particles. *Environ Sci Technol*. 2018;52:13195–13201. November 20, 2018. http://pubs.acs.org/doi/10.1021/acs.est.8b03880.

35. Wang C, Collins DB, Hems RF, Borduas N, Antiñolo M, Abbatt JPD. Exploring Conditions for Ultrafine Particle Formation from Oxidation of Cigarette Smoke in Indoor Environments. *Environ Sci Technol*. 2018;52:4623–4631.

36. Jordan A, Hansel A, Holzinger R, Lindinger W. Acetonitrile and benzene in the breath of smokers and non-smokers investigated by proton transfer reaction mass spectrometry (PTR-MS). *Int J Mass Spectrom Ion Process*. 1995;148:L1–L3. September 1995. https://linkinghub.elsevier.com/retrieve/pii/016811769504236E.

37. Gordon SM, Wallace LA, Brinkman MC, Callahan PJ, Kenny D V. Volatile organic

compounds as breath biomarkers for active and passive smoking. *Environ Health Perspect*. 2002;110. 2002. http://ehpnet1.niehs.nih.gov/docs/2002/110p689-698gordon/abstract.html. Accessed May 22, 2021.

38. Li M, Ding J, Gu H, et al. Facilitated Diffusion of Acetonitrile Revealed by Quantitative Breath Analysis Using Extractive Electrospray Ionization Mass Spectrometry. *Sci Reports 2013 31*. 2013;3:1–6. February 5, 2013. https://www.nature.com/articles/srep01205. Accessed August 24, 2021.

39. Wallace LA, Pellizzari E, Leaderer B, Zelon H, Sheldon L. Emissions of volatile organic compounds from building materials and consumer products. *Atmos Environ*. 1987.

40. Ueta I, Saito Y, TERAOKA K, Miura T, JINNO K. Determination of Volatile Organic Compounds for a Systematic Evaluation of Third-Hand Smoking. *Anal Sci*. 2010;26:569–574. 2010. http://joi.jlc.jst.go.jp/JST.JSTAGE/analsci/26.569?from=CrossRef.

41. Prazeller P, Karl T, Jordan A, Holzinger R, Hansel A, Lindinger W. Quantification of passive smoking using proton-transfer-reaction mass spectrometry. *Int J Mass Spectrom*. 1998.

42. Metsälä M, Schmidt FM, Skyttä M, Vaittinen O, Halonen L. Acetylene in breath: background levels and real-time elimination kinetics after smoking. *J Breath Res*. 2010;4:046003. November 15, 2010. https://iopscience.iop.org/article/10.1088/1752-7155/4/4/046003. Accessed August 8, 2021.

43. Sanchez JMM, Sacks RDD. Development of a multibed sorption trap, comprehensive two-dimensional gas chromatography, and time-of-flight mass spectrometry system for the analysis of volatile organic compounds in human breath. *Anal Chem*. 2006;78:3046–3054. May 1, 2006. https://pubs.acs.org/doi/pdf/10.1021/ac060053k. Accessed August 8, 2021.

44. Benowitz NL. Biomarkers of environmental tobacco smoke exposure. *Environ Health Perspect*. 1999;107:349–355. May 18, 1999. https://pubs.acs.org/sharingguidelines. Accessed June 20, 2021.

45. Liu J, Benowitz NL, Hatsukami DK, et al. 3-Ethenylpyridine Measured in Urine of Active and Passive Smokers: A Promising Biomarker and Toxicological Implications. *Chem Res Toxicol*. 2021;34:1630–1639. May 17, 2021. https://doi.org/10.1021/acs.chemrestox.1c00064. Accessed June 20, 2021.

46. Torres S, Merino C, Paton B, Correig X, Ramírez N. Biomarkers of exposure to secondhand and thirdhand Tobacco smoke: Recent advances and future perspectives. *Int J Environ Res Public Health*. 2018;15:2693. November 29, 2018. http://webofscience.com. Accessed June 20, 2021.

47. Baker RR, Dixon M. The retention of tobacco smoke constituents in the human respiratory tract. *Inhal Toxicol*. 2006;18:255–294. 2006. https://www.tandfonline.com/action/journalInformation?journalCode=iiht20. Accessed June 27, 2021.

48. Pankow JF. A consideration of the role of gas/particle partitioning in the deposition of

nicotine and other tobacco smoke compounds in the respiratory tract. *Chem Res Toxicol*. 2001;14:1465–1481.

49. Gueneron M, Erickson MH, Vanderschelden GS, Jobson BT. PTR-MS fragmentation patterns of gasoline hydrocarbons. *Int J Mass Spectrom*. 2015;379:97–109. 2015. http://dx.doi.org/10.1016/j.ijms.2015.01.001.

50. Erickson MH, Gueneron M, Jobson BT. Measuring long chain alkanes in diesel engine exhaust by thermal desorption PTR-MS. *Atmos Meas Tech*. 2014;7:225–239. January 27, 2014. www.atmos-meas-tech.net/7/225/2014/. Accessed August 8, 2021.

51. Eichler CMA, Cao J, Isaacman-VanWertz G, Little JC. Modeling the formation and growth of organic films on indoor surfaces. *Indoor Air*. 2019;29:17–29.

52. Anderson PJ, Wilson JD, Hiller FC. Particle size distribution of mainstream tobacco and marijuana smoke. Analysis using the electrical aerosol analyzer. *Am Rev Respir Dis*. 1989;140:202–205. July 17, 1989. http://www.atsjournals.org/doi/abs/10.1164/ajrccm/140.1.202. Accessed June 26, 2021.

53. Sander R. Compilation of Henry's law constants (version 4.0) for water as solvent. *Atmos Chem Phys*. 2015;15:4399–4981.

54. Appel BR, Guirguis G, Kim IS, et al. Benzene, benzo(a)pyrene, and lead in smoke from tobacco products other than cigarettes. *Am J Public Health*. 1990;80:560–564. May 1990. /pmc/articles/PMC1404640/?report=abstract. Accessed June 24, 2021.

55. Ayer HE, Yeager DW. Irritants in cigarette smoke plumes. *Am J Public Health*. 1982;72:1283–1285. October 7, 1982. http://ajph.aphapublications.org/. Accessed July 15, 2021.

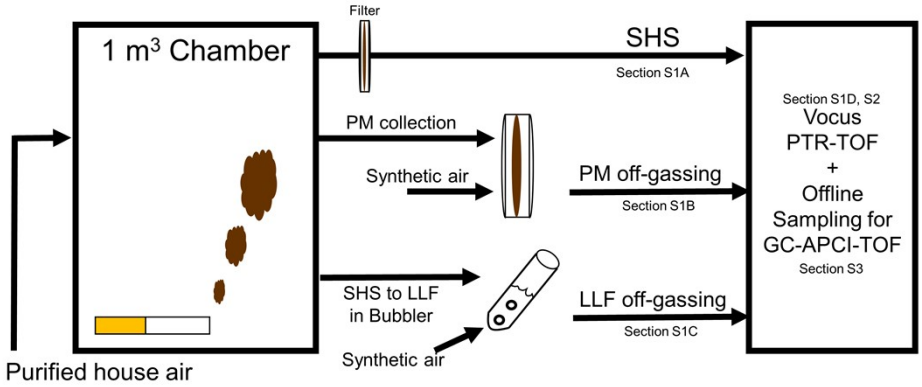

Figure S1. Generalized schematic for sample collection. Three different sets of experiments evaluated by the PTR-TOF: gas-phase secondhand smoke (SHS), PM off-gassing, and surrogate LLF off-gassing. Adsorbent tubes for each of these three sampling pathways were also collected for offline analysis. PM collection and SHS exposure to LLF occurred during cigarette combustion, and the passage of purified air through the filter or bubbler took place after the filter/bubbler was disconnected from the smoking chamber and connected to the PTR-TOF for data collection. More details for each method of sample collection and analysis have been provided for convenience elsewhere in the SI.

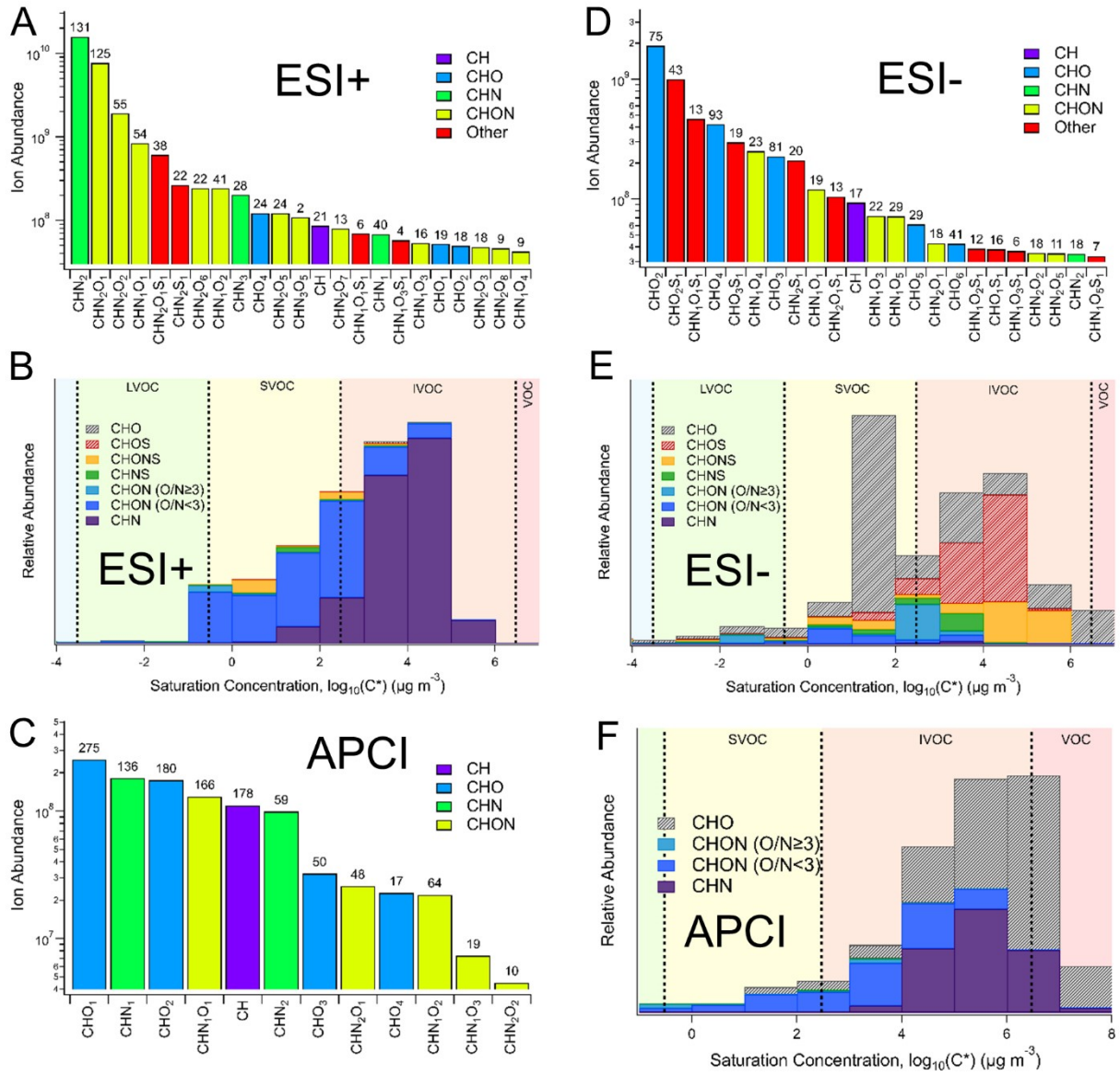

Figure S2. Elemental compositions and volatility distributions for aerosol- and gas-phase SHS samples. Elemental composition (A, D) and volatility (B, E) distributions in a non-targeted analysis of particle-phase organic compounds from combined LC-TOF results of fresh and off-gassed PM filters, with (A,D) showing the rank-ordered list of the most abundant compound formula types (number of observed formulas indicated above the bars) and the volatility distribution of all observed compounds that passed QA/QC [4]. Followed by the elemental composition distribution (C) for the most abundant formula types and volatility distribution (F) in the non-targeted gas-phase analysis (GC-TOF). Non-targeted analysis in (C, F) was run on gas-phase SHS samples to identify elemental compositions that cover the majority of species and ion abundance observed in the GC-TOF, and seven of the top eight elemental compositions shown in panel C (with the exception of CHO_3) were selected to be featured in Figure 2 of this manuscript.

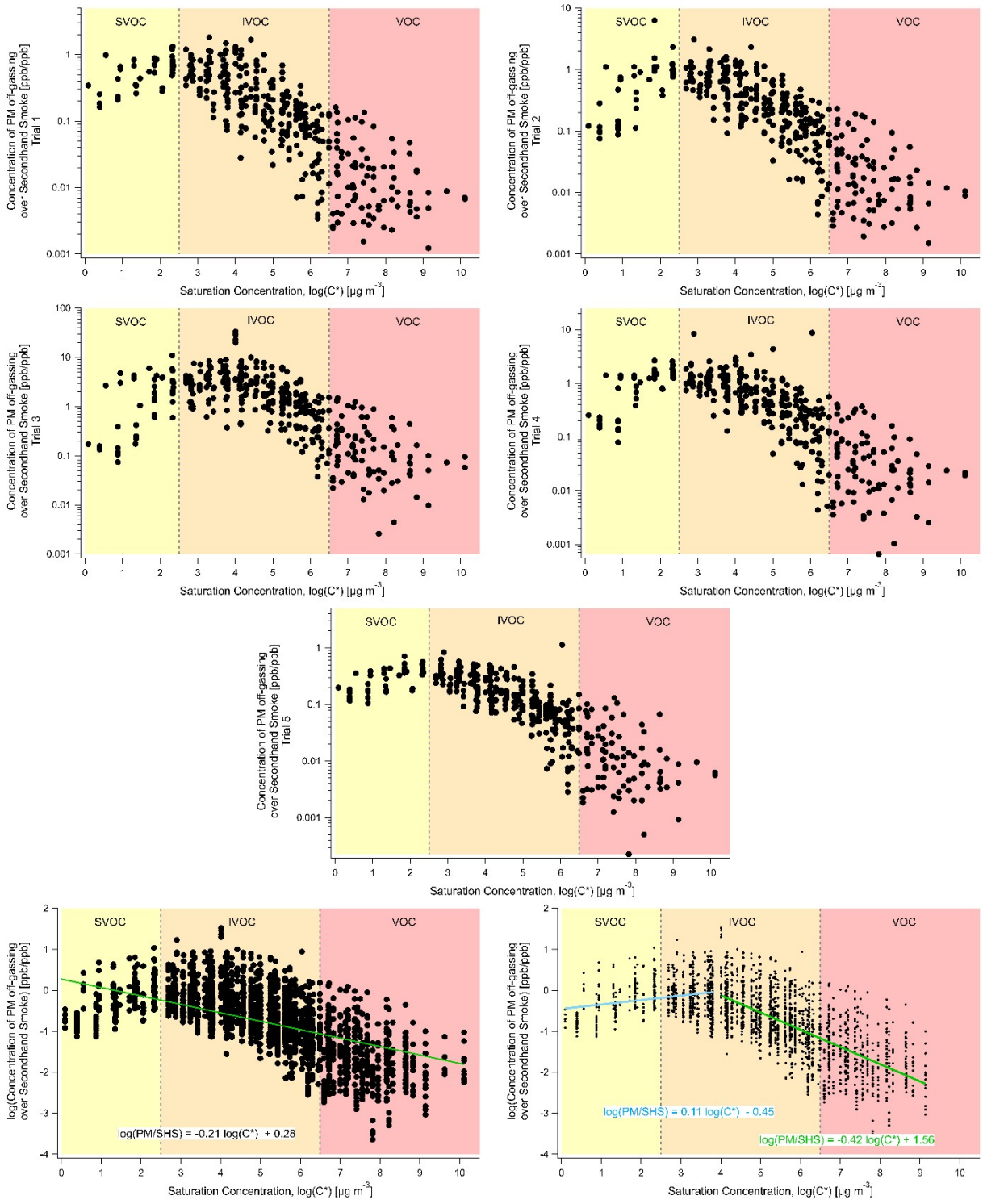

Figure S3. Ratio of fresh PM off-gassing over SHS concentrations vs. saturation concentration for gas-phase samples. The last two panels include points from all trials. In the last panel, a saturation concentration of log(C*) = 4 µg m^{-3} was used as the cut-off for the piecewise function. Select saturation concentrations on either end were truncated to avoid over-weighting. Data from PTR-TOF.

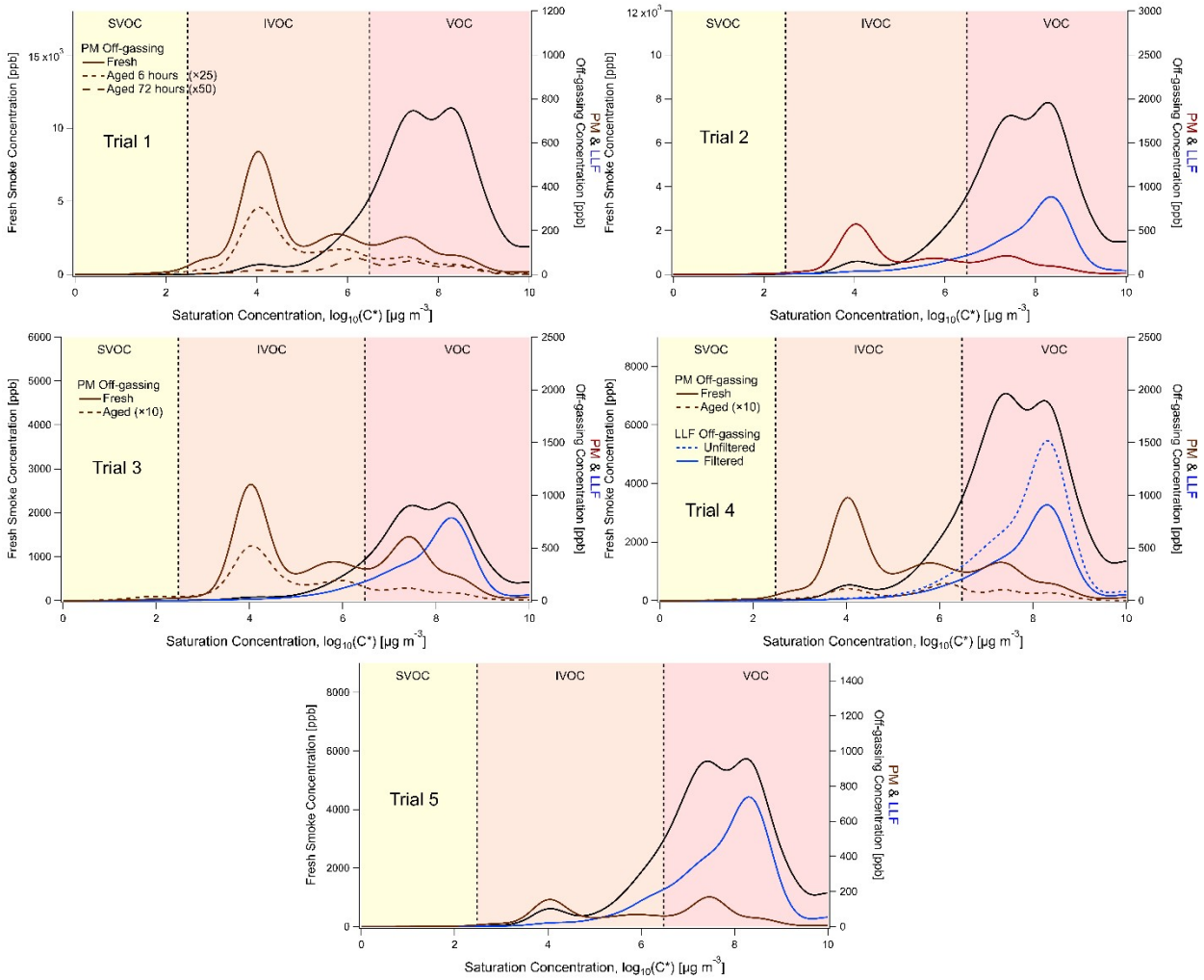

Figure S4. Volatility distributions from Trials 1–5, including data for secondhand smoke (black), PM off-gassing (brown), and LLF off-gassing (blue). These provide trial-specific data for the distributions shown in Figure 3A. A Gaussian distribution was used instead of bins to display the impact of prominent individual compounds (e.g, nicotine). For the purposes of graphical comparison, traces were adjusted by scaling factors as indicated with an (x10), (x25), or (x50). Data from PTR-TOF.

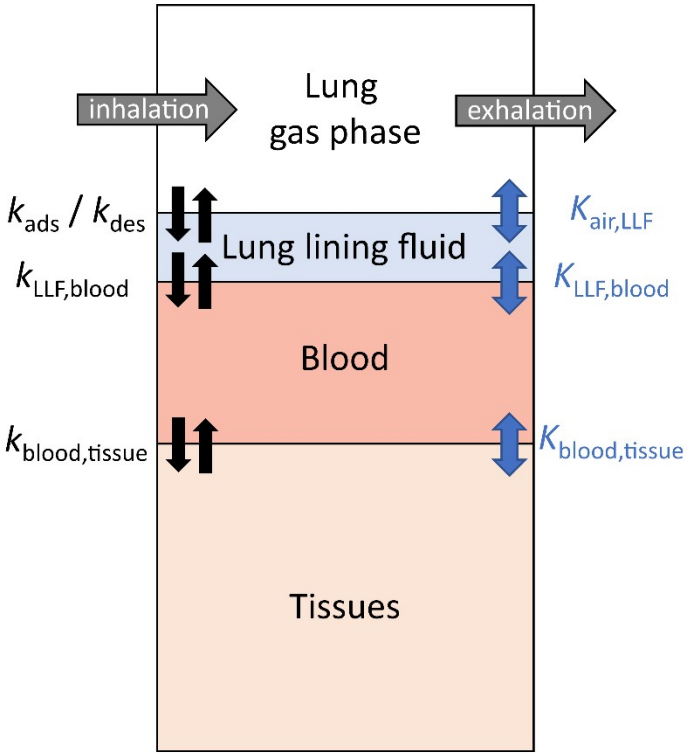

Figure S5. Multi-compartment model of transport of organic compounds in the body through inhalation. The flux between body compartments was treated with kinetic transport (black) and thermodynamic partitioning (blue) coefficients. Compartment sizes shown here are not an accurate depiction of relative volumes of these aqueous phases in the body. Transfer of lipophilic organic compounds from blood into adipose tissue can lead to greater persistence.

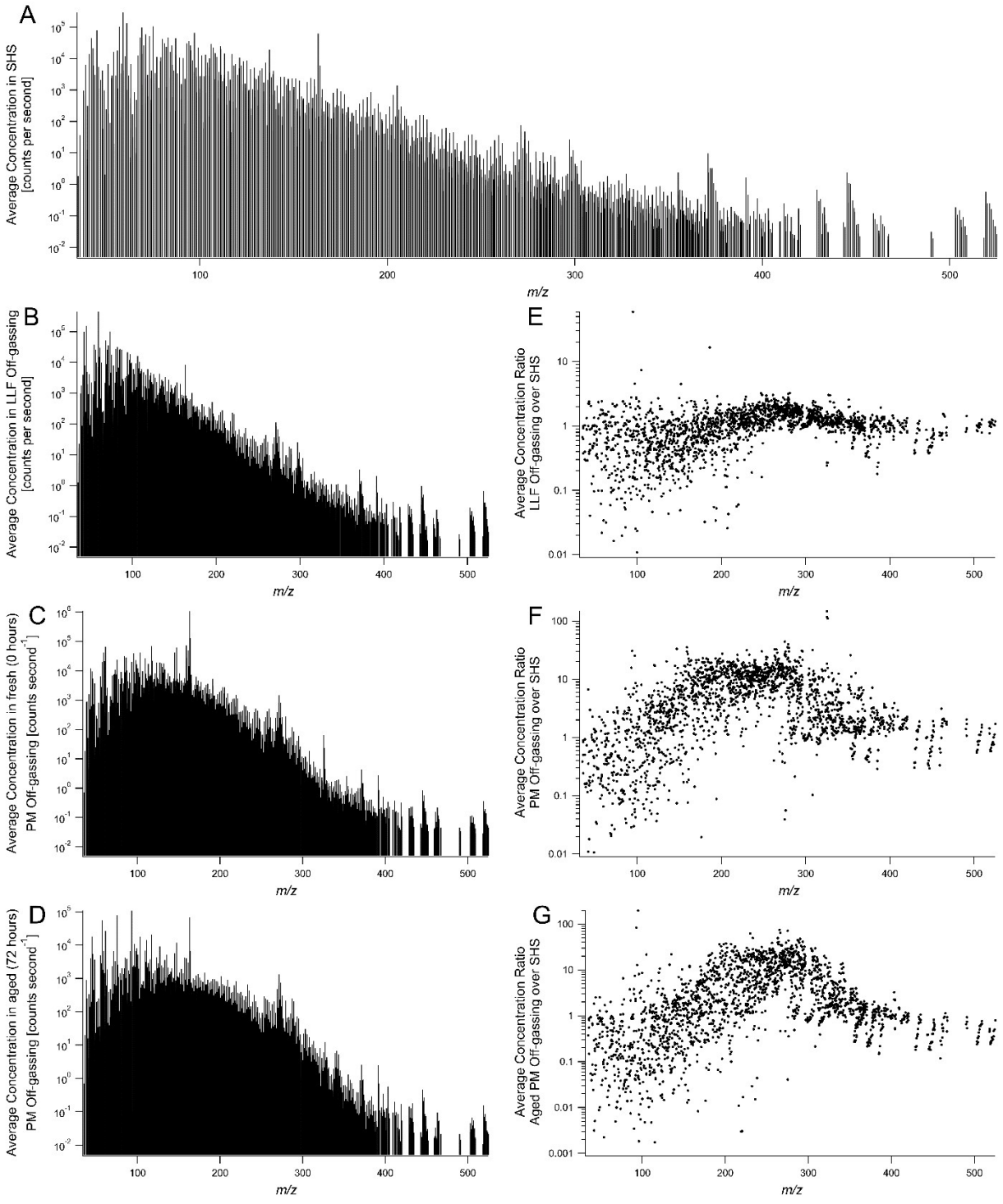

Figure S6. Average PTR-TOF spectra from (A) SHS, (B) LLF off-gassing, (C) fresh PM off-gassing, and (D) aged PM off-gassing, along with ratios to SHS for (E) LLF off-gassing, (F) fresh PM off-gassing, and (G) aged PM off-gassing. Data presented in A–D were prior to accounting for sub-sample dilution during PTR-TOF sampling, so abundances in E, F, G are intended to illustrate relative patterns, not absolute ratios. They show that the LLF off-gassing spectra distribution was generally consistent with secondhand smoke, while the PM off-gassing

had *m/z*-dependent (and by proxy, volatility-dependent) behavior. Aged PM off-gassing showed some small shift in *m/z* (F, G) relative to fresh PM off-gassing, though was still generally similar in terms of abundance (prior to accounting for dilution).

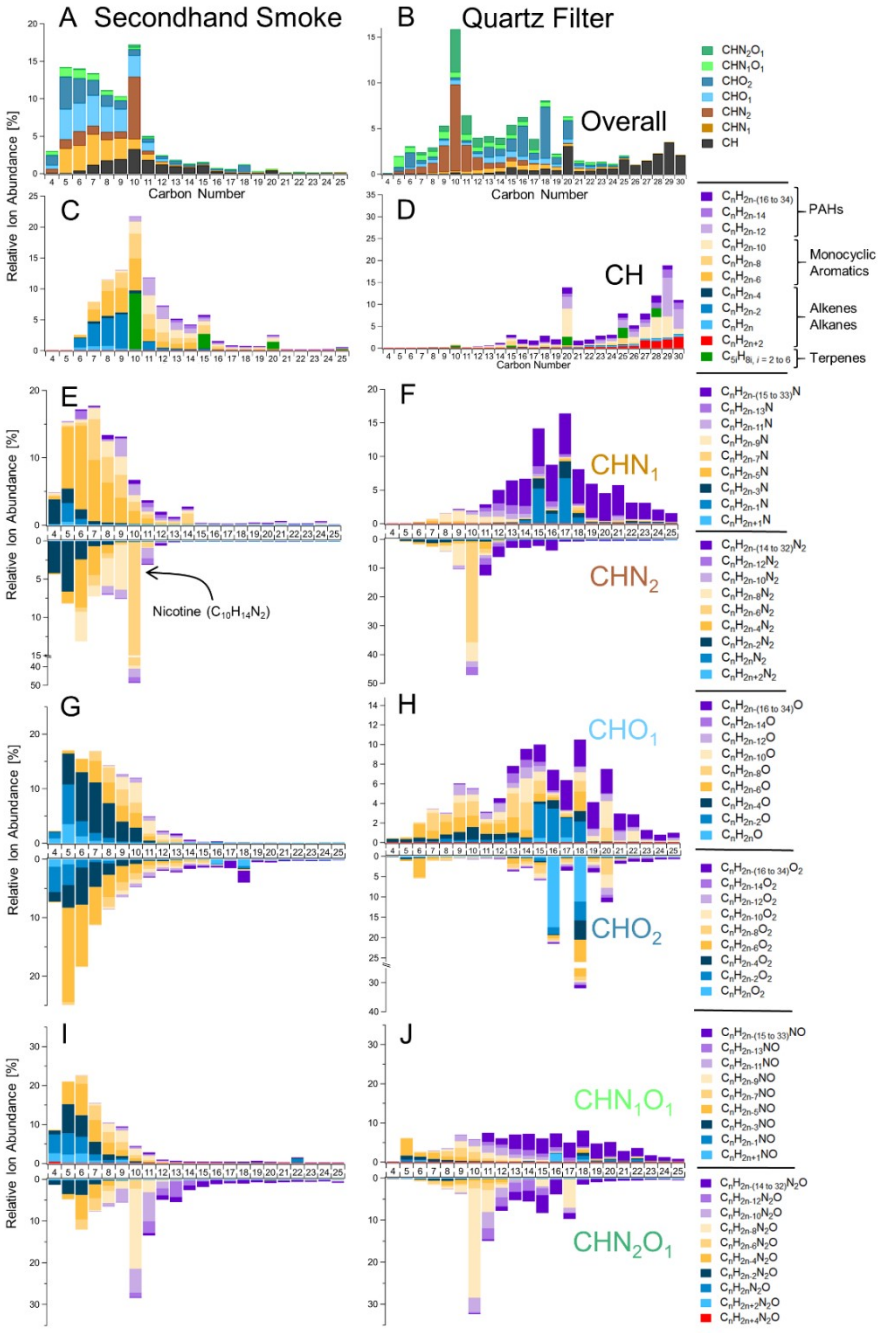

Figure S7. Secondhand smoke gas-phase and particle-phase chemical composition, provided to accompany chemical composition data in Figure 2 on PM and LLF off-gassing. Ion abundance data collected with GC-TOF for gas-phase SHS samples collected on adsorbent tubes (left) and particle-phase SHS samples on quartz filters via thermal desorption (right). Hydrocarbon data ranged from $C_{6\text{-}30}$, while other compounds ranged $C_{4\text{–}25}$. Contributions of aliphatic hydrocarbons (i.e., alkanes, alkenes) may be underestimated due to lower relative response factors, especially for lighter compounds. Note, some compound class distributions in the PM samples (Panels F upper, H upper, and J) have relatively low overall abundance.

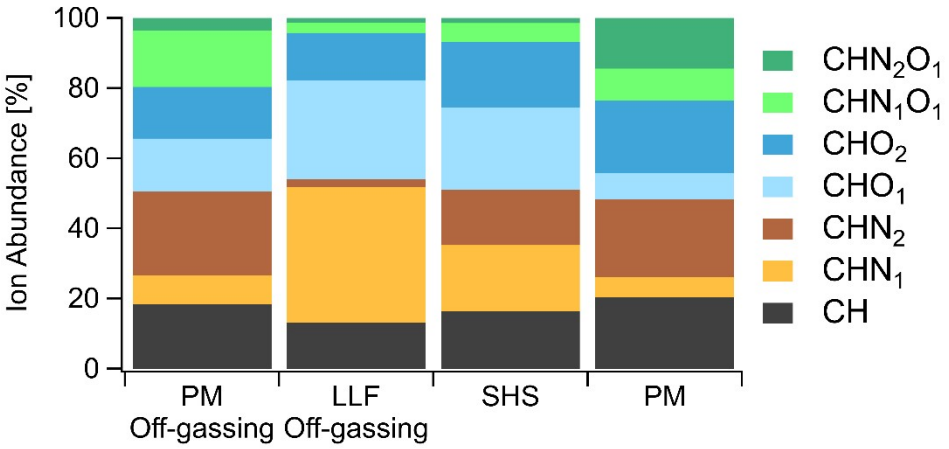

Figure S8. Distribution of compound classes across PM off-gassing, LLF off-gassing, SHS, and PM filter samples measured via GC-TOF. Arithmetic means were averaged across adsorbent tube samples and filters to accompany Figures 1C and 1D, with sample sizes of *N*=4 for PM off-gassing, *N*=3 for LLF off-gassing, *N*=4 for SHS, and *N*=3 for PM. For further breakdowns, see Figures 2 and S2, and for numeric data, see Table 1.

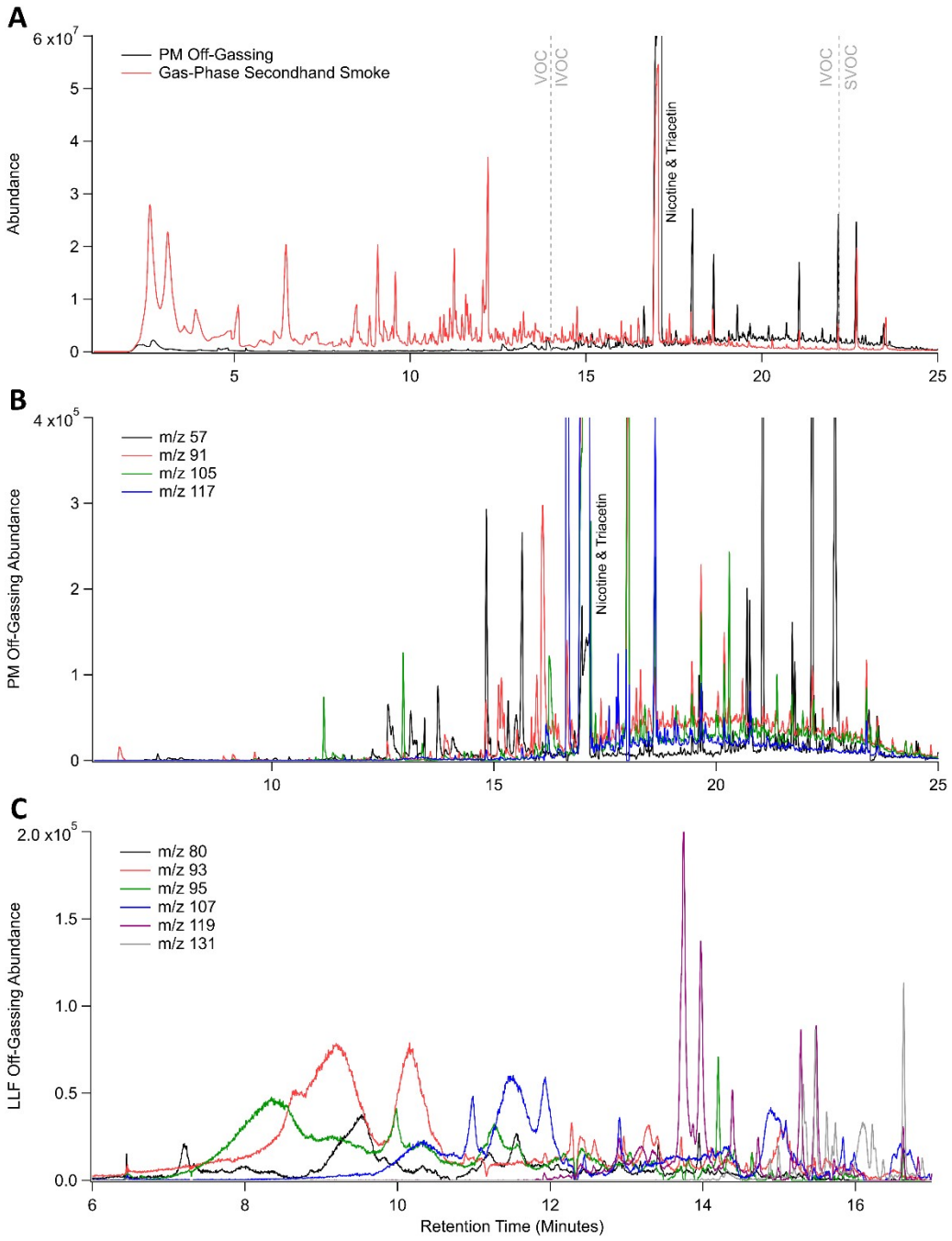

Figure S9. Traditional GC-EIMS chromatogram data. PM off-gassing in panel B is shown with a selection of extracted ion chromatograms to supplement the GC-TOF data in Figure 2, including contributions from typical compound groups for *m/z* 57 (e.g., linear/branched alkanes), *m/z* 91 (e.g., single-ring aromatics), *m/z* 105 (e.g., single-ring aromatics), and *m/z* 117 (e.g., alkylindanes, single-ring aromatics with unsaturated alkyl groups). LLF off-gassing is shown with a selection of extracted ion chromatograms that focus on oxygen- and nitrogen-containing compounds, with *m/z* 80 (incl. alkyl-pyrroles), *m/z* 93 (incl. alkyl-pyridines), *m/z* 95 (incl. furans, alkyl-pyrroles), *m/z* 107 (incl. alkyl-phenols (e.g., cresols), alkyl-pyridines), *m/z* 119 (incl.

methyl-benzaldehydes), and *m/z* 131 (e.g., alkyl-benzofurans). It should be noted that the *m/z*'s chosen are often not unique to isolated compound classes when present in complex mixtures and are included here as supporting GC-EI-MS data, with primary speciation done via GC-TOF (e.g., Figure 2).

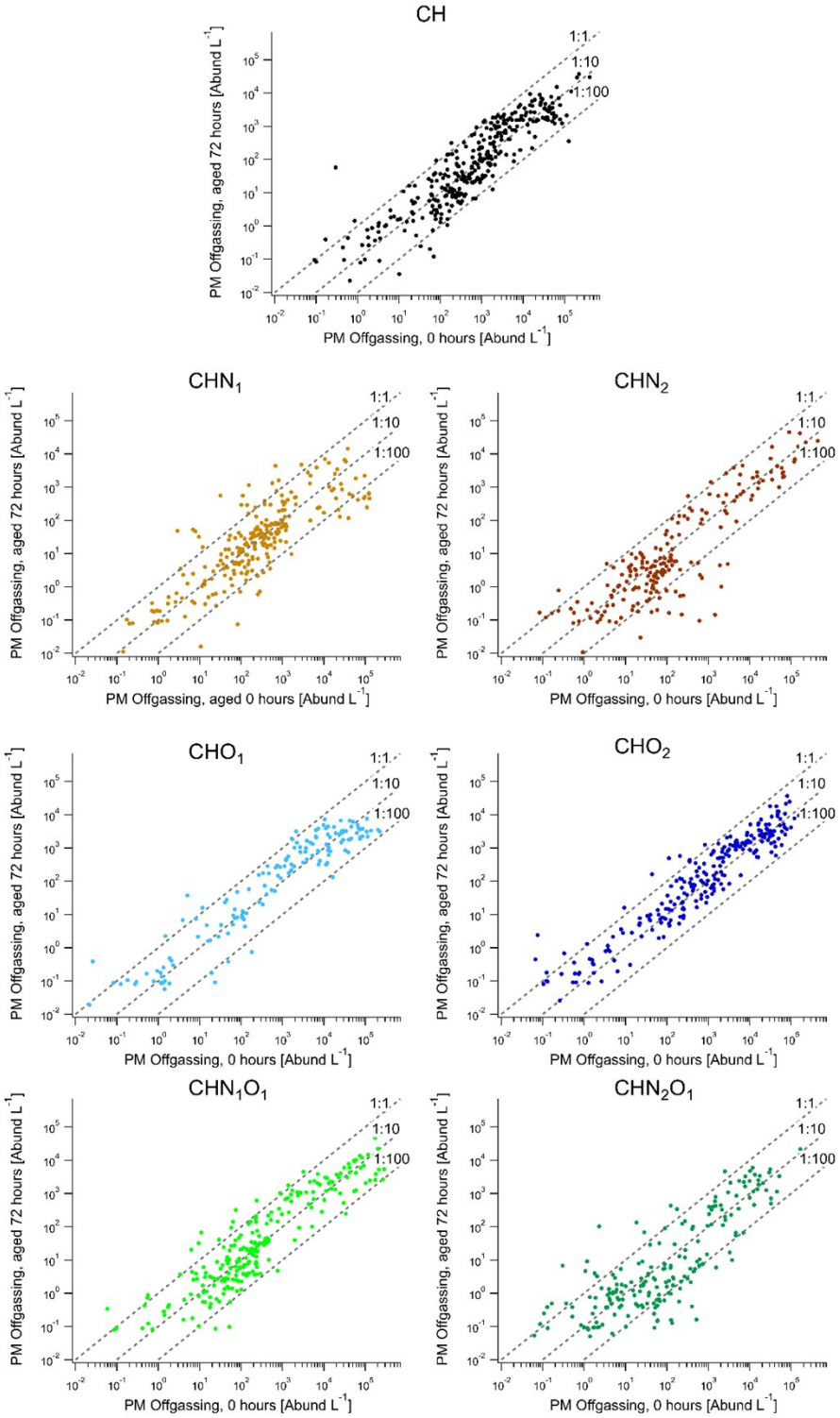

Figure S10A. Log-log comparison of normalized abundances for aged (72 h; y-axis) vs. PM off-gassing after 10 min (x-axis) across elemental types. In all of the panels, the top dashed line is 1:1, while the other dashed lines denote 1:10 and 1:100 ratios.

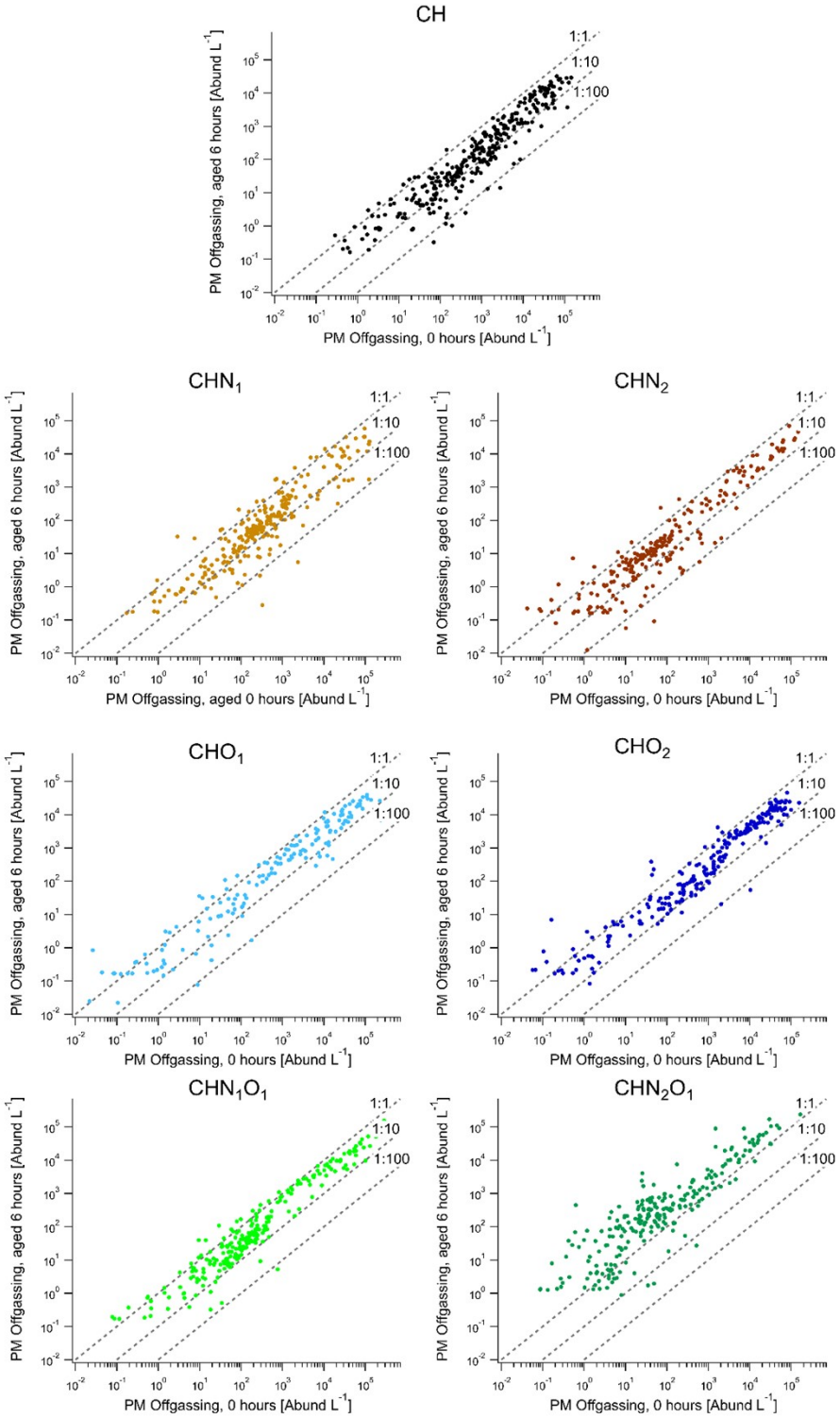

Figure S10B. Log-log comparison of normalized abundances for slightly aged (6 hr; y-axis) vs. PM off-gassing after 10 min (x-axis) across elemental types. In all of the panels, the top dashed line is 1:1, while the other dashed lines denote 1:10 and 1:100 ratios.

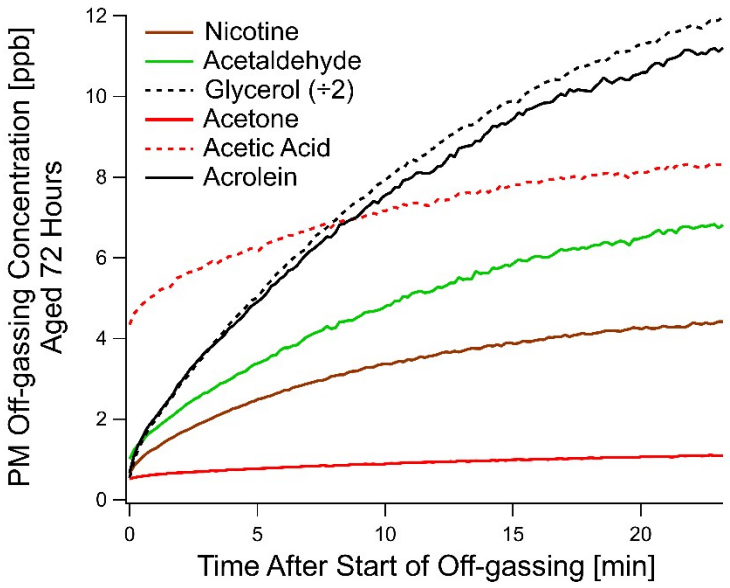

Figure S11. The evolution of PM off-gassing as PM ages. The gradual increase in concentration for the off-gassing from PM in the PTR-TOF setup after being aged 72 hours. This time series provides a contrast to the time series in Figure 1A. The concentration increases monotonically for the 72 hour aged PM off-gassing, while the fresh PM drops off somewhat substantially initially for most compounds.

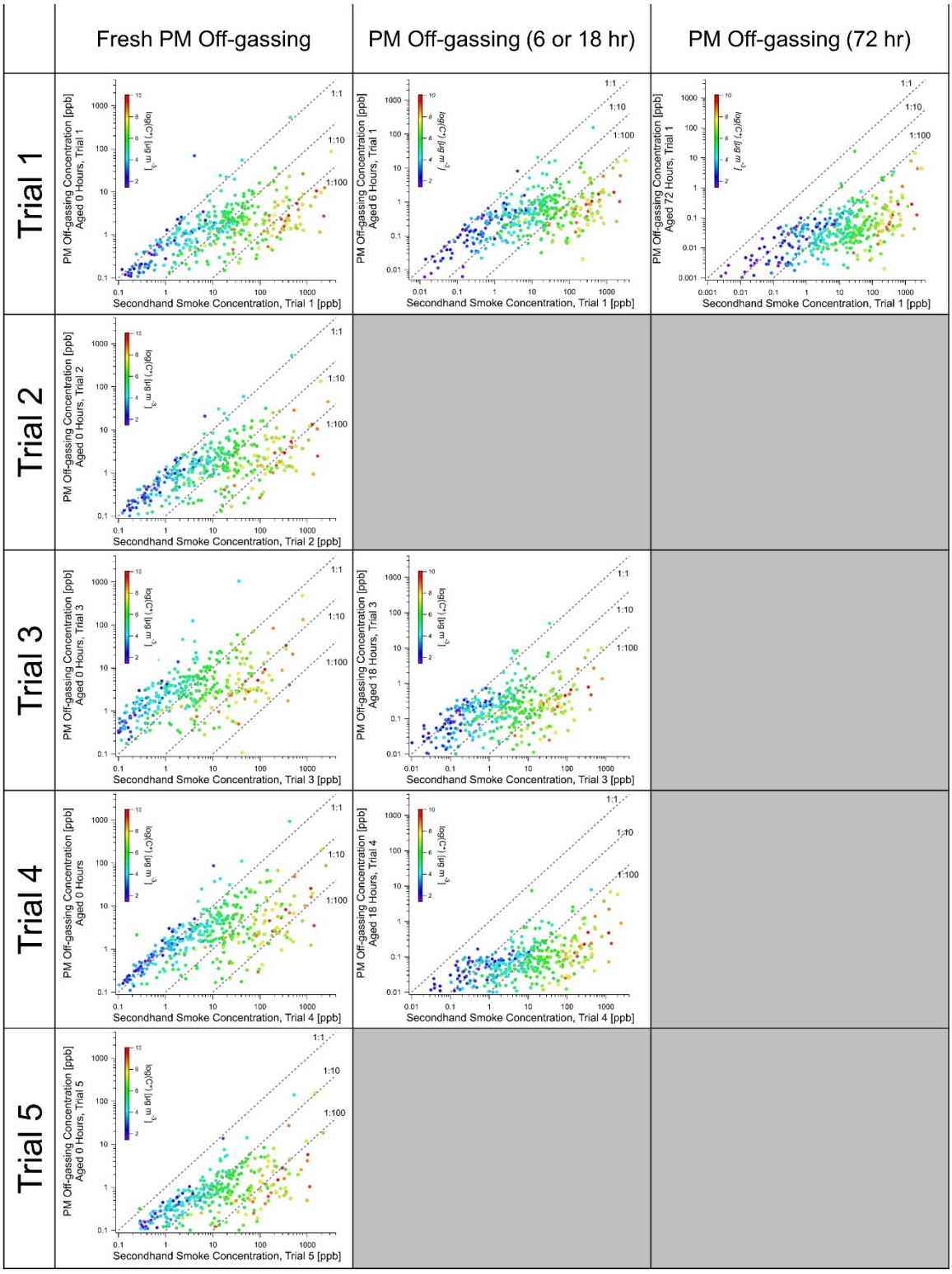

Figure S12. Scatterplots of compound concentrations comparing PM off-gassing to gas-phase SHS for all trials. Data from PTR-TOF.

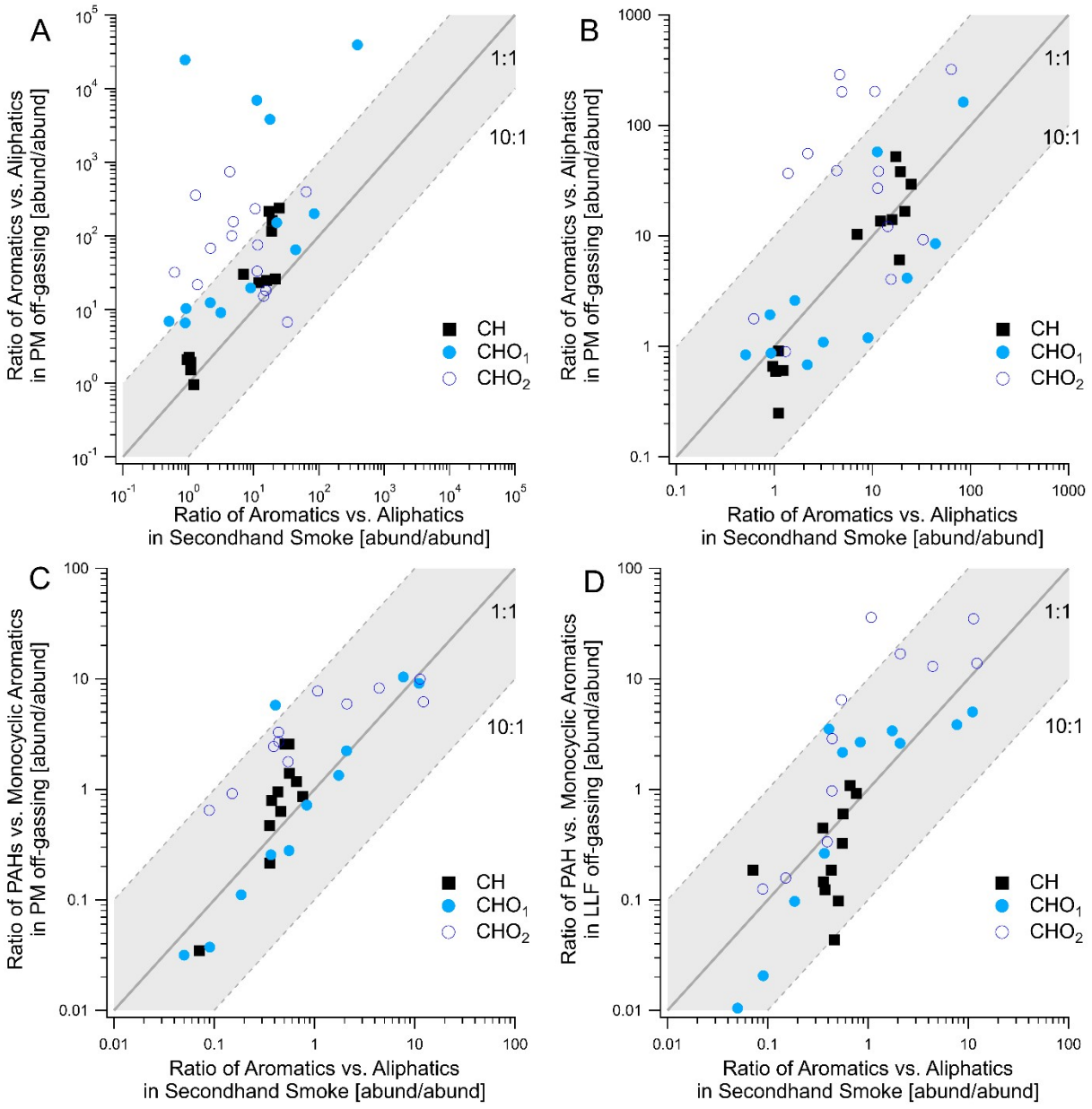

Figure S13. Comparison of compound class ratios in THS vs. SHS. Ratios of compound classes are shown for each carbon number point for hydrocarbons and oxygenated compounds based on molecular formulas measured by GC-TOF. (A, B) All aromatic formulas (DBE 4–15) vs. aliphatics (DBE 0–3; i.e., alkanes, alkenes) and (C, D) PAC-related formulas (DBE 7–15) vs. monocyclic aromatics (DBE 4–6), shown for PM off-gassing vs. SHS in (A, C) and LLF off-gassing vs. SHS in (B, D). The plots show that while LLF off-gassing does not exhibit any trends, PM off-gassing shows distinct aromatic enhancements in (A) for most, but not all carbon numbers, and suggests PAC enhancements in (C) for some CH and CHO_2 compounds. Only $C_{8–20}$ hydrocarbons and $C_{7–20}$ oxygenated compounds were included to avoid the relatively low abundances at either carbon number extreme that could skew some ratios and interpretations. Data from GC-TOF, using the slightly-aged samples after initial off-gassing into PTR-TOF.

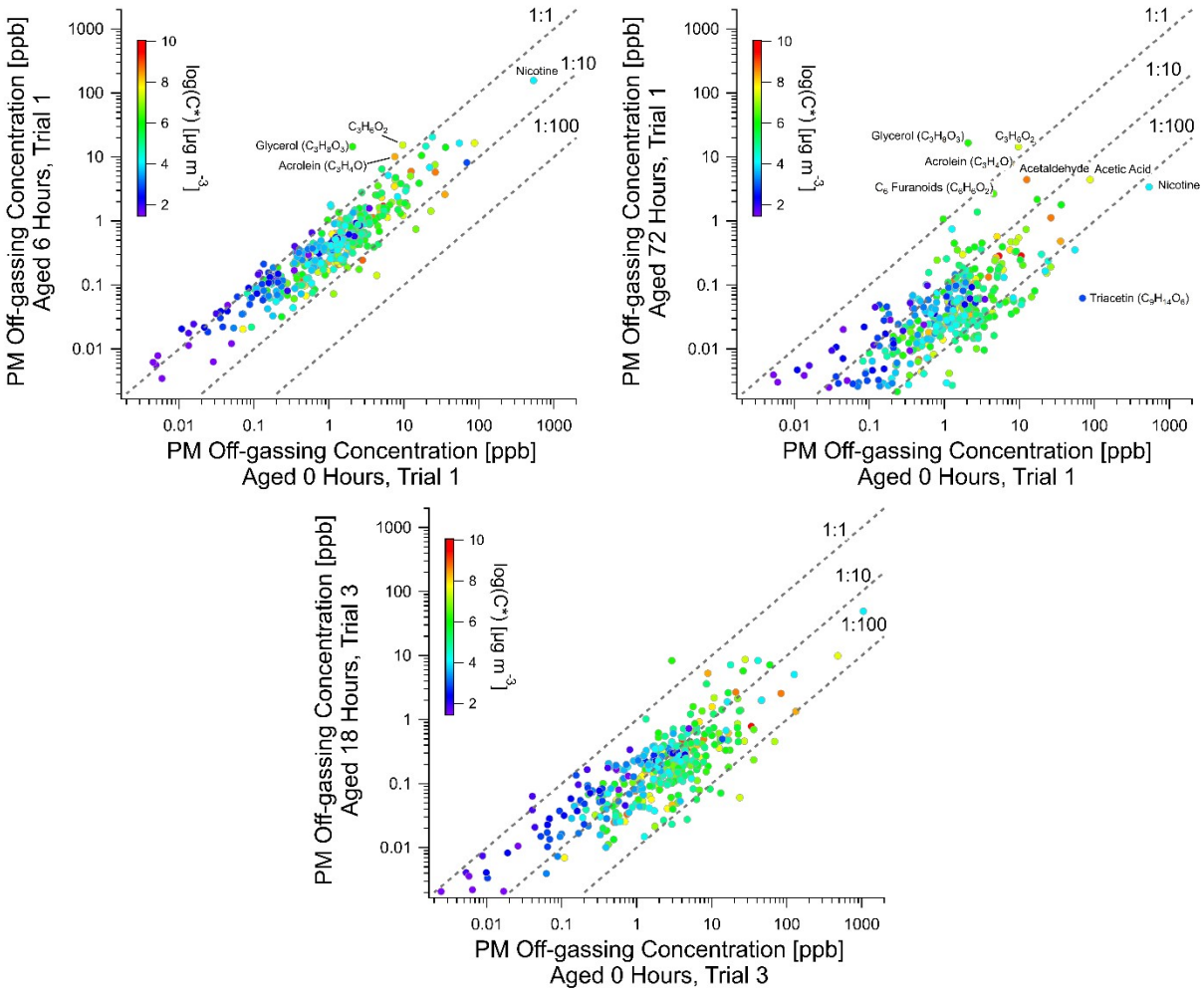

Figure S14. Scatterplots of compound concentrations from aged vs. fresh PM off-gassing experiments within individual trials. Points are colored by saturation concentration. We note reduced concentrations with longer aging. Data from PTR-TOF for experiments with PM off-gassing checked at multiple ages.

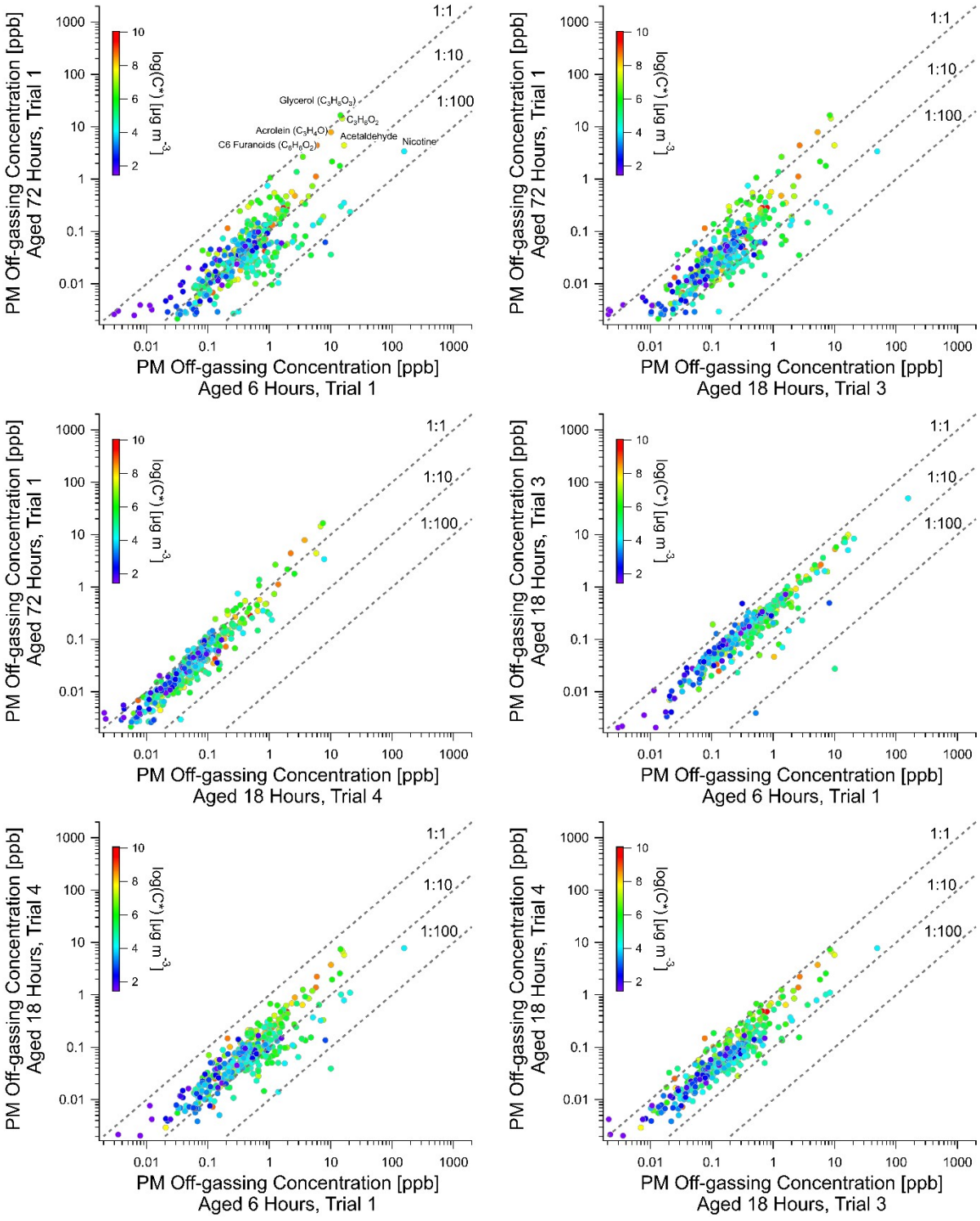

Figure S15. Scatterplots of compound concentrations from PM off-gassing experiments for various PM off-gassing ages, across different trials. Data from PTR-TOF.

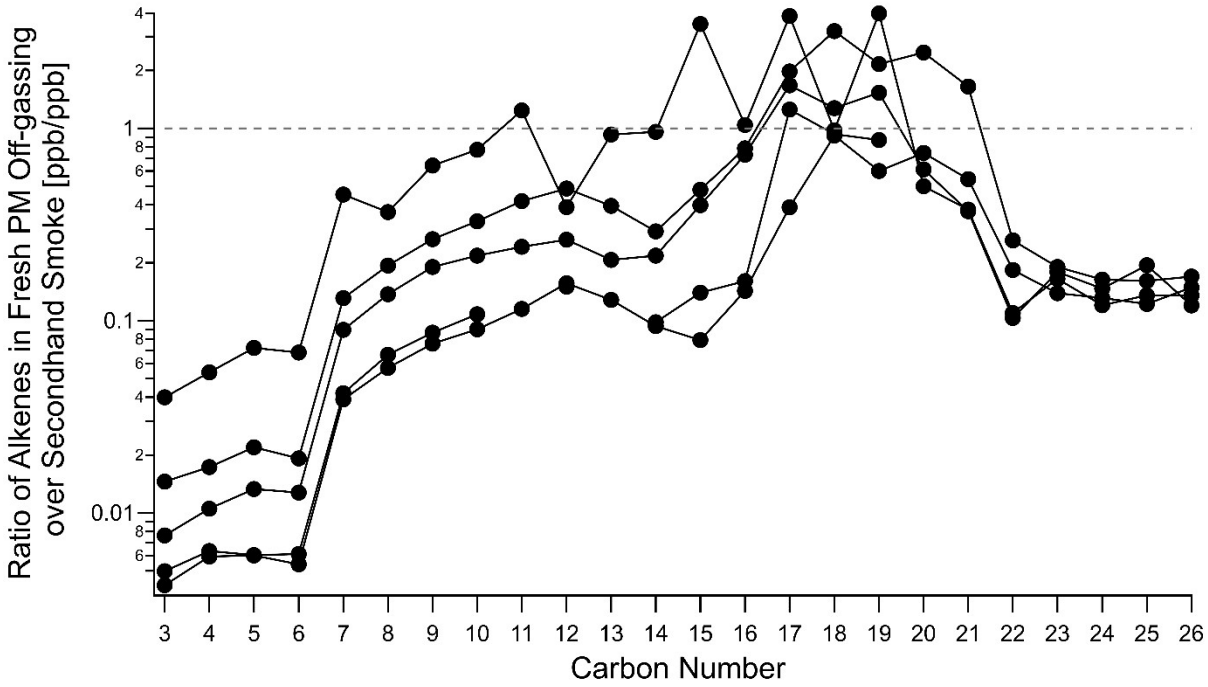

Figure S16. Comparison of PM off-gassing over SHS ratios by carbon number for acyclic alkene formulas (i.e., C_nH_{2n}, e.g., 1-tetradecene) in PTR-TOF data. Data for each alkene's formula may include other species, including fragments from larger alkyl chains that could affect observed alkene abundances, especially for smaller species. The alkenes shown here include only acyclic (e.g., linear/branched) alkenes, which have larger enhancement ratios in PM off-gassing vs. SHS but comprise a smaller fraction of PM off-gassing concentrations than DBE 2-3 alkene formulas (e.g., dienes, cyclic alkenes), which have greater concentrations with generally lower concentration enhancements in PM off-gassing vs. SHS (Table S3). We note that the observed formulas attributable to $C_{3–18}$ alkenes in the PTR-TOF data are more likely than cycloalkanes with the same formula since alkenes are generally more sensitive to PTR ionization.[49] Lighter masses might also contain contributions from neutral water loss by-products or from smaller fragments of larger alkanes.[49,50]

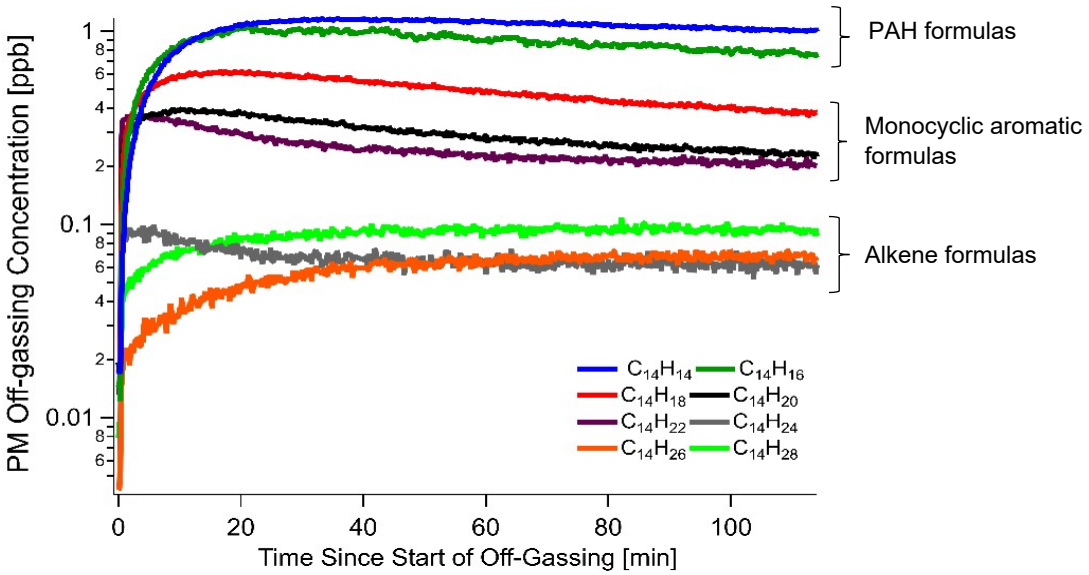

Figure S17. Comparison of non-aromatic, monocyclic aromatic, and polycyclic aromatic compounds in online PM off-gassing data. Comparison of hydrocarbon formulas at various DBEs for C_{14} hydrocarbons (located near the middle of the PM off-gassing volatility distribution) with online PTR-TOF data from Trial 5. Results demonstrate the prevalence of PAH and monocyclic aromatic compound formulas (similar to offline GC-TOF observations, e.g., Figure 2C), as well as variations in the shape of the initial off-gassing curve that can be compared to nicotine, which has a similar volatility.

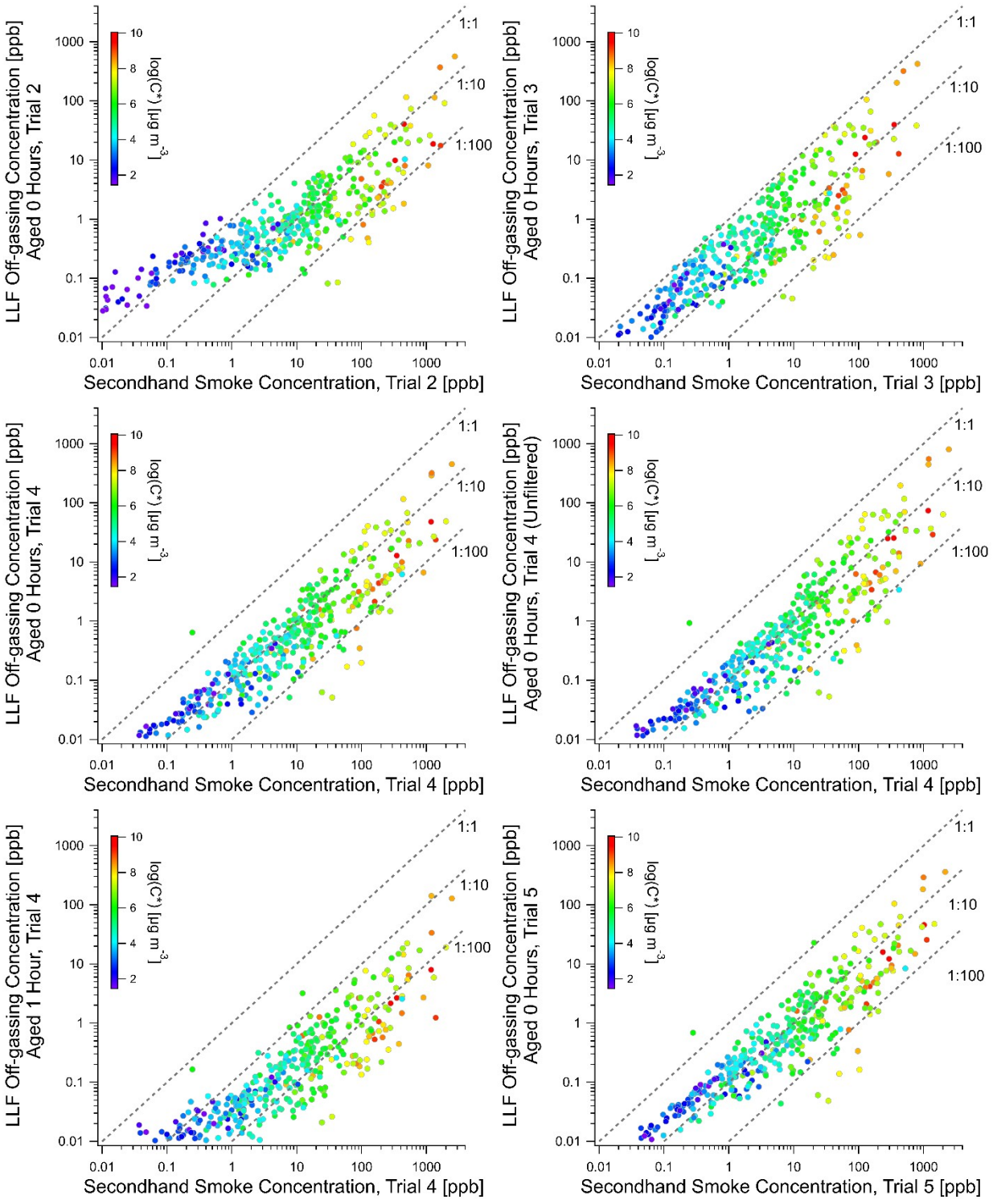

Figure S18. Scatterplots of compound concentrations comparing LLF off-gassing to gas-phase SHS across different trials. Data from PTR-TOF.

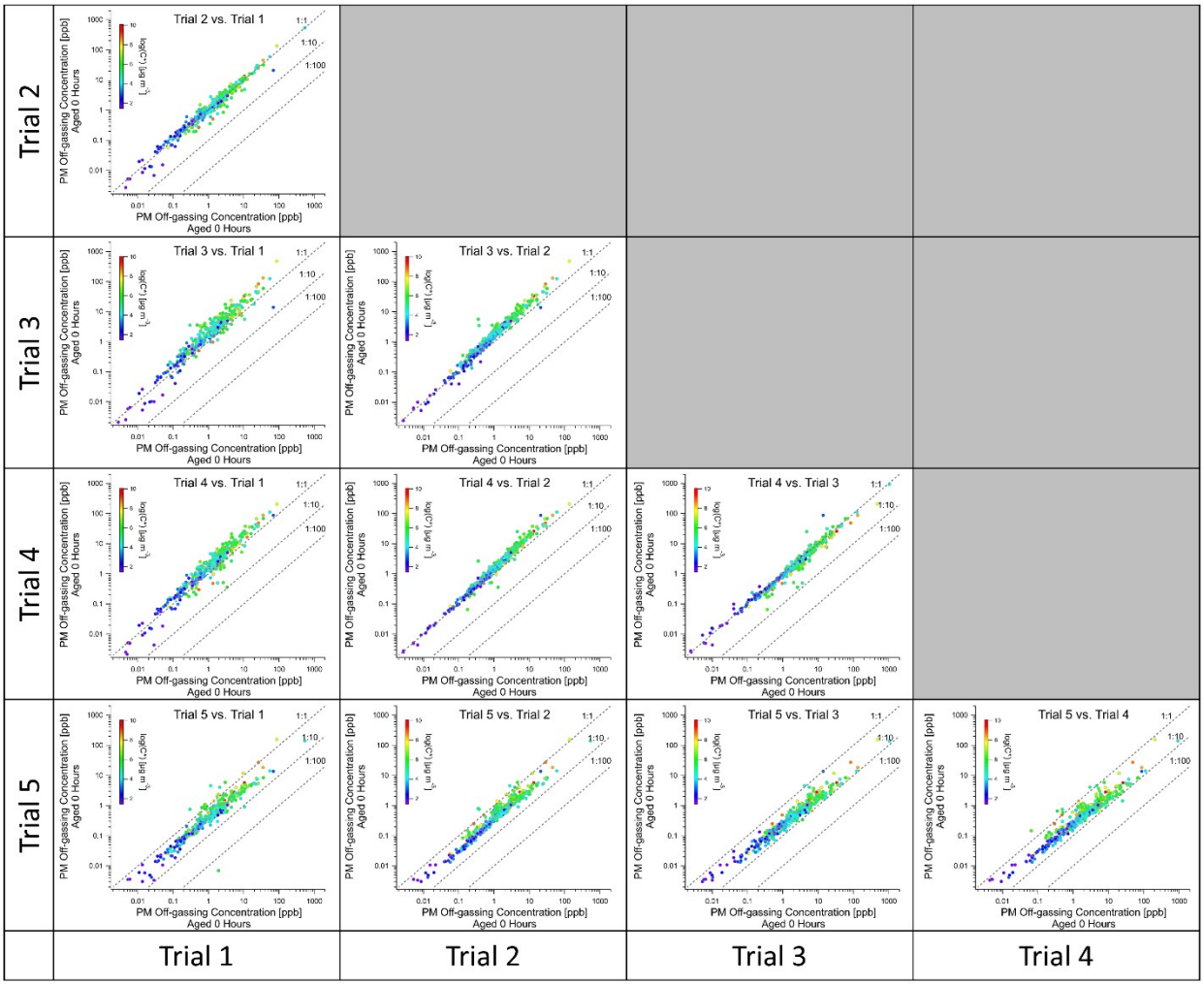

Figure S19. Scatterplots of compound concentrations from fresh PM off-gassing experiments, compared across trials. Data from PTR-TOF.

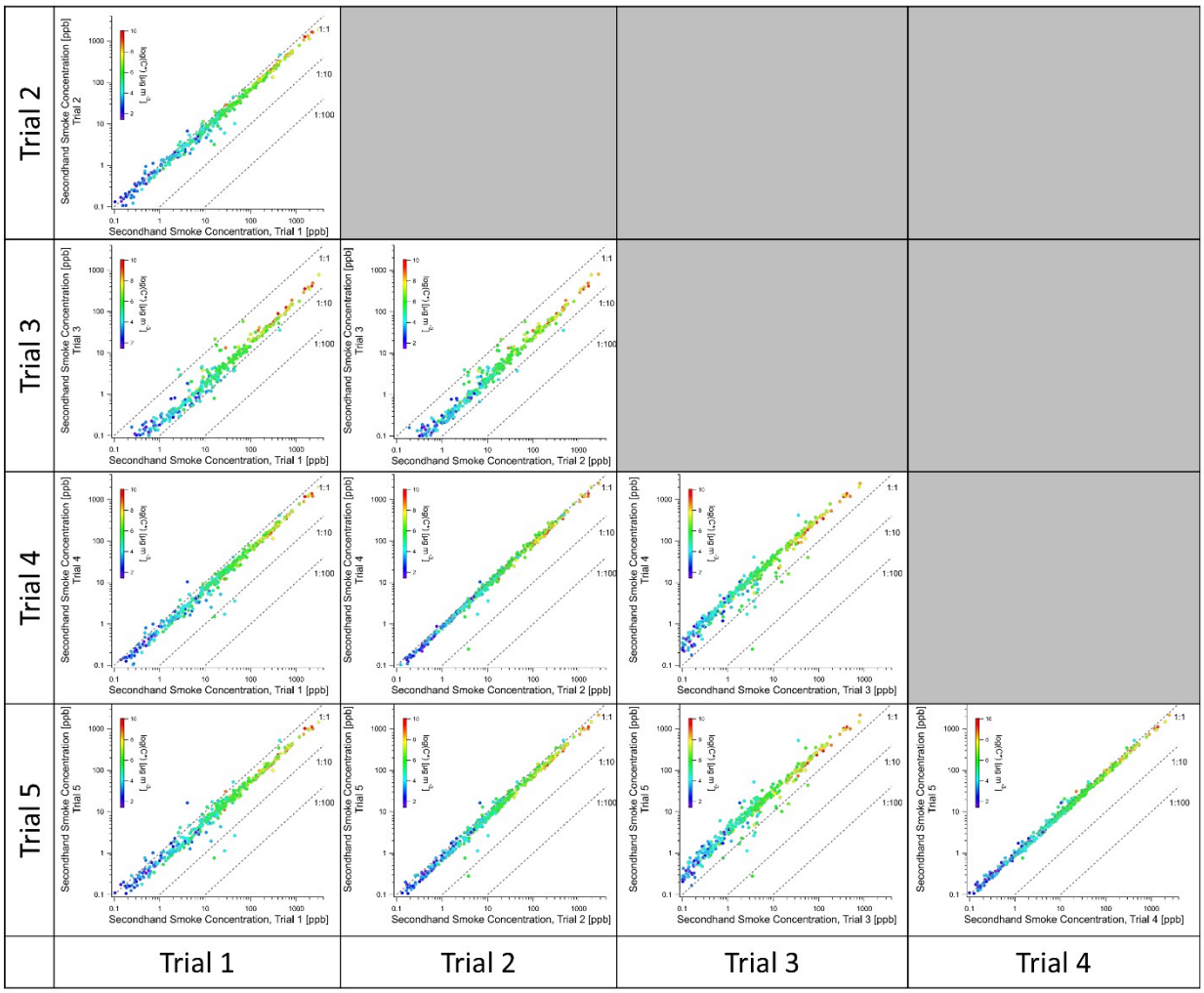

Figure S20. Gas-phase secondhand smoke concentration distributions across different trials. Data from PTR-TOF.

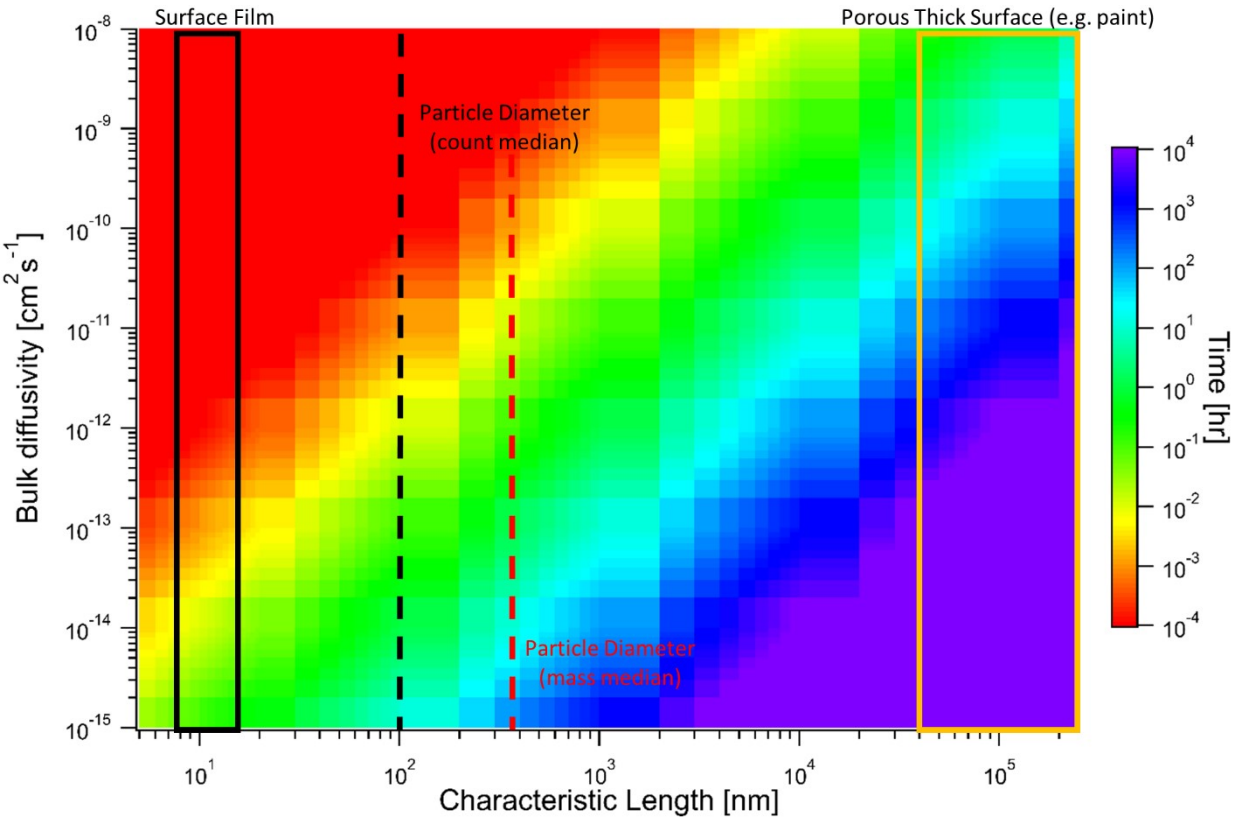

Figure S21. Modeled timescales for equilibrium partitioning to/from surfaces or particles. A longer characteristic length represents the possibility of compound diffusion through thick layers (e.g., paint). These calculations only take into account the timescale for diffusion through a bulk/surface (see *Methods*). Characteristic lengths were also indicated for surface films (8–15 nm; black box),[28,51] particles (100 nm (count median) and 380 nm (mass median)[52] with black and red dashed lines, respectively), and thick surface layers (40–250 μm; orange box).[27] See Section S4 for an explanation of equilibrium timescale calculations.

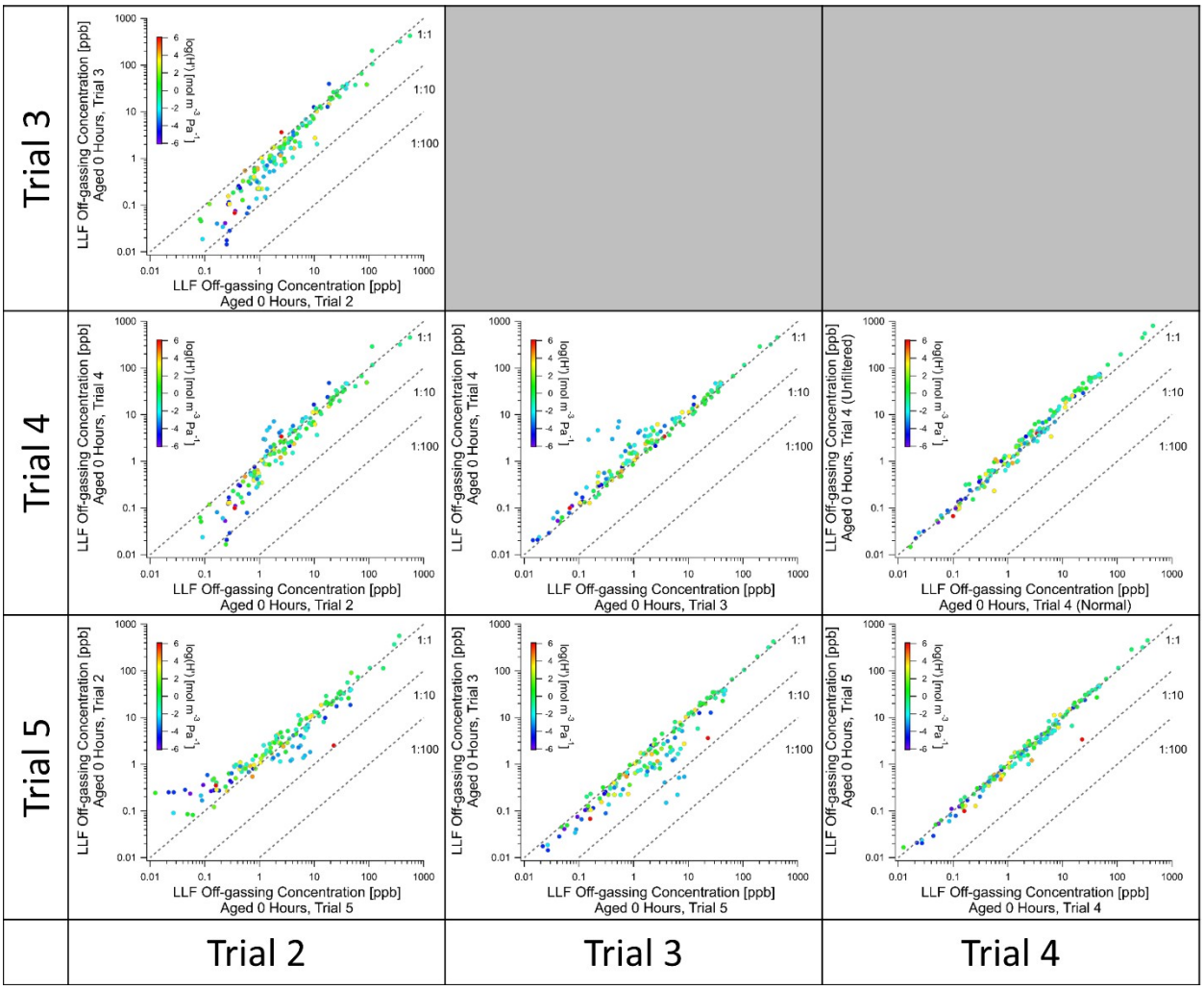

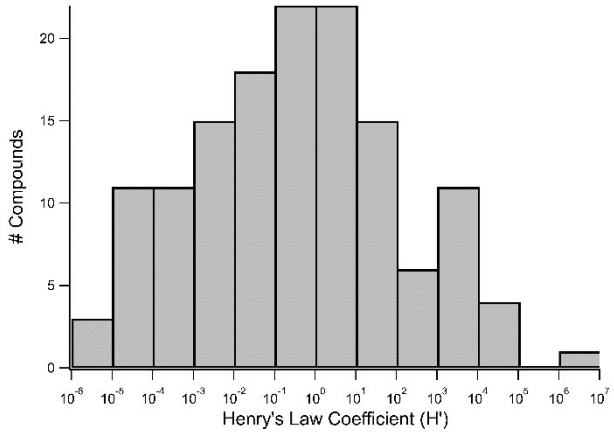

Figure S22. Scatterplots of compound concentrations comparing fresh LLF off-gassing experiments across different trials and the distribution of the compounds observed in PTR-TOF data as binned by Henry's law constant. Values for Henry's law constant from Sander et al.[53] Data from PTR-TOF.

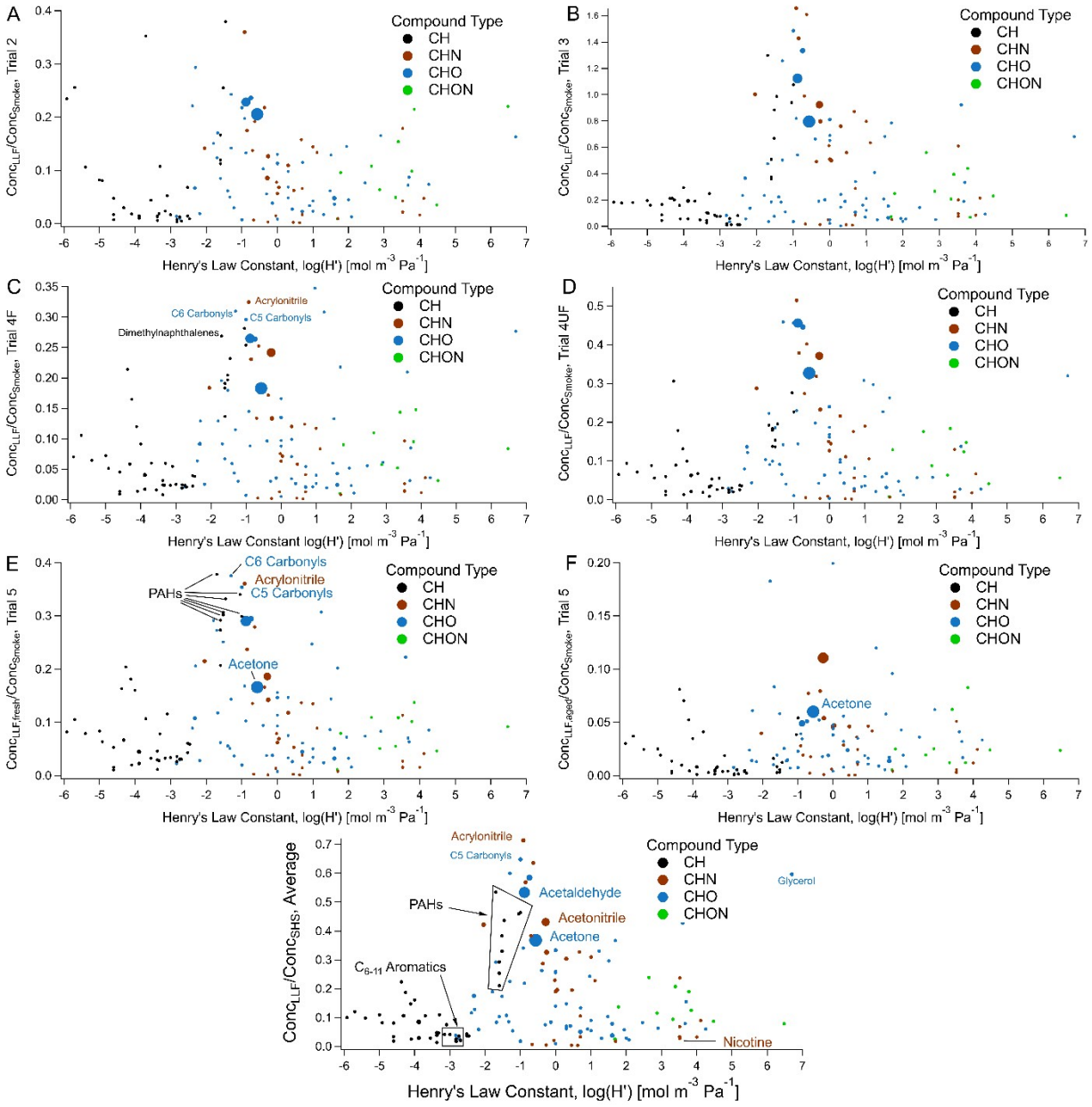

Figure S23. Comparison of $Conc_{LLF}/Conc_{Smoke}$ vs. Henry's law constant for individual trials (fresh, A–E; aged, F) and the average of the fresh trials (G). Concentration ratios for the last two panels were calculated by averaging LLF off-gassing concentrations during the 0–20 (fresh, bottom left) and 60–80 (aged, bottom right) minute intervals. In the bottom two panels, markers for each compound are sized based on their concentration in LLF off-gassing. Data from PTR-TOF.

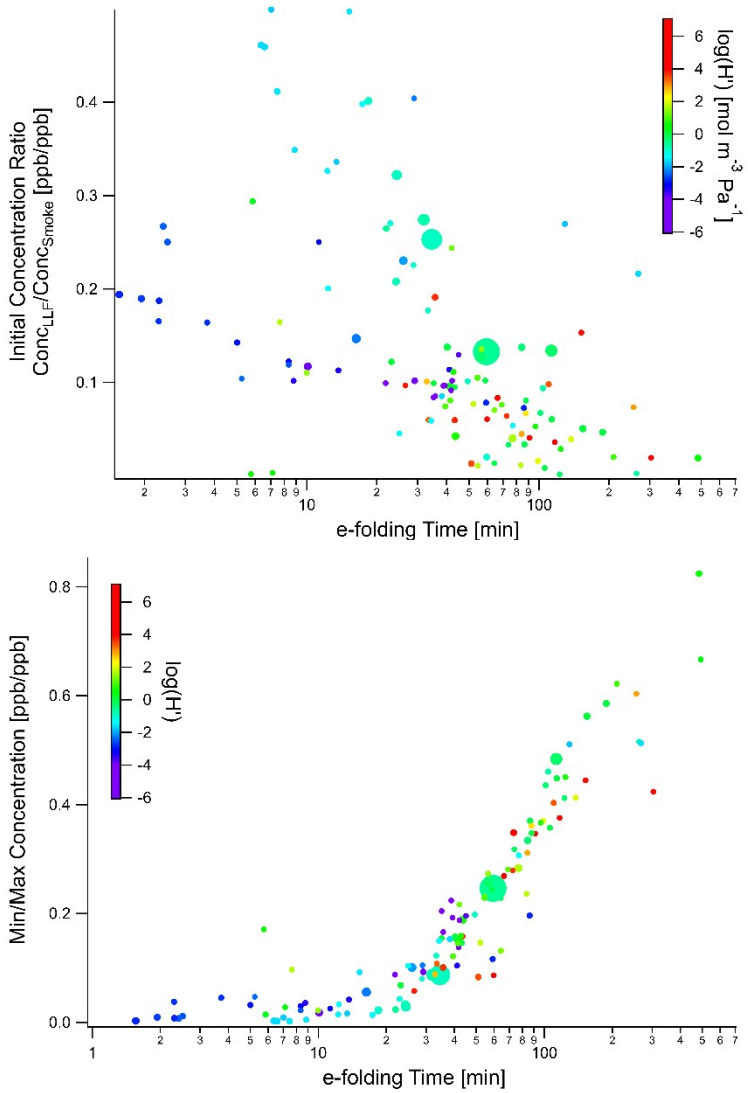

Figure S24. Persistence of compounds from LLF off-gassing lab experiments by residence time. Residence times (i.e., e-folding times) were calculated via an exponential fit on the LLF off-gassing time series (Trial 5). The exponential fit also takes into account the likely elevated concentration baseline these compounds can exhibit after initial off-gassing. A large majority of compounds have a positive "steady state" concentration as fit by the exponential function, though certain prominent compounds, such as acetaldehyde, acetone, and acetonitrile, would likely stabilize if a longer duration of time were sampled, also implying that their decay may be best fit by a multi-exponential process. For most of the compounds, their minimum concentrations (bottom panel) came at the end of the 80 minute sampling time, while their maximum concentrations came at the beginning of sampling. Thus, the trend seen here would be expected, since a factor increase in e-folding time would lead to exponentially slower concentration decay. Data from PTR-TOF.

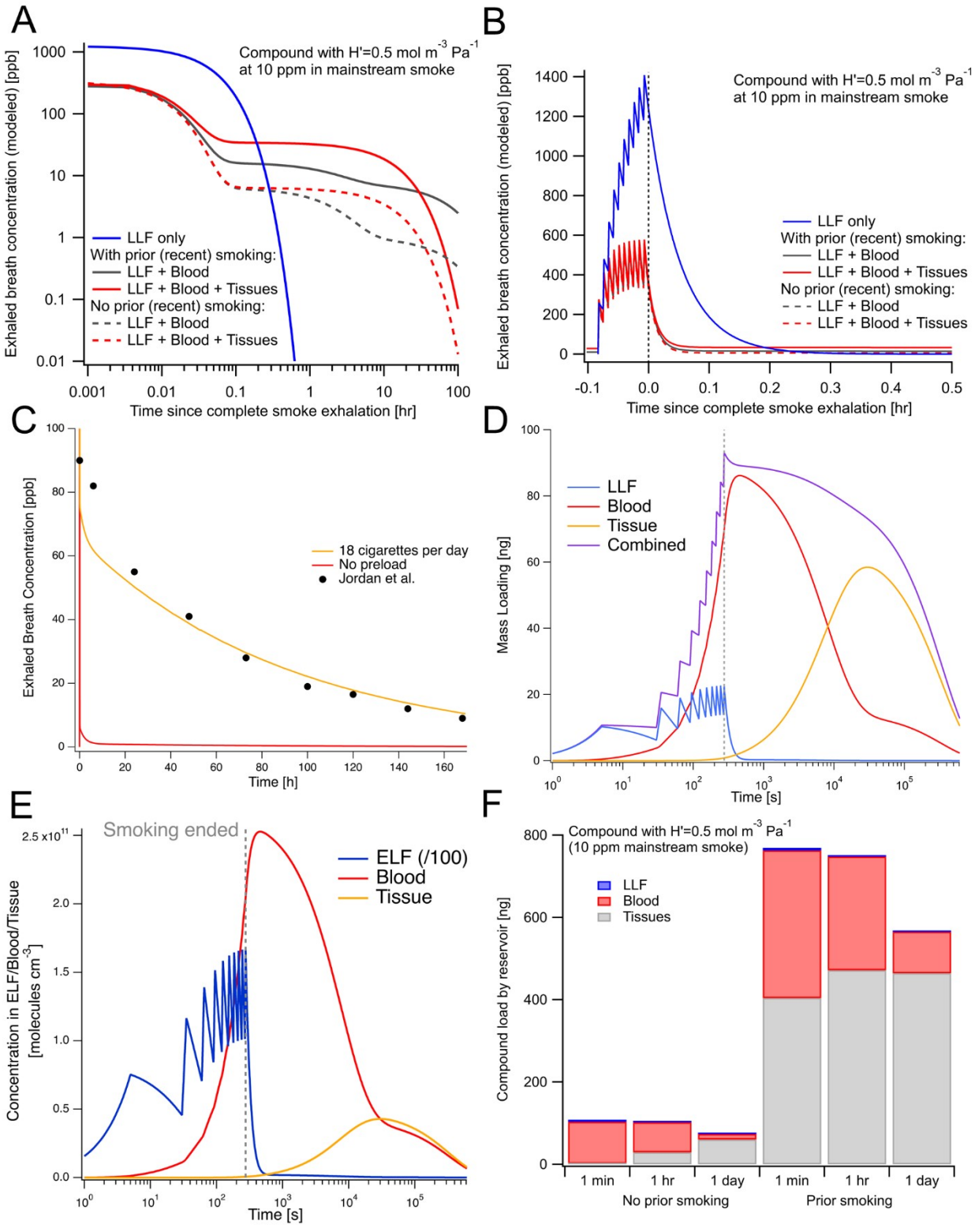

Figure S25: Evaluating THS uptake and off-gassing from bodily reservoirs via multi-compartment modeling, including the role of prior smoking, and model QA/QC. (A) Log-log plot showing dynamics with multi-compartment modeling as indicated in legend, shown with

and without prior smoking (8 cigarettes total, 1 per hour), and (B) short-term behavior on a linear axis (also showing multi-puff smoking pattern prior to dotted vertical line indicating the completion of smoke exhalation). Both panels depict the same results as Figure 5E with variations in axis settings for comparison, where Figure 5E shows multi-compartment results with prior smoking. (C) Model performance for a highly-persistent compound was checked against prior human subject data on long-term off-gassing of acetonitrile (H'= 0.52 mol m^{-3} Pa^{-1}), and verifies the importance of multicompartment modeling and accounting for prior smoking (the simulated smoker consumed 18 cigarettes per day for 30 days in panel C to best reproduce the human subject data in Jordan et al., which is consistent with that subject who smoked "approximately 20 cigarettes per day"[36]). (D-E) Compound loads (D) and concentrations (E) by reservoir demonstrates the transport between reservoirs, shown without prior smoking for clarity. The presence of LLF-to-blood transport enables greater uptake of compounds with both high and low H' values and leads to slower off-gassing via breath than considering LLF alone. Compounds entering LLF during smoking will transfer to blood quickly with equilibration times of minutes, while the subsequent transport to/from moderately-perfused tissues occurs over timescales of hours ($\tau \sim 3$ h).[37] (F) A comparison without and with recent prior smoking (8 total cigarettes at a rate of 1 per hr) shows the magnitude of in-body loads, the large existing reservoir with recent prior smoking, and the distribution across reservoirs as a function of time after smoking (modeled a H' = 0.5 mol m^{-3} Pa^{-1} compound at 10 ppm in mainstream smoke).

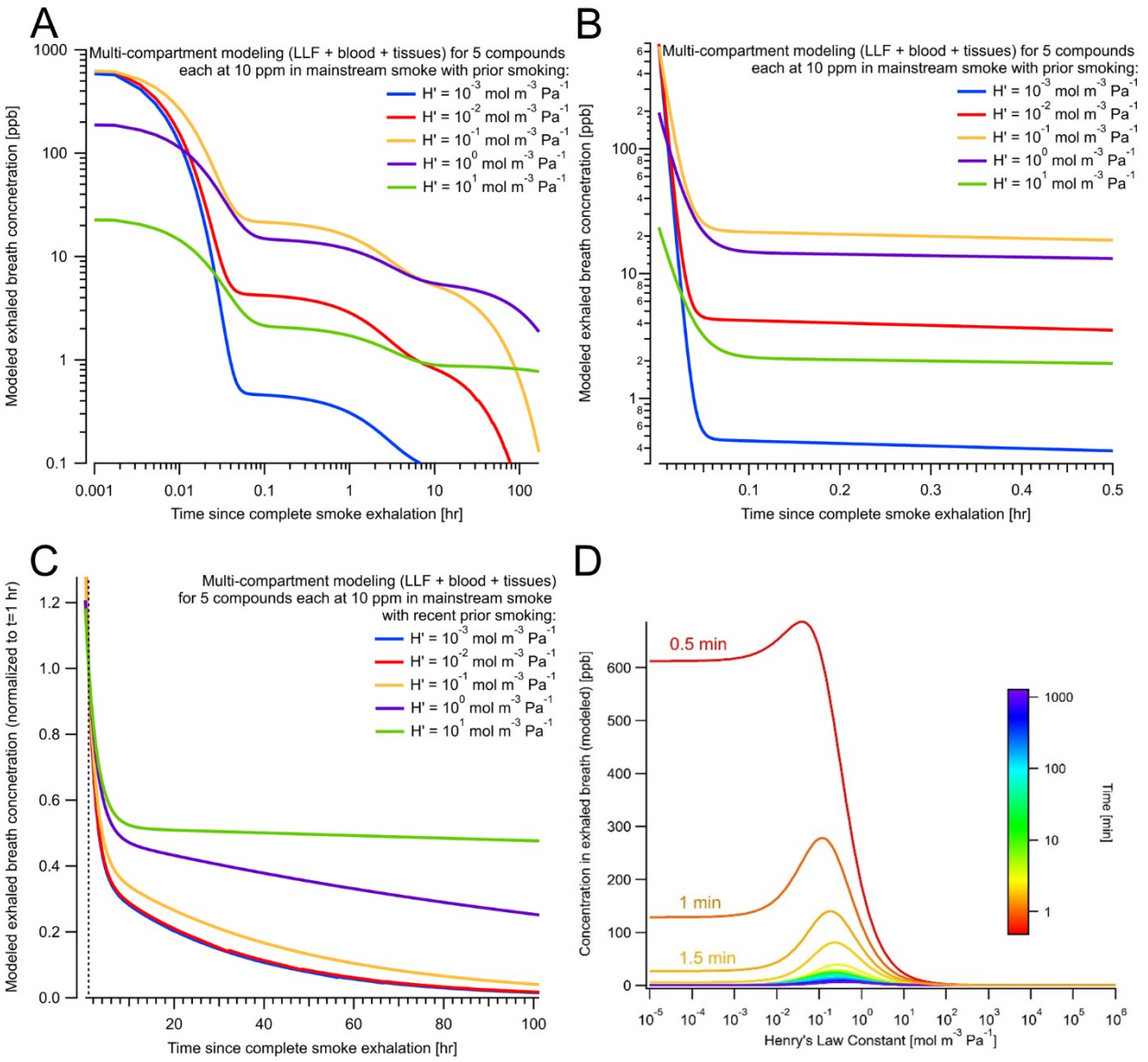

Figure S26: Multicompartment modeling and the role of Henry's Law Constants. (A-C) Detailed multi-compartment modeling over 100 hrs was conducted for compounds with H' = 10^{-3} to 10^{1} mol m^{-3} Pa^{-1}, which span the range of the most abundant THS compounds observed in lab experiments with LLF off-gassing (Figure 5D, S20). Each was modeled at 10 ppm in mainstream smoke, a concentration relevant to many tobacco smoke compounds (for comparison, benzene is at approx. 30-60 ppm[54] and acrolein can be found at approx. 100 ppm[55]). (A) log-log plot showing the dynamics starting 30 s after the last cigarette puff, allowing for complete exhalation, and (B) short-term off-gassing dynamics in the first 30 min. The concentration time series in A-B show that the relative concentrations of H' 10^{-1}-10^{0} mol m^{-3} Pa^{-1} compounds are enhanced, similar to experimental data (Figure 5), as they are readily taken up and off-gassed from aqueous bodily reservoirs. Compounds with H' 10^{-3}-10^{-2} mol m^{-3} Pa^{-1} also show large initial emissions, but drop off, while compounds with H' 10^{-1}-10^{0} expectedly remain higher. (C) Normalization to concentrations at 1 hour demonstrates that even after 1 hour, there

is still active off-gassing, with a halving of concentrations over the next 5 hours (with transport from blood) and then a slower decline in concentrations thereafter resulting from partitioning with moderately-perfused aqueous tissues. (D) Non-normalized distributions of off-gassing concentrations from compounds with H' = 10^{-5}-10^{6} mol m^{-3} Pa^{-1}, for comparison to normalized version in Figure 5F. For consistent comparison, all compounds here were modeled in mainstream smoke at 10 ppm each. See text for discussion of model constraints and limitations.

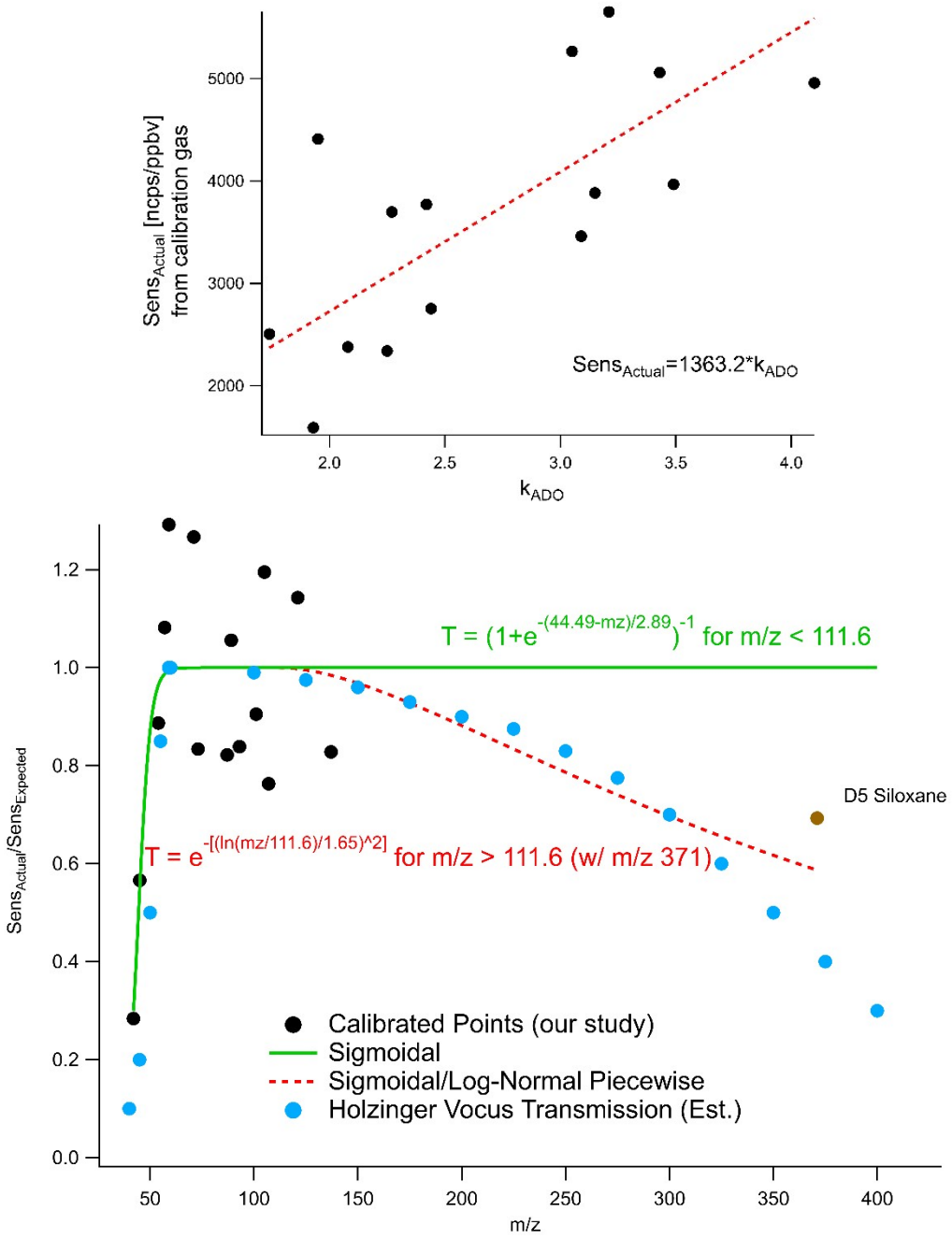

Figure S27. Fits to convert k_{ADO} and *m/z* data into sensitivities (top) and transmission efficiencies (bottom), which can then be used to convert signal abundance (in ions per second) to concentrations (in ppb). Data from literature were estimated from Holzinger et al.[14] Explanations for these calculations, including the estimation of the D5 siloxane point, can be found in the SI Sections S2.2 and S2.3.

Table S1. Experiment Information

	Trial #	Cigarette Pair	Experiment Type	Sample Time [mins]
Adsorbent Tube GC-APCI-TOF-MS	*1*	Cigarette A & Cigarette B	Secondhand Smoke	3
	1	Cigarette A & Cigarette B	Secondhand Smoke	3
	1	Cigarette A & Cigarette B	PM Off-gassing (aged 10 minutes)	3
	1	Cigarette A & Cigarette B	PM Off-gassing (aged 6 hours)	23
	1	Cigarette A & Cigarette B	PM Off-gassing (aged 72 hours)	46
	2	Cigarette A & Cigarette B	Secondhand Smoke	1.5
	2	Cigarette A & Cigarette B	PM Off-gassing (aged 1.5 hours)	30
	3	Cigarette A & Cigarette B	LLF Off-gassing (aged 1 hour)	40
	4	Cigarette C & Cigarette D	Secondhand Smoke	3
	4	Cigarette C & Cigarette D	LLF Off-gassing (aged 0.5 hours)	15
	4	Cigarette C & Cigarette D	LLF Off-gassing (aged 0.8 hours)	16
	4	Cigarette C & Cigarette D	PM Off-gassing (aged 1 hour)	15
	5	Cigarette E & Cigarette F	Secondhand Smoke	3
	5	Cigarette E & Cigarette F	PM Off-gassing (aged 2 hours)	30
Vocus PTR-TOF	*1*	Cigarette A & Cigarette B	Secondhand Smoke	7
	1	Cigarette A & Cigarette B	PM Off-gassing (aged 0 hours)	25
	1	Cigarette A & Cigarette B	PM Off-gassing (aged 6 hours)	42
	1	Cigarette A & Cigarette B	PM Off-gassing (aged 72 hours)	25
	2	Cigarette A & Cigarette B	Secondhand Smoke	14
	2	Cigarette A & Cigarette B	LLF Off-gassing (fresh)	18
	2	Cigarette A & Cigarette B	PM Off-gassing (aged 0 hours)	20
	3	Cigarette A & Cigarette B	Secondhand Smoke	11
	3	Cigarette A & Cigarette B	LLF Off-gassing (fresh)	37
	3	Cigarette A & Cigarette B	PM Off-gassing (aged 0 hours)	40
	3	Cigarette A & Cigarette B	PM Off-gassing (aged 18 hours)	19
	4	Cigarette C & Cigarette D	Secondhand Smoke	9
	4	Cigarette C & Cigarette D	LLF Off-gassing (fresh)	35
	4	Cigarette C & Cigarette D	LLF Off-gassing (fresh, no filter)	31
	4	Cigarette C & Cigarette D	LLF Off-gassing (aged 1 hour)	4
	4	Cigarette C & Cigarette D	PM Off-gassing (aged 0 hours)	68
	4	Cigarette C & Cigarette D	PM Off-gassing (aged 18 hours)	66
	5	Cigarette E & Cigarette F	Secondhand Smoke	8
	5	Cigarette E & Cigarette F	LLF Off-gassing (fresh)	86
	5	Cigarette E & Cigarette F	PM Off-gassing (aged 0 hours)	114

PM and LLF samples were collected from the most recent secondhand smoke cigarette trial (i.e., "burn") above and subsequently off-gassed. "Aged" indicates the amount of time spent off-gassing with active flow of purified air. "Fresh" in the case of LLF indicates that it was immediately transferred from exposure to SHS to off-gassing into the VOCUS. The cigarettes used in the study are common, highly sold brands purchased in Germany (Mainz) from a major commercial retailer in Fall 2019, where Cigarettes A, B, D, and E represent "original" style cigarettes while Cigarette C and F are purportedly "lighter" style cigarettes.

Table S2A. Compounds in the 12 component calibration gas

Compound	Formula	MW
Acetonitrile	C_2H_3N	41.0265
Acetaldehyde	C_2H_4O	44.0262
Acetone	C_3H_6O	58.0418
Dimethyl Sulfide	C_2H_6S	62.0189
Isoprene	C_5H_8	68.0626
Methacrolein/Methyl Vinyl Ketone	C_4H_6O	70.0418
Methyl Ethyl Ketone	C_4H_8O	72.0575
Benzene	C_6H_6	78.0469
Toluene	C_7H_8	92.0626
m-Xylene	C_8H_{10}	106.0782
1,3,5-Trimethylbenzene	C_9H_{12}	120.0938
α-Pinene	$C_{10}H_{16}$	136.1251

Compounds were present at equal concentrations and were diluted to 1, 2, and 10 ppb to give a four-point calibration (including 0 ppb).

Table S2B. Compounds in the 79 component calibration gas

Compound	Formula	MW	Conc. [ppb]
Methanol	CH_4O	32.0262	28.9
Acetonitrile	C_2H_3N	41.0265	47.7
Propene	C_3H_6	42.0469	55.5
Acetaldehyde	C_2H_4O	44.0262	76.6
Ethanol	C_2H_6O	46.0418	45.5
Chloromethane	CH_3Cl	49.9925	58.5
Acrylonitrile	C_3H_3N	53.0265	54.8
1,3-Butadiene	C_4H_6	54.0469	52.2
Acrolein	C_3H_4O	56.0262	47.1
Isobutene	C_4H_8	56.0624	52.3
Propanal	C_3H_6O	58.0418	51.4
Acetone	C_3H_6O	58.0418	56.9
1-Propanol	C_3H_8O	60.0575	49.2
2-Propanol	C_3H_8O	60.0575	55.3
Vinyl Chloride	C_2H_3Cl	61.9900	55.1
Chloroethane	C_2H_5Cl	64.0081	55.5
Isoprene	C_5H_8	68.0626	51.1
Methyl Vinyl Ketone	C_4H_6O	70.0418	50.3
Methacrolein	C_4H_6O	70.0418	55.6
Cyclopentane	C_5H_{10}	70.0782	47.5
Methyl Ethyl Ketone	C_4H_8O	72.0575	55.6
Butanal	C_4H_8O	72.0575	52.9
Pentane	C_5H_{12}	72.0938	56
1-Butanol	$C_4H_{10}O$	74.0731	34.5
Carbon Disulfide	CS_2	75.9441	55.2
Benzene	C_6H_6	78.0469	51.6
Dichloromethane	CH_2Cl_2	83.9536	48.1

Cyclohexane	C_6H_{12}	84.0938	51.7
Chlorodifluoromethane (HCFC-22)	$CHClF_2$	85.9728	53.5
Vinyl Acetate	$C_4H_6O_2$	86.0367	57.7
2-Pentanone	$C_5H_{10}O$	86.0731	55.2
3-Pentanone	$C_5H_{10}O$	86.0731	56.8
Pentanal	$C_5H_{10}O$	86.0731	47.8
Hexane	C_6H_{14}	86.1095	54.6
1,4-Dioxane	$C_4H_8O_2$	88.0524	53.4
Methyl Tertiary Butyl Ether (MTBE)	$C_5H_{12}O$	88.0887	56.6
Toluene	C_7H_8	92.0626	53.6
Bromomethane	CH_3Br	93.9415	53.1
1,1-Dichloroethene	$C_2H_2Cl_2$	95.9536	54
cis-1,2-Dichloroethene	$C_2H_2Cl_2$	95.9536	52.5
trans-1,2-Dichloroethene	$C_2H_2Cl_2$	95.9536	52.2
1,1-Dichloroethane	$C_2H_4Cl_2$	97.9693	56.4
1,2-Dichloroethane	$C_2H_4Cl_2$	97.9693	54.8
Hexanal	$C_6H_{12}O$	100.0887	24.7
2-Hexanone	$C_6H_{12}O$	100.0887	50
3-Hexanone	$C_6H_{12}O$	100.0887	52.3
4-Methyl-2-Pentanone	$C_6H_{12}O$	100.0887	53.1
Styrene	C_8H_8	104.0626	27.5
m-Xylene	C_8H_{10}	106.0782	54.6
p-Xylene	C_8H_{10}	106.0782	54.9
Ethyl Benzene	C_8H_{10}	106.0782	51.1
o-Xylene	C_8H_{10}	106.0782	54.4
cis-1,3-Dichloropropene	$C_3H_4Cl_2$	109.9693	52.6
trans-1,3-Dichloropropene	$C_3H_4Cl_2$	109.9693	56.3
1,2-Dichloropropane	$C_3H_6Cl_2$	111.9849	50.4
Chlorobenzene	C_6H_5Cl	112.0081	51.1

Chloroform	$CHCl_3$	117.9148	52.9
Dichlorodifluoromethane (F-12)	CCl_2F_2	119.9340	52.1
1,3,5-Trimethylbenzene	C_9H_{12}	120.0938	47.1
1,2,4-Trimethylbenzene	C_9H_{12}	120.0938	44.8
1,2,3-Trimethylbenzene	C_9H_{12}	120.0938	40.7
Benzyl Chloride	C_7H_7Cl	126.0237	48.2
Trichloroethylene	C_2HCl_3	129.9148	54.2
1,1,1-Trichloroethane	$C_2H_3Cl_3$	131.9305	52.4
1,1,2-Trichloroethane	$C_2H_3Cl_3$	131.9305	54.2
Trichlorofluoromethane (F-11)	CCl_3F	135.9050	54.9
Methyl Iodide	CH_3I	141.9279	53.5
o-Dichlorobenzene	$C_6H_4Cl_2$	145.9693	50.8
m-Dichlorobenzene	$C_6H_4Cl_2$	145.9693	50.1
p-Dichlorobenzene	$C_6H_4Cl_2$	145.9693	51
Tetrachloromethane	CCl_4	151.8760	50.2
Bromodichloromethane	$CHCl_2Br$	161.8638	54.9
Tetrachloroethylene	C_2Cl_4	163.8760	53.6
1,1,2,2-Tetrachloroethane	$C_2H_2Cl_4$	165.8916	55
1,2-Dichlorotetrafluoroethane (F-114)	$C_2Cl_2F_4$	169.9300	59.9
1,2,4-Trichlorobenzene	$C_6H_3Cl_3$	179.9305	46.8
1,2-Dibromoethane	$C_2H_4Br_2$	185.8673	52.5
1,1,2-Trichloro-1,2,2-Trifluoroethane (CFC-113)	$C_2Cl_3F_3$	185.9010	54.3
Bromoform	$CHBr_3$	249.7618	47

Table S3. Compounds analyzed via Vocus PTR-TOF: relevant compound parameters; average concentrations found in SHS, PM off-gassing, and LLF off-gassing samples

Molecular Formula	Ion *m/z*	Potential Compound IDs*	Type	k_{cap}	$Sens_{calc}$ [cps $ppbv^{-1}$]	H' [mol m^{-3} Pa^{-1}]	log(C*) [µg m-3]	$Conc_{Smoke}$ [ppb]	$Conc_{PM}$ [ppb]	$Conc_{LLF}$ [ppb]	$\frac{Conc_{PM}}{Conc_{PM,Nic}}$
CH_2OH^+	31.0163	Formaldehyde	CHO_1	2.94	19	32	8.83	†	†	†	†
CH_4OH^+	33.0322	Methanol	CHO_1	2.06	30	2	8.83	†	†	†	†
$C_3H_4H^+$	41.0376	Alkyl fragment, Isoprene fragment	CH	1.50	428		10.11	1257.4	20.8	51.9	2.7E-02
$C_2H_3NH^+$	42.0329	Acetonitrile	CHN_1	3.55	1365	0.52	8.22	1336.7	1.3	280.1	1.7E-03
$C_2H_2OH^+$	43.0170	Acetic acid fragment	CHO_1	2.96	1484		8.64	566.3	46.9	24.8	6.1E-02
$C_3H_6H^+$	43.0533	Propene, Alkyl fragment	CH	1.53	774	0.000048	10.11	311.5	4.1	17.5	5.3E-03
$C_2H_5NH^+$	44.0488	Vinylamine	CHN_1	1.88	1201		8.22	117.5	2.5	0.3	3.2E-03
$C_2H_4OH^+$	45.0328	Acetaldehyde	CHO_1	2.97	2286	0.13	8.64	1537.9	15.1	370.1	2.0E-02
CH_3NOH^+	46.0280	Formamide	CHN_1O_1	3.35	3007	7000	6.67	17.0	2.4	2.1	3.1E-03
$C_2H_7NH^+$	46.0643	Ethylmethylamine, Dimethylamine	CHN_1	2.54	2293	0.9	8.22	21.7	1.4	0.2	1.8E-03
$CH_2O_2H^+$	47.0120	Formic acid	CHO_2	1.75	1767	88	7.43	6.4	1.3	0.3	1.8E-03
$C_2H_6OH^+$	47.0484	Ethanol	CHO_1	2.06	2090	2	8.64	27.6	0.8	1.8	1.1E-03
$CH_4O(H_2O)H^+$	51.0435	Methanol-water adduct	CHO_1	2.06	2620		8.83	102.6	0.4	3.8	5.2E-04
$C_3H_3NH^+$	54.0334	Acrylonitrile	CHN_1	3.55	4742	0.12	7.82	155.6	0.08	45.7	1.0E-04
$C_3H_5NH^+$	56.0453	Propionitrile	CHN_1	3.87	5230	0.43	7.82	163.6	1.7	23.5	2.2E-03
$C_3H_4OH^+$	57.0332	Acrolein	CHO_1	3.01	4077	0.1	8.32	1043.6	8.1	9.2	1.1E-02
$C_4H_8H^+$	57.0694	Butenes, Alkyl/Butanol/Hexanol fragment	CH	1.71	2315		9.62	424.8	7.1	18.6	9.3E-03
$C_3H_7NH^+$	58.0644	Propenamine	CHN_1	1.95	2647	0.54	7.82	127.3	1.2	0.2	1.6E-03

$C_3H_6OH^+$	59.0490	Acetone	CHO_1	3.02	4101	0.27	8.32	2877.2	75.2	510.1	9.9E-02
$C_2H_5NOH^+$	60.0438	Acetamide	CHN_1O_1	3.60	4896	2500	6.33	73.9	12.3	10.1	1.6E-02
$C_3H_9NH^+$	60.0802	C_3 amines	CHN_1	1.96	2671	0.215	7.82	68.1	0.6	0.2	7.4E-04
$C_2H_4O_2H^+$	61.0282	Acetic acid	CHO_2	1.80	2457	40	7.50	2136.0	227.5	49.7	3.0E-01
$C_2H_6O_2H^+$	63.0436	Ethylene glycol	CHO_2	2.26	3079	4000	7.50	80.9	4.1	17.1	5.4E-03
$CH_2O(H_2O)_2H^+$	67.0410	Formaldehyde-water Adduct	CHO_1	3.04	4144	32	8.83	16.9	0.5	1.9	7.2E-04
$C_5H_6H^+$	67.0538	1,3-Cyclopentadiene	CH	1.83	2489	0.00047	9.14	218.6	2.1	4.6	2.8E-03
$C_4H_5NH^+$	68.0492	Pyrrole	CHN_1	2.50	3414	0.55	7.41	588.2	1.5	78.5	1.9E-03
$C_4H_4OH^+$	69.0330	Furan	CHO_1	1.75	2392	0.0018	7.95	254.6	8.8	4.0	1.2E-02
$C_5H_8H^+$	69.0695	Isoprene	CH	1.85	2520	0.00013	9.14	1594.6	3.2	22.8	4.2E-03
$C_4H_7NH^+$	70.0651	Pyrroline	CHN_1	2.50	3414	2	7.41	329.3	1.3	39.9	1.7E-03
$C_3H_2O_2H^+$	71.0124	Propiolic acid	CHO_2	2.28	3104		7.37	34.9	2.1	1.4	2.7E-03
$C_4H_6OH^+$	71.0489	Methacrolein, MVK	CHO_1	3.05	4157	0.0048	7.95	571.1	5.7	48.4	7.5E-03
$C_5H_{10}H^+$	71.0851	Pentenes, Cyclopentanes, Alkyl fragment	CH	1.87	2551	0.000025	9.14	193.6	3.7	2.5	4.8E-03
$C_3H_5NOH^+$	72.0440	Acrylamide	CHN_1O_1	3.64	4966	6000	5.98	19.5	3.6	1.9	4.7E-03
$C_4H_9NH^+$	72.0795	Pyrrolidine	CHN_1	2.51	3416	4.2	7.41	43.2	1.0	0.05	1.3E-03
$C_3H_4O_2H^+$	73.0280	Methylglyoxal, acrylic acid	CHO_2	2.28	3108	100	7.37	71.0	18.1	1.4	2.4E-02
$C_4H_8OH^+$	73.0644	2-Butanone, MEK	CHO_1	3.05	4163	0.18	7.95	498.4	1.9	130.6	2.4E-03
$C_3H_7NOH^+$	74.0595		CHN_1O_1	3.44	4686	750	5.98	32.0	6.2	1.9	8.2E-03
$C_3H_6O_2H^+$	75.0440	C_3 ester, C_3 acid, hydroxyacetone, glycidol	CHO_2	2.28	3112	5	7.37	1334.7	17.4	32.2	2.3E-02

$C_3H_8O_2H^+$	77.0595	C_3 diols, Propylene glycol	CHO_2	2.29	3117	5000	7.37	151.7	12.8	12.3	1.7E-02
$C_2H_6O_3H^+$	79.0388		CHO_3	2.64	3602		6.16	86.7	8.2	2.4	1.1E-02
$C_6H_6H^+$	79.0537	Benzene	CH	1.96	2668	0.0018	8.65	181.9	1.4	3.4	1.8E-03
$C_5H_5NH^+$	80.0494	Pyridine	CHN_1	2.54	3462	1.1	7.00	498.9	9.2	39.1	1.2E-02
$C_5H_4OH^+$	81.0333	2,4-Cyclopentadiene-1-one	CHO_1	3.07	4182		7.56	208.6	8.0	1.4	1.0E-02
$C_4H_4N_2H^+$	81.0437		CHN_2	3.20	4368		6.45	12.7	0.2	0.3	2.6E-04
$C_6H_8H^+$	81.0696	Hexatriene, Monoterpene fragment	CH	1.98	2697		8.65	462.9	5.7	10.0	7.4E-03
$C_5H_7NH^+$	82.0651	Methylpyrrole	CHN_1	2.52	3441	0.009	7.00	289.0	2.4	51.1	3.1E-03
$C_5H_6OH^+$	83.0490	2-Methylfuran	CHO_1	3.07	4186	0.00146	7.56	469.6	3.4	8.3	4.4E-03
$C_6H_{10}H^+$	83.0853	Hexenes, Monoterpene fragment, C_6 fragment (e.g., hexanal or hexenols)	CH	2.00	2725		8.65	243.0	2.4	4.6	3.1E-03
$C_4H_5NOH^+$	84.0440	Methyloxazoles	CHN_1O_1	3.48	4737		5.62	10.2	1.1	1.3	1.5E-03
$C_5H_9NH^+$	84.0808	Pentanenitrile	CHN_1	2.53	3448	0.14	7.00	187.7	33.8	42.9	4.4E-02
$C_4H_4O_2H^+$	85.0282	2-(3H)Furanone	CHO_2	2.31	3152	1	7.13	263.3	8.8	1.2	1.1E-02
$C_5H_8OH^+$	85.0646	Cyclopentanone	CHO_1	3.07	4190	1	7.56	247.1	2.5	34.7	3.3E-03
$C_6H_{12}H^+$	85.1009	Hexenes	CH	2.02	2753	0.000025	8.65	101.0	1.8	0.8	2.3E-03
$C_4H_7NOH^+$	86.0601	2-Pyrrolidinone	CHN_1O_1	3.48	4747		5.62	33.1	13.0	1.9	1.7E-02
$C_5H_{11}NH^+$	86.0953	Piperidine	CHN_1	2.54	3457	2.8	7.00	28.4	1.5	0.06	1.9E-03
$C_4H_6O_2H^+$	87.0439	2,3-Butanedione, Butyrolactone	CHO_2	2.32	3164	0.73	7.13	572.6	14.4	21.8	1.9E-02
$C_5H_{10}OH^+$	87.0800	Pentanone, pentanal, and others	CHO_1	3.08	4193	0.1	7.56	121.6	0.5	35.3	5.9E-04
$C_4H_9NOH^+$	88.0752	C_4 amide	CHN_1O_1	3.49	4756	440	5.62	26.7	3.8	3.1	4.9E-03

$C_3H_4O_3H^+$	89.0231	Pyruvic acid	CHO_3	2.66	3630		6.18	16.1	2.1	0.8	2.7E-03
$C_4H_8O_2H^+$	89.0595	Butanoic acid, ethyl acetate, C_4 esters	CHO_2	2.33	3176	0.06	7.13	133.9	3.6	3.8	4.7E-03
$C_2H_3NO_3H^+$	90.0183		$CHNO_3$	2.50	3414		4.87	2.8	0.8	0.4	1.1E-03
$C_4H_{11}NOH^+$	90.0910	C_4 amine alcohol	CHN_1O_1	3.50	4765	48	5.62	13.9	5.6	0.1	7.4E-03
$C_3H_6O_3H^+$	91.0383		CHO_3	2.67	3634	0.016	6.18	8.8	1.5	1.3	2.0E-03
$C_7H_6H^+$	91.0540	Monoterpene fragment, Cresol fragment	CH	2.08	2835		8.17	164.5	9.0	3.7	1.2E-02
$C_3H_8O_3H^+$	93.0549	Glycerol	CHO_3	2.67	3638	5000000	6.18	19.4	3.0	8.5	3.9E-03
$C_7H_8H^+$	93.0694	Toluene	CH	2.10	2862	0.0015	8.17	438.4	2.1	5.8	2.7E-03
$C_6H_7NH^+$	94.0649	Methylpyridines	CHN_1	2.58	3520	1	6.60	423.1	2.0	29.8	2.6E-03
$C_6H_6OH^+$	95.0490	Phenol	CHO_1	3.08	4204	20	7.14	274.5	46.6	4.1	6.1E-02
$C_5H_6N_2H^+$	95.0606	Methylpyrazines, Methylpyrimidines	CHN_2	3.23	4400	10000	6.04	59.0	2.3	0.7	3.0E-03
$C_7H_{10}H^+$	95.0853	Monoterpene fragment	CH	2.12	2889		8.17	271.1	4.4	5.8	5.8E-03
$C_5H_5NOH^+$	96.0440	4-Pyridinol	CHN_1O_1	3.51	4791		5.26	10.2	4.4	1.2	5.7E-03
$C_6H_9NH^+$	96.0804	C_2 Pyrroles	CHN_1	2.57	3507		6.60	117.8	0.4	18.9	5.5E-04
$C_5H_4O_2H^+$	97.0285	Furfural	CHO_2	2.37	3231	2.6	6.83	846.3	4.5	22.6	5.9E-03
$C_6H_8OH^+$	97.0644	2,5-Dimethylfuran	CHO_1	3.09	4206	0.0015	7.14	386.4	2.1	9.6	2.8E-03
$C_5H_8N_2H^+$	97.0751	Pyrazine + C_2 or Imidazole + C_2	CHN_2	3.23	4403		6.04	1.4	1.9	0.7	2.5E-03
$C_7H_{12}H^+$	97.1010	Heptanal fragment, Methylcyclohexane ion	CH	2.14	2915		8.17	85.9	1.8	1.7	2.4E-03
$C_5H_7NOH^+$	98.0597	Furfurylamine, Dimethyloxazoles	CHN_1O_1	3.52	4799		5.26	20.9	7.8	1.8	1.0E-02
$C_6H_{11}NH^+$	98.0958	Isoamyl cyanide, 4-Methylpentanenitrile	CHN_1	2.58	3518	0.23	6.60	59.6	0.3	14.7	4.4E-04
$C_5H_6O_2H^+$	99.0439	Furfuryl alcohol	CHO_2	2.38	3246	120	6.83	261.7	17.0	2.9	2.2E-02

$C_6H_{10}OH^+$	99.0801	Cyclohexanone, Methylcyclopentanone	CHO_1	3.09	4208		7.14	74.3	1.4	11.9	1.8E-03
$C_7H_{14}H^+$	99.1165	Heptenes	CH	2.16	2941	0.000025	8.17	8.2	1.0	0.3	1.3E-03
$C_4H_5NO_2H^+$	100.0392		CHN_1O_2	3.53	4807		4.93	3.6	1.3	0.4	1.7E-03
$C_5H_9NOH^+$	100.0757	Methylpyrrolidione	CHN_1O_1	3.53	4807	2100	5.26	24.0	7.9	1.1	1.0E-02
$C_4H_4O_3H^+$	101.0231	Succinic anhydride	CHO_3	2.68	3651		6.06	13.7	2.2	0.9	2.9E-03
$C_5H_8O_2H^+$	101.0597	Methyl methacrylate	CHO_2	2.39	3262	0.04	6.83	146.1	9.3	8.2	1.2E-02
$C_6H_{12}OH^+$	101.0955	Hexanals, hexanones	CHO_1	3.09	4210	0.05	7.14	25.2	0.2	7.6	2.9E-04
$C_5H_{11}NOH^+$	102.0911		CHN_1O_1	3.53	4814		5.26	25.3	4.2	4.5	5.5E-03
$C_4H_6O_3H^+$	103.0389	Acetic anhydride	CHO_3	2.68	3654		6.06	137.9	24.0	2.1	3.1E-02
$C_5H_{10}O_2H^+$	103.0751	C_5 aldehydes, C_5 ketones, C_5 esters, C_5 acids	CHO_2	2.40	3277	0.046	6.83	35.5	4.4	1.5	5.8E-03
$C_7H_5NH^+$	104.0479	Benzonitrile	CHN_1	2.61	3555	0.2	6.19	95.7	1.0	13.4	1.3E-03
$C_6H_4N_2H^+$	105.0438	Pyridinecarbonitriles	CHN_2	3.24	4415	50	5.63	52.7	1.6	0.3	2.1E-03
$C_4H_8O_3H^+$	105.0540	4-Hydroxybutanoic acid	CHO_3	2.68	3657		6.06	35.9	1.7	1.9	2.3E-03
$C_8H_8H^+$	105.0696	Styrene	CH	2.21	3018	0.0034	7.68	143.7	5.0	3.9	6.6E-03
$C_7H_7NH^+$	106.0655	3-Ethenylpyridine	CHN_1	2.62	3567	2.9	6.19	342.9	10.3	21.9	1.3E-02
$C_7H_6OH^+$	107.0491	Benzaldehyde	CHO_1	3.09	4215	0.4	6.72	82.4	2.6	8.1	3.5E-03
$C_8H_{10}H^+$	107.0854	C_8 aromatics	CH	2.23	3044	0.002	7.68	298.4	2.2	4.5	3.0E-03
$C_6H_5NOH^+$	108.0437	Pyridine aldehyde	CHN_1O_1	3.55	4835	60	4.89	17.8	3.6	1.4	4.8E-03
$C_7H_9NH^+$	108.0807	C_7 Pyridine	CHN_1	2.63	3580	0.95	6.19	172.6	1.5	14.8	2.0E-03
$C_6H_4O_2H^+$	109.0282	Benzoquinones	CHO_2	2.44	3327	0.021	6.49	54.6	6.5	3.6	8.5E-03
$C_7H_8OH^+$	109.0642	Cresols and anisole	CHO_1	3.09	4217	10	6.72	108.6	25.6	2.7	3.4E-02

$C_6H_8N_2H^+$	109.0748	C_6 Pyrazines, Benzenediamines, Methylpyridinamines, C_6 Pyrimidines	CHN_2	3.24	4420	5	5.63	50.8	3.2	0.6	4.2E-03
$C_8H_{12}H^+$	109.1010		CH	2.25	3069		7.68	138.5	3.1	4.1	4.0E-03
$C_6H_7NOH^+$	110.0594	Aminophenol	CHN_1O_1	3.55	4842	30000	4.89	16.4	4.8	0.6	6.3E-03
$C_7H_{11}NH^+$	110.0961	C_7 Pyrroles	CHN_1	2.64	3593		6.19	51.1	0.3	7.6	3.5E-04
$C_6H_6O_2H^+$	111.0441	5-Methylfurfural, 2-Acetylfuran, Catechols	CHO_2	2.45	3343		6.49	291.1	5.3	6.9	7.0E-03
$C_5H_6N_2OH^+$	111.0555	Methoxypyrazine	CHN_2O	2.59	3531		4.14	15.3	1.5	0.5	1.9E-03
$C_7H_{10}OH^+$	111.0794	C_7 Furan	CHO_1	3.09	4218		6.72	189.5	2.1	7.0	2.7E-03
$C_8H_{14}H^+$	111.1168		CH	2.27	3094		7.68	40.6	1.7	1.0	2.2E-03
$C_6H_9NOH^+$	112.0753		CHN_1O_1	3.56	4848		4.89	15.1	2.9	0.8	3.8E-03
$C_5H_4O_3H^+$	113.0230	2,5-Furandione, 3-methyl-	CHO_3	2.69	3666		5.87	24.7	2.5	0.4	3.3E-03
$C_6H_8O_2H^+$	113.0596	2-hydroxy-3-methyl-2-cyclopenten-1-one	CHO_2	2.47	3360		6.49	161.5	24.4	1.7	3.2E-02
$C_5H_8N_2OH^+$	113.0731		CHN_2O	2.60	3544		4.14	8.9	1.1	0.1	1.4E-03
$C_7H_{12}OH^+$	113.0955	Ethyl cyclopentanone	CHO_1	3.10	4220		6.72	27.1	0.4	5.8	5.1E-04
$C_8H_{16}H^+$	113.1323	Octene	CH	2.29	3118	0.00001	7.68	4.9	0.9	0.3	1.1E-03
$C_6H_{11}NOH^+$	114.0908	C_2 Pyrrolidinone, Acetylpyrrolidine	CHN_1O_1	3.56	4854		4.89	11.2	4.7	0.6	6.2E-03
$C_5H_6O_3H^+$	115.0388	5-Hydroxymethyl-2[3H]-furanone	CHO_3	2.69	3669		5.87	39.9	6.9	0.7	9.0E-03
$C_6H_{10}O_2H^+$	115.0750	C_6 diketones, C_6 esters, C_6 acid	CHO_2	2.48	3378		6.49	40.2	3.3	2.2	4.4E-03
$C_6H_{13}NOH^+$	116.1071		CHN_1O_1	3.56	4860		4.89	18.0	3.5	4.3	4.6E-03
$C_5H_8O_3H^+$	117.0552	1-(Acetyloxy)-2-propanone	CHO_3	2.69	3673		5.87	150.5	48.8	2.1	6.4E-02

$C_6H_{12}O_2H^+$	117.0905	C_6 esters	CHO_2	2.49	3395	0.025	6.49	15.2	5.0	0.9	6.6E-03
$C_8H_7NH^+$	118.0645	Benzeneacetonitrile	CHN_1	2.68	3648	10	5.78	69.4	19.5	8.2	2.6E-02
$C_8H_6OH^+$	119.0474	Benzofuran	CHO_1	3.10	4230	0.02	6.30	13.8	0.2	2.2	2.6E-04
$C_7H_6N_2H^+$	119.0588		CHN_2	3.25	4430		5.23	11.3	3.2	0.4	4.2E-03
$C_5H_{10}O_3H^+$	119.0691		CHO_3	2.70	3678		5.87	10.6	2.5	0.9	3.2E-03
$C_9H_{10}H^+$	119.0850	Indane, Cyclopropylbenzene, α-Methylstyrene	CH	2.34	3191	0.003	7.19	85.0	3.3	2.4	4.3E-03
$C_8H_9NH^+$	120.0806	Dihydropyridine or Methylethenylpyridine	CHN_1	2.69	3662		5.78	34.0	5.4	3.7	7.0E-03
$C_8H_8OH^+$	121.0637	Acetophenone and tolualdehydes	CHO_1	3.11	4235	1	6.30	44.8	5.1	4.6	6.7E-03
$C_7H_8N_2H^+$	121.0728		CHN_2	3.25	4432		5.23	22.1	1.6	1.0	2.1E-03
$C_9H_{12}H^+$	121.1010	C_9 Aromatics	CH	2.36	3215	0.0015	7.19	141.1	1.9	2.5	2.5E-03
$C_7H_7NOH^+$	122.0592		CHN_1O_1	3.58	4876		4.53	17.2	3.2	1.4	4.2E-03
$C_8H_{11}NH^+$	122.0965	Pyridine + C_3	CHN_1	2.70	3676		5.78	66.6	1.6	6.6	2.2E-03
$C_7H_6O_2H^+$	123.0438	Benzoic acid	CHO_2	2.53	3448	290	6.13	17.9	1.6	0.9	2.1E-03
$C_6H_6N_2OH^+$	123.0558	Acetylpyrazine	CHN_2O	2.65	3613		3.78	10.9	1.3	0.4	1.6E-03
$C_8H_{10}OH^+$	123.0797	C_8 Phenol, Methylanisole	CHO_1	3.11	4240	10	6.30	62.4	16.1	2.7	2.1E-02
$C_7H_{10}N_2H^+$	123.0920	C_7 Pyrazines	CHN_2	3.25	4434	13000	5.23	17.5	1.2	0.7	1.6E-03
$C_9H_{14}H^+$	123.1168		CH	2.38	3238		7.19	106.9	2.0	2.2	2.6E-03
$C_7H_9NOH^+$	124.0750		CHN_1O_1	3.58	4881		4.53	12.7	3.4	0.5	4.5E-03
$C_8H_{13}NH^+$	124.1097		CHN_1	2.71	3691		5.78	16.3	0.3	2.8	4.0E-04
$C_6H_4O_3H^+$	125.0232	Hydroxybenzoquinone or Furandicarboxaldehyde	CHO_3	2.71	3694		5.61	17.4	1.7	0.7	2.3E-03

$C_7H_8O_2H^+$	125.0589	Guaiacol	CHO_2	2.54	3466	8	6.13	95.0	7.8	2.2	1.0E-02
$C_6H_8N_2OH^+$	125.0702	Methoxymethylpyrazine	CHN_2O	2.66	3627		3.78	9.8	2.7	0.2	3.5E-03
$C_8H_{12}OH^+$	125.0958		CHO_1	3.11	4245		6.30	81.3	2.0	4.8	2.6E-03
$C_9H_{16}H^+$	125.1324		CH	2.39	3262		7.19	20.0	1.0	0.4	1.3E-03
$C_7H_{11}NOH^+$	126.0909		CHN_1O_1	3.58	4885		4.53	8.2	2.2	0.5	2.9E-03
$C_6H_6O_3H^+$	127.0386	5-Hydroxymethyl, 2-furfural	CHO_3	2.71	3700	18000	5.61	35.9	11.9	1.5	1.6E-02
$C_7H_{10}O_2H^+$	127.0750		CHO_2	2.56	3484		6.13	50.2	10.4	0.7	1.4E-02
$C_6H_{10}N_2OH^+$	127.0879		CHN_2O	2.67	3641		3.78	5.5	0.9	0.05	1.1E-03
$C_8H_{14}OH^+$	127.1113	6-Methyl-5-hepten-2-one (6-MHO)	CHO_1	3.12	4251		6.30	15.3	0.4	3.9	5.9E-04
$C_9H_{18}H^+$	127.1480	Nonene	CH	2.41	3285	0.000012	7.19	3.2	0.8	0.1	1.0E-03
$C_{10}H_8H^+$	128.0597	Naphthalene (ionized)	CH	2.42	3297		6.71	9.5	2.0	1.2	2.6E-03
$C_7H_{13}NOH^+$	128.1072		CHN_1O_1	3.59	4890		4.53	8.5	2.5	0.6	3.3E-03
$C_6H_8O_3H^+$	129.0543		CHO_3	2.72	3706		5.61	52.1	16.9	0.3	2.2E-02
$C_{10}H_8H^+$	129.0683	Naphthalene	CH	2.43	3308	0.025	6.71	33.1	2.3	4.4	3.0E-03
$C_9H_7NH^+$	130.0646	Quinoline/Isoquinoline	CHN_1	2.74	3734	5	5.38	23.8	14.9	1.0	2.0E-02
$C_7H_{15}NOH^+$	130.1234		CHN_1O_1	3.59	4894		4.53	2.4	0.7	0.3	9.8E-04
$C_9H_6OH^+$	131.0492		CHO_1	3.13	4264		5.87	11.9	1.7	0.1	2.3E-03
$C_6H_{10}O_3H^+$	131.0695		CHO_3	2.72	3713		5.61	30.6	8.0	0.6	1.0E-02
$C_{10}H_{10}H^+$	131.0843		CH	2.44	3331		6.71	30.2	1.8	2.0	2.3E-03
$C_9H_9NH^+$	132.0810	Skatole	CHN_1	2.75	3749	4.7	5.38	45.9	16.8	5.6	2.2E-02
$C_9H_8OH^+$	133.0644	Methylbenzofuran	CHO_1	3.13	4271	2	5.87	26.0	3.5	2.1	4.6E-03
$C_8H_8N_2H^+$	133.0771		CHN_2	3.27	4452		4.82	22.9	10.4	0.7	1.4E-02

$C_{10}H_{12}H^+$	133.1008	Ethylstyrene, Methylindanes	CH	2.46	3354		6.71	61.3	2.2	1.9	2.8E-03
$C_8H_7NOH^+$	134.0598		CHN_1O_1	3.60	4903		4.17	7.0	1.8	0.5	2.3E-03
$C_9H_{11}NH^+$	134.0947		CHN_1	2.76	3764		5.38	18.7	3.7	2.3	4.8E-03
$C_9H_{10}OH^+$	135.0803	Methyl acetophenone	CHO_1	3.14	4279	1	5.87	29.7	4.1	3.1	5.4E-03
$C_8H_{10}N_2H^+$	135.0962		CHN_2	3.27	4457		4.82	7.6	1.9	0.4	2.5E-03
$C_{10}H_{14}H^+$	135.1166	C_{10} Aromatics	CH	2.48	3377	0.001	6.71	90.9	3.7	1.9	4.8E-03
$C_8H_9NOH^+$	136.0752		CHN_1O_1	3.60	4907		4.17	11.5	2.2	0.9	2.8E-03
$C_9H_{13}NH^+$	136.1126		CHN_1	2.77	3778		5.38	26.5	4.2	3.3	5.5E-03
$C_8H_8O_2H^+$	137.0591		CHO_2	2.62	3574		5.75	18.8	3.1	0.8	4.1E-03
$C_7H_8N_2OH^+$	137.0711		CHN_2O	2.73	3715		3.42	7.7	1.5	0.3	2.0E-03
$C_9H_{12}OH^+$	137.0957		CHO_1	3.14	4286		5.87	31.9	7.3	1.9	9.6E-03
$C_{10}H_{16}H^+$	137.1326	Monoterpenes	CH	2.49	3400	0.00042	6.71	223.9	2.1	1.5	2.8E-03
$C_8H_{11}NOH^+$	138.0930		CHN_1O_1	3.60	4911		4.17	6.9	2.2	0.2	2.9E-03
$C_7H_6O_3H^+$	139.0386	Salicylic acid	CHO_3	2.75	3744	800	5.32	6.5	1.4	0.3	1.8E-03
$C_8H_{10}O_2H^+$	139.0747	Methylguaiacol	CHO_2	2.63	3592		5.75	34.4	7.6	1.1	9.9E-03
$C_7H_{10}N_2OH^+$	139.0866	Ethylmethoxypyrazine	CHN_2O	2.74	3730		3.42	5.5	2.2	0.1	2.9E-03
$C_9H_{14}OH^+$	139.1105		CHO_1	3.15	4294		5.87	36.1	1.9	4.0	2.4E-03
$C_{10}H_{18}H^+$	139.1479	Monoterpenoids	CH	2.51	3422	0.00008	6.71	14.5	0.5	0.2	6.6E-04
$C_8H_{13}NOH^+$	140.1075		CHN_1O_1	3.60	4914		4.17	4.9	1.3	0.6	1.6E-03
$C_7H_8O_3H^+$	141.0541		CHO_3	2.75	3753		5.32	7.2	2.0	0.2	2.6E-03
$C_8H_{12}O_2H^+$	141.0907		CHO_2	2.65	3610		5.75	15.0	4.4	0.4	5.8E-03
$C_7H_{12}N_2OH^+$	141.1043		CHN_2O	2.75	3745		3.42	2.4	0.7	0.07	8.9E-04
$C_{10}H_{20}H^+$	141.1637	Decene	CH	2.53	3444	0.000004	6.71	2.3	0.7	0.1	8.8E-04

$C_8H_{15}NOH^+$	142.1230		CHN_1O_1	3.61	4918		4.17	2.9	0.9	0.2	1.2E-03
$C_7H_{10}O_3H^+$	143.0690		CHO_3	2.76	3761		5.32	8.4	3.6	0.10	4.7E-03
$C_{11}H_{10}H^+$	143.0847	Methylnaphthalenes	CH	2.54	3466	0.025	6.22	31.8	5.0	4.9	6.6E-03
$C_9H_{18}OH^+$	143.1430	Nonanal	CHO_1	3.16	4311	0.03	5.87	3.5	0.3	0.4	3.8E-04
$C_{10}H_9NH^+$	144.0804	Methylquinolines or Naphthylamine	CHN_1	2.82	3838	13	4.97	6.5	5.3	0.6	7.0E-03
$C_8H_{17}NOH^+$	144.1416		CHN_1O_1	3.61	4921		4.17	1.2	0.3	0.2	3.4E-04
$C_6H_8O_4H^+$	145.0495	Triacetin fragment (-$C_3H_5O_2$), Levoglucosan fragment (-OH)	CHO_4	2.79	3806		4.58	22.9	21.6	0.4	2.8E-02
$C_{10}H_8OH^+$	145.0637	2-Ethenylbenzofuran	CHO_1	3.17	4320	30	5.43	13.1	3.4	0.6	4.4E-03
$C_9H_8N_2H^+$	145.0803		CHN_2	3.29	4488		4.42	4.5	2.7	0.2	3.5E-03
$C_{11}H_{12}H^+$	145.0992	Ethylindene	CH	2.56	3488		6.22	30.0	2.4	2.0	3.2E-03
$C_{10}H_{11}NH^+$	146.0961	C_{10} Indole	CHN_1	2.83	3853		4.97	16.0	4.6	2.3	6.1E-03
$C_8H_6N_2OH^+$	147.0544		CHN_2O	2.78	3790		3.05	3.3	2.5	0.07	3.3E-03
$C_{10}H_{10}OH^+$	147.0794	C_{10} Benzofuran	CHO_1	3.18	4329		5.43	21.4	2.5	1.7	3.2E-03
$C_9H_{10}N_2H^+$	147.0919	Myosmine	CHN_2	3.30	4495		4.42	13.9	33.4	1.3	4.4E-02
$C_{11}H_{14}H^+$	147.1153		CH	2.57	3510		6.22	26.6	1.5	0.8	2.0E-03
$C_9H_9NOH^+$	148.0761		CHN_1O_1	3.62	4928		3.80	7.7	2.6	0.6	3.4E-03
$C_{10}H_{13}NH^+$	148.1136		CHN_1	2.84	3868		4.97	10.2	2.7	1.2	3.6E-03
$C_8H_4O_3H^+$	149.0229	Phthalic anhydride	CHO_3	2.78	3788	1600	5.00	*0.4*	*0.09*		1.2E-04
$C_8H_8N_2OH^+$	149.0747		CHN_2O	2.79	3805		3.05	2.3	1.2	0.1	1.6E-03
$C_{10}H_{12}OH^+$	149.0943	Estragole	CHO_1	3.18	4338		5.43	12.9	3.7	1.2	4.8E-03
$C_9H_{12}N_2H^+$	149.1067	Nornicotine	CHN_2	3.30	4503		4.42	4.6	2.0	0.3	2.7E-03
$C_{11}H_{16}H^+$	149.1321	C_{11} Aromatics	CH	2.59	3532	0.0007	6.22	27.7	1.6	0.5	2.1E-03

$C_9H_{11}NOH^+$	150.0920		CHN_1O_1	3.62	4931		3.80	7.8	3.0	0.7	3.9E-03
$C_{10}H_{15}NH^+$	150.1286		CHN_1	2.85	3884		4.97	13.1	1.4	2.0	1.8E-03
$C_9H_{10}O_2H^+$	151.0743	Vinylguaiacol	CHO_2	2.71	3701	0.5	5.36	15.4	7.2	0.5	9.5E-03
$C_8H_{10}N_2OH^+$	151.0873		CHN_2O	2.80	3820		3.05	4.3	1.8	0.1	2.3E-03
$C_{10}H_{14}OH^+$	151.1108	Carvone	CHO_1	3.19	4348	0.13	5.43	20.9	4.1	2.0	5.4E-03
$C_{11}H_{18}H^+$	151.1469		CH	2.61	3553		6.22	19.3	0.7	0.3	9.0E-04
$C_9H_{13}NOH^+$	152.1094		CHN_1O_1	3.62	4934		3.80	4.1	1.7	0.2	2.2E-03
$C_8H_8O_3H^+$	153.0544	Vanillin	CHO_3	2.79	3807	4700	5.00	4.1	2.1	0.2	2.8E-03
$C_{12}H_8H^+$	153.0688	Acenaphthylene	CH	2.62	3575	0.09	5.74	2.0	1.2	0.4	1.6E-03
$C_9H_{12}O_2H^+$	153.0901		CHO_2	2.73	3719		5.36	12.6	4.6	0.5	6.1E-03
$C_8H_{12}N_2OH^+$	153.1040		CHN_2O	2.81	3836		3.05	2.9	1.5	0.05	2.0E-03
$C_{10}H_{16}OH^+$	153.1259	Camphor, Monoterpenoids	CHO_1	3.20	4357	0.12	5.43	17.4	1.8	2.6	2.4E-03
$C_{11}H_{20}H^+$	153.1632		CH	2.62	3575		6.22	1.8	0.3	0.05	3.8E-04
$C_{11}H_7NH^+$	154.0649		CHN_1	2.87	3914		4.56	1.5	1.6	0.1	2.1E-03
$C_8H_{10}O_3H^+$	155.0687	Syringol	CHO_3	2.80	3817		5.00	4.2	2.7	0.1	3.5E-03
$C_{12}H_{10}H^+$	155.0841	Biphenyl and Acenaphthene	CH	2.64	3596	0.035	5.74	5.2	2.6	1.0	3.4E-03
$C_{10}H_{18}OH^+$	155.1417	Cineole, Monoterpenoids	CHO_1	3.20	4367	0.05	5.43	5.1	0.3	0.5	4.5E-04
$C_{11}H_{22}H^+$	155.1794	Undecene	CH	2.64	3596		6.22	1.6	0.5	0.08	7.0E-04
$C_{11}H_9NH^+$	156.0793		CHN_1	2.88	3929		4.56	1.7	2.3	0.2	3.0E-03
$C_{10}H_8N_2H^+$	157.0755	Dipyridyl	CHN_2	3.33	4534	18000	4.01	1.4	1.0	9.6	1.4E-03
$C_{12}H_{12}H^+$	157.1010	C_{12} Naphthalenes	CH	2.65	3617	0.03	5.74	20.2	8.6	3.2	1.1E-02
$C_{10}H_{20}OH^+$	157.1583	Decanal	CHO_1	3.21	4377	0.005	5.43	2.8	0.3	0.3	3.9E-04

$C_{11}H_{11}NH^+$	158.0969		CHN_1	2.89	3944		4.56	3.2	3.5	0.3	4.5E-03
$C_7H_{10}O_4H^+$	159.0656	Triacetin fragment	CHO_4	2.84	3870		2.90	9.4	47.8	0.1	6.3E-02
$C_{11}H_{10}OH^+$	159.0794		CHO_1	3.22	4387		5.00	6.0	11.5	0.5	1.5E-02
$C_{10}H_{10}N_2H^+$	159.0915	Nicotyrine	CHN_2	3.33	4543		4.01	8.5	7.7	0.5	1.0E-02
$C_{12}H_{14}H^+$	159.1144		CH	2.67	3638		5.74	19.8	4.5	1.2	5.8E-03
$C_{11}H_{13}NH^+$	160.1141		CHN_1	2.90	3959		4.56	6.2	3.0	0.8	3.9E-03
$C_9H_8N_2OH^+$	161.0701		CHN_2O	2.86	3897		2.69	2.1	3.0	0.08	3.9E-03
$C_{11}H_{12}OH^+$	161.0943		CHO_1	3.23	4397		5.00	10.8	1.2	1.0	1.5E-03
$C_{10}H_{12}N_2H^+$	161.1073	Anatabine, Anabaseine	CHN_2	3.34	4552		4.01	17.3	33.9	0.4	4.4E-02
$C_{12}H_{16}H^+$	161.1303		CH	2.68	3659		5.74	15.4	1.9	0.4	2.5E-03
$C_{10}H_{14}N_2H^+$	162.0924	Nicotine ionized	CHN_2	3.34	4556		4.01	4.5	2.3	0.4	3.1E-03
$C_{10}H_{14}N_2H^+$	162.1138	Nicotine ionized	CHN_2	3.34	4556		4.01	6.3	11.2	0.1	1.5E-02
$C_{11}H_{15}NH^+$	162.1302		CHN_1	2.92	3975		4.56	5.7	3.1	0.6	4.1E-03
$C_{10}H_{14}N_2H^+$	163.1248	Nicotine	CHN_2	3.35	4561	3300	4.01	461.9	762.7	5.2	1.0E+00
$C_{12}H_{18}H^+$	163.1620	C_{12} Aromatics	CH	2.70	3680	0.0008	5.74	5.3	0.5	0.07	6.3E-04
$C_{10}H_{14}N_2$ $(^{13}C)H^+$	164.1266	Nicotine (^{13}C)	CHN_2	3.35	4565		4.01	44.9	87.9	0.5	1.2E-01
$C_{11}H_{17}NH^+$	164.1416		CHN_1	2.93	3990		4.56	8.9	7.4	1.0	9.6E-03
$C_{10}H_{12}O_2H^+$	165.0896	Eugenol	CHO_2	2.81	3827	5.1	4.96	6.0	3.2	0.3	4.1E-03
$C_9H_{12}N_2OH^+$	165.0998		CHN_2O	2.88	3928		2.69	2.6	1.5	0.1	1.9E-03
$C_{11}H_{16}OH^+$	165.1277		CHO_1	3.24	4419		5.00	9.0	5.7	0.7	7.5E-03
$C_{12}H_{20}H^+$	165.1633		CH	2.71	3701		5.74	5.4	0.3	0.1	4.3E-04
$C_{10}H_{15}NOH^+$	166.1271		CHN_1O_1	3.63	4954		3.44	1.8	0.8	0.1	1.1E-03
$C_{13}H_{10}H^+$	167.0842	Phenalene, Fluorene	CH	2.73	3721	0.1	5.25	1.5	1.5	0.3	2.0E-03

$C_9H_{14}N_2OH^+$	167.1184		CHN_2O	2.89	3943		2.69	1.7	1.2	0.06	1.5E-03
$C_{11}H_{18}OH^+$	167.1418		CHO_1	3.25	4429		5.00	4.2	0.8	0.7	1.1E-03
$C_{12}H_{22}H^+$	167.1788		CH	2.73	3721		5.74	0.8	0.2	0.04	2.5E-04
$C_{12}H_9NH^+$	168.0806	Carbazole	CHN_1	2.95	4020		4.16	0.6	0.8	0.1	1.1E-03
$C_{13}H_{12}H^+$	169.0989	Methylbiphenyl	CH	2.74	3742	0.02	5.25	3.8	3.4	0.9	4.4E-03
$C_{12}H_{24}H^+$	169.1950	Dodecene	CH	2.74	3742	0.000002	5.74	1.3	0.4	0.09	5.7E-04
$C_{12}H_{11}NH^+$	170.0958		CHN_1	2.96	4035		4.16	1.2	1.7	0.2	2.3E-03
$C_{13}H_{14}H^+$	171.1151	C_{13} Naphthalenes	CH	2.76	3762	0.03	5.25	8.4	6.9	1.4	9.1E-03
$C_{12}H_{13}NH^+$	172.1153		CHN_1	2.97	4051		4.16	2.7	2.8	0.4	3.7E-03
$C_{11}H_{12}N_2H^+$	173.1060		CHN_2	3.38	4607		3.60	1.8	2.6	0.2	3.4E-03
$C_{13}H_{16}H^+$	173.1314		CH	2.77	3782		5.25	11.8	4.1	0.6	5.3E-03
$C_{11}H_{11}NOH^+$	174.0934		CHN_1O_1	3.64	4964		3.07	1.0	1.1	0.1	1.5E-03
$C_{12}H_{15}NH^+$	174.1316		CHN_1	2.98	4066		4.16	2.9	1.6	0.3	2.1E-03
$C_{10}H_{10}N_2OH^+$	175.0854		CHN_2O	2.94	4004		2.32	0.9	1.5	0.04	1.9E-03
$C_7H_{14}N_2O_3H^+$	175.1092		CHN_2O_3	2.94	4004		2.06	5.1	3.0	0.4	3.9E-03
$C_{12}H_{14}OH^+$	175.1111		CHO_1	3.28	4473		4.56			*0.5*	
$C_{13}H_{18}H^+$	175.1470		CH	2.79	3802		5.25	9.8	1.7	0.3	2.2E-03
$C_{11}H_{13}NOH^+$	176.1104		CHN_1O_1	3.64	4966		3.07	2.0	1.5	0.2	2.0E-03
$C_{12}H_{17}NH^+$	176.1459		CHN_1	2.99	4081		4.16	1.9	1.0	0.2	1.3E-03
$C_{10}H_{12}N_2OH^+$	177.1014	Cotinine	CHN_2O	2.95	4020	3000000	2.32	1.6	2.9	0.10	3.9E-03
$C_{12}H_{16}OH^+$	177.1238		CHO_1	3.29	4484		4.56	3.0	1.6	0.4	2.1E-03
$C_{11}H_{16}N_2H^+$	177.1372		CHN_2	3.39	4627		3.60	1.8	1.6	0.2	2.1E-03
$C_{13}H_{20}H^+$	177.1629	C_{13} Aromatics	CH	2.80	3822	0.0005	5.25	7.9	1.3	0.4	1.7E-03

$C_{10}H_{14}N_2OH^+$	179.1170	Hydroxynicotine	CHN_2O	2.96	4035		2.32	1.5	0.7	0.4	9.7E-04
$C_{12}H_{18}OH^+$	179.1413		CHO_1	3.30	4496		4.56	2.4	1.2	0.3	1.6E-03
$C_{13}H_{22}H^+$	179.1789		CH	2.82	3842		5.25	3.1	0.4	0.09	4.7E-04
$C_{11}H_{16}O_2H^+$	181.1221		CHO_2	2.91	3970		4.55	1.7	1.1	0.1	1.5E-03
$C_{10}H_{16}N_2OH^+$	181.1335		CHN_2O	2.97	4050		2.32	1.6	2.3	0.05	3.0E-03
$C_{12}H_{20}OH^+$	181.1554		CHO_1	3.31	4507		4.56	1.7	0.6	0.3	8.1E-04
$C_{13}H_{24}H^+$	181.1945		CH	2.83	3862		5.25	0.5	0.1	0.02	1.8E-04
$C_{13}H_{11}NH^+$	182.0954	Methylcarbazole	CHN_1	3.03	4127		3.75	0.2	0.4	0.05	5.4E-04
$C_{13}H_{10}OH^+$	183.0787	Benzophenone	CHO_1	3.31	4519	17	4.12	0.6	0.7	0.1	9.1E-04
$C_{10}H_{14}O_3H^+$	183.0993		CHO_3	2.91	3966		4.30	0.6	0.5	0.04	5.9E-04
$C_{14}H_{14}H^+$	183.1157	Dimethylbiphenyls	CH	2.85	3882		4.76	2.1	2.9	0.5	3.8E-03
$C_{13}H_{26}H^+$	183.2105		CH	2.85	3882		5.25	1.1	0.3	0.06	4.0E-04
$C_{13}H_{13}NH^+$	184.1122		CHN_1	3.04	4142		3.75	0.6	1.0	0.1	1.4E-03
$C_{14}H_{16}H^+$	185.1308	Naphthalene + C_4	CH	2.86	3901		4.76	3.8	3.5	0.5	4.6E-03
$C_{13}H_{15}NH^+$	186.1305		CHN_1	3.05	4157		3.75	1.2	1.3	0.2	1.7E-03
$C_{13}H_{14}OH^+$	187.1085		CHO_1	3.33	4542		4.12	1.2	1.2	0.1	1.5E-03
$C_{14}H_{18}H^+$	187.1464		CH	2.88	3921		4.76	5.2	2.7	0.3	3.5E-03
$C_{13}H_{17}NH^+$	188.1490		CHN_1	3.06	4172		3.75	1.3	0.9	0.1	1.1E-03
$C_{13}H_{16}OH^+$	189.1249		CHO_1	3.34	4553		4.12	1.8	1.5	0.2	1.9E-03
$C_{14}H_{20}H^+$	189.1623		CH	2.89	3940		4.76	6.1	1.7	0.2	2.2E-03
$C_{13}H_{19}NH^+$	190.1648		CHN_1	3.07	4187		3.75	1.3	0.6	0.08	7.4E-04
$C_{10}H_{14}N_2$ $(^+N_2)H^+$	191.1400	Nicotine-nitrogen adduct	CHN_2	3.06	4171		1.71	4.5	4.1	0.4	5.4E-03
$C_{13}H_{18}OH^+$	191.1458		CHO_1	3.35	4565		4.12	1.6	2.0	0.2	2.6E-03

$C_{14}H_{22}H^+$	191.1776	C_{14} Aromatics	CH	2.90	3960		4.76	7.9	1.3	0.2	1.7E-03
$C_{13}H_{21}NH^+$	192.1805		CHN_1	3.08	4202		3.75	1.6	0.4	0.06	4.7E-04
$C_{13}H_{20}OH^+$	193.1574		CHO_1	3.36	4577		4.12	2.2	1.2	0.3	1.6E-03
$C_{14}H_{24}H^+$	193.1926		CH	2.92	3979		4.76	2.2	0.3	0.05	4.1E-04
$C_{13}H_{22}OH^+$	195.1734	Solanone	CHO_1	3.37	4589		4.12	3.2	1.2	0.6	1.5E-03
$C_{14}H_{26}H^+$	195.2089		CH	2.93	3998		4.76	0.4	0.1	0.03	1.8E-04
$C_{14}H_{12}OH^+$	197.0961		CHO_1	3.37	4601		3.68	0.3	0.4	0.06	5.4E-04
$C_{12}H_{20}O_2H^+$	197.1559	Geranyl acetate	CHO_2	3.01	4110	0.0041	4.14	0.4	0.4	0.02	5.1E-04
$C_{14}H_{28}H^+$	197.2260	Tetradecene	CH	2.95	4017	0.0000012	4.76	0.9	0.3	0.05	3.6E-04
$C_{14}H_{15}NH^+$	198.1300		CHN_1	3.12	4247		3.34	0.3	0.5	0.06	6.3E-04
$C_{15}H_{18}H^+$	199.1464	Naphthalene + C_5	CH	2.96	4036		4.28	1.5	1.6	0.2	2.1E-03
$C_{14}H_{17}NH^+$	200.1468		CHN_1	3.13	4262		3.34	0.5	0.6	0.07	7.4E-04
$C_{14}H_{16}OH^+$	201.1283		CHO_1	3.39	4625		3.68	0.7	0.8	0.09	1.1E-03
$C_{15}H_{20}H^+$	201.1621		CH	2.97	4055		4.28	3.0	2.0	0.2	2.6E-03
$C_{13}H_{14}O_2H^+$	203.1047		CHO_2	3.05	4161		3.72	0.7	0.8	0.04	1.1E-03
$C_{14}H_{18}OH^+$	203.1424		CHO_1	3.40	4637		3.68	0.9	0.9	0.1	1.2E-03
$C_{15}H_{22}H^+$	203.1785		CH	2.99	4074		4.28	6.7	2.7	0.2	3.6E-03
$C_{13}H_{16}O_2H^+$	205.1228		CHO_2	3.07	4179		3.72	0.5	0.5	0.05	6.0E-04
$C_{14}H_{20}OH^+$	205.1585		CHO_1	3.41	4649		3.68	1.3	1.1	0.2	1.5E-03
$C_{15}H_{24}H^+$	205.1941	Sesquiterpenes and C_{15} Aromatics	CH	3.00	4092		4.28	13.7	3.5	0.2	4.5E-03
$C_{13}H_{18}O_2H^+$	207.1382		CHO_2	3.08	4196		3.72	0.7	0.6	0.06	7.7E-04
$C_{14}H_{22}OH^+$	207.1729		CHO_1	3.42	4661		3.68	1.3	0.9	0.3	1.2E-03
$C_{15}H_{26}H^+$	207.2085		CH	3.02	4111	0.003	4.28	3.0	0.8	0.06	1.0E-03

$C_{10}H_{13}N_3O_2H^+$	208.1059	Nicotine-derived nitrosamine ketone	CHN_3O_2	4.00	5457		0.55	0.05	0.06	<0.01	7.3E-05
$C_{13}H_{20}O_2H^+$	209.1528		CHO_2	3.09	4213		3.72	1.2	1.0	0.1	1.3E-03
$C_{14}H_{24}OH^+$	209.1861		CHO_1	3.43	4673		3.68	0.5	0.3	0.06	3.8E-04
$C_{15}H_{28}H^+$	209.2252		CH	3.03	4129		4.28	0.3	0.1	0.02	1.8E-04
$C_{12}H_{19}NO_2H^+$	210.1471		CHN_1O_2	3.71	5052		2.05	0.8	0.5	0.1	6.7E-04
$C_{11}H_{18}N_2O_2H^+$	211.1442		CHN_2O_2	3.14	4278		1.30	0.4	0.5	0.08	6.3E-04
$C_{13}H_{22}O_2H^+$	211.1667		CHO_2	3.10	4230		3.72	0.5	0.4	0.06	5.1E-04
$C_{15}H_{30}H^+$	211.2403	Pentadecene	CH	3.04	4148		4.28	0.7	0.4	0.03	5.1E-04
$C_{11}H_{20}N_2O_2H^+$	213.1601		CHN_2O_2	3.15	4293		1.30	0.6	0.6	0.07	8.2E-04
$C_{16}H_{20}H^+$	213.1654	Naphthalene + C_6	CH	3.06	4166		3.79	0.2	0.2	0.03	2.7E-04
$C_{16}H_{22}H^+$	215.1783		CH	3.07	4184		3.79	1.0	0.9	0.08	1.2E-03
$C_{14}H_{16}O_2H^+$	217.1244		CHO_2	3.14	4280		3.30	0.3	0.5	0.02	6.0E-04
$C_{15}H_{20}OH^+$	217.1579		CHO_1	3.46	4722		3.24	0.6	0.6	0.10	8.4E-04
$C_{16}H_{24}H^+$	217.1931		CH	3.08	4203		3.79	1.5	0.9	0.08	1.2E-03
$C_{15}H_{22}OH^+$	219.1730		CHO_1	3.47	4734		3.24	0.9	0.9	0.2	1.1E-03
$C_{16}H_{26}H^+$	219.2085	C_{16} Aromatics	CH	3.10	4221	0.0002	3.79	1.5	0.8	0.09	1.0E-03
$C_{14}H_{20}O_2H^+$	221.1536		CHO_2	3.16	4314		3.30	0.3	0.2	0.04	2.9E-04
$C_{15}H_{24}OH^+$	221.1915	Sesquiterpenoids	CHO_1	3.48	4747		3.24	0.7	0.7	0.2	8.7E-04
$C_{16}H_{28}H^+$	221.2227		CH	3.11	4239		3.79	0.4	0.2	0.03	3.0E-04
$C_{14}H_{22}O_2H^+$	223.1690		CHO_2	3.18	4331		3.30	0.2	0.2	0.03	2.9E-04
$C_{15}H_{26}OH^+$	223.2026	Sesquiterpenoids	CHO_1	3.49	4759		3.24	0.3	0.2	0.05	3.2E-04
$C_{16}H_{30}H^+$	223.2423		CH	3.12	4257		3.79	0.1	0.1	0.01	1.7E-04
$C_{17}H_{20}H^+$	225.1617		CH	3.14	4275		3.31	0.2	0.2	0.03	2.8E-04

$C_{15}H_{28}OH^+$	225.2183		CHO_1	3.50	4771	3.24	0.2	0.1	0.03	1.5E-04
$C_{16}H_{32}H^+$	225.2563	Hexadecenes	CH	3.14	4275	3.79	0.3	0.3	0.05	3.6E-04
$C_{12}H_{22}N_2O_2H^+$	227.1724		CHN_2O_2	3.23	4397	0.94	0.3	0.3	0.04	3.5E-04
$C_{17}H_{22}H^+$	227.1818	Naphthalene + C_7	CH	3.15	4292	3.31	0.2	0.2	0.02	2.7E-04
$C_{15}H_{30}OH^+$	227.2359	C_{15} Carbonyls	CHO_1	3.51	4784	3.24	0.2	0.09	0.04	1.2E-04
$C_{12}H_{24}N_2O_2H^+$	229.1923		CH	3.16	4310	0.94	0.5	0.5	0.05	6.2E-04
$C_{14}H_{28}O_2H^+$	229.2136		CHO_2	3.21	4380	3.30	0.2	0.1	0.02	1.4E-04
$C_{16}H_{22}OH^+$	231.1744		CHO_1	3.53	4808	2.79	0.2	0.2	0.03	2.1E-04
$C_{17}H_{26}H^+$	231.2087		CH	3.17	4328	3.31	0.5	0.4	0.05	5.7E-04
$C_{15}H_{20}O_2H^+$	233.1534		CHO_2	3.24	4413	2.87	0.2	0.2	0.02	2.2E-04
$C_{16}H_{24}OH^+$	233.1892		CHO_1	3.54	4821	2.79	0.2	0.2	0.04	2.4E-04
$C_{17}H_{28}H^+$	233.2247	C_{17} Aromatics	CH	3.19	4345	3.31	0.4	0.3	0.03	4.0E-04
$C_{15}H_{22}O_2H^+$	235.1671		CHO_2	3.25	4430	2.87	0.4	0.3	0.07	3.3E-04
$C_{17}H_{30}H^+$	235.2426		CH	3.20	4363	3.31	0.05	0.06	<0.01	8.2E-05
$C_{17}H_{32}H^+$	237.2561		CH	3.21	4380	3.31	0.05	0.07	<0.01	9.6E-05
$C_{16}H_{30}OH^+$	239.2349	Hexadecanoic acid fragment	CHO_1	3.56	4858	2.79	0.06	0.04	0.01	5.7E-05
$C_{17}H_{34}H^+$	239.2714	Heptadecenes	CH	3.23	4398	3.31	0.07	0.2	0.02	2.3E-04
$C_{18}H_{24}H^+$	241.1925	C_{18} Naphthalene	CH	3.24	4415	2.82	0.2	0.2	0.03	2.7E-04
$C_{18}H_{26}H^+$	243.2090		CH	3.25	4432	2.82	0.3	0.3	0.04	3.9E-04
$C_{15}H_{30}O_2H^+$	243.2300		CHO_2	3.30	4495	2.87	0.10	0.07	0.02	9.7E-05
$C_{17}H_{24}OH^+$	245.1898		CHO_1	3.59	4895	2.35	0.06	0.06	0.01	7.7E-05
$C_{18}H_{28}H^+$	245.2245		CH	3.26	4449	2.82	0.3	0.3	0.03	3.8E-04
$C_{15}H_{32}O_2H^+$	245.2457		CHO_2	3.31	4511	2.87	0.1	0.07	0.02	9.8E-05

$C_{17}H_{26}OH^+$	247.2051		CHO_1	3.60	4908		2.35	0.06	0.06	0.01	7.7E-05
$C_{18}H_{30}H^+$	247.2410	C_{18} Aromatics	CH	3.28	4467		2.82	0.2	0.2	0.02	2.2E-04
$C_{18}H_{32}H^+$	249.2558		CH	3.29	4484		2.82	0.06	0.05	<0.01	7.0E-05
$C_{18}H_{34}H^+$	251.2737		CH	3.30	4501		2.82	0.02	0.02	<0.01	2.1E-05
$C_{18}H_{36}H^+$	253.2879	Octadecenes	CH	3.31	4517		2.82	0.05	0.08	0.02	1.1E-04
$C_{19}H_{26}H^+$	255.2080	Naphthalene + C_9	CH	3.33	4534		2.33	0.1	0.1	0.02	1.6E-04
$C_{19}H_{28}H^+$	257.2241		CH	3.34	4551		2.33	0.2	0.2	0.03	2.8E-04
$C_{19}H_{30}H^+$	259.2396		CH	3.35	4568		2.33	0.3	0.3	0.04	3.7E-04
$C_{18}H_{28}OH^+$	261.2194	Linolenic acid fragment	CHO_1	3.66	4995	49	1.91	0.04	0.04	<0.01	5.4E-05
$C_{19}H_{32}H^+$	261.2555	C_{19} Aromatics	CH	3.36	4584		2.33	0.1	0.1	0.02	1.9E-04
$C_{19}H_{34}H^+$	263.2719		CH	3.38	4601		2.33	0.02	0.02	<0.01	2.0E-05
$C_{19}H_{36}H^+$	265.2857		CH	3.39	4618		2.33	0.02	0.02	<0.01	2.3E-05
$C_{19}H_{38}H^+$	267.3046	Nonadecenes	CH	3.40	4634		2.33	0.08	0.1	0.02	1.8E-04
$C_{20}H_{28}H^+$	269.2245	Naphthalene + C_{10}	CH	3.41	4651		1.85	0.2	0.2	0.03	2.2E-04
$C_{20}H_{30}H^+$	271.2400		CH	3.42	4667		1.85	0.6	0.7	0.1	9.5E-04
$C_{20}H_{30}H^+$	271.2486		CH	3.42	4667		1.85	0.3	0.3	0.06	4.4E-04
$C_{20}H_{32}H^+$	273.2553	Diterpenes	CH	3.44	4683		1.85	0.4	0.4	0.06	4.9E-04
$C_{20}H_{34}H^+$	275.2734	C_{20} Aromatics	CH	3.45	4699		1.85	0.07	0.07	<0.01	9.4E-05
$C_{20}H_{36}H^+$	277.2900		CH	3.46	4716		1.85	0.01	<0.01	<0.01	1.2E-05
$C_{16}H_{22}O_4H^+$	279.1581	Dibutyl phthalate	CHO_4	3.34	4547	9.3	1.35	0.09	0.03	0.01	3.3E-05
$C_{20}H_{38}H^+$	279.3049	Neophytadiene	CH	3.47	4732		1.85	0.03	0.08	0.01	1.1E-04
$C_{20}H_{40}H^+$	281.3227	Eicosenes	CH	3.48	4748		1.85	0.01	0.01	<0.01	1.5E-05
$C_{22}H_{18}H^+$	283.1490		CH	3.49	4764		0.87	0.07	0.01	<0.01	1.6E-05

$C_{19}H_{38}OH^+$	283.2975		CHO_1	3.76	5132	1.46	0.03	0.02	<0.01	2.8E-05
$C_{21}H_{38}H^+$	291.3030		CH	3.54	4828	1.36	<0.01	<0.01	<0.01	3.3E-06
$C_{21}H_{40}H^+$	293.3154		CH	3.55	4843	1.36	<0.01	<0.01	<0.01	4.0E-06
$C_{22}H_{30}H^+$	295.2399		CH	3.56	4859	0.87	<0.01	<0.01	<0.01	3.2E-06
$C_{21}H_{42}H^+$	295.3299		CH	3.56	4859	1.36	0.01	<0.01	<0.01	7.0E-06
$C_{22}H_{38}H^+$	303.3021	C_{22} Aromatics	CH	3.61	4921	0.87	0.03	<0.01	<0.01	7.4E-06
$C_{22}H_{40}H^+$	305.3169		CH	3.62	4937	0.87	<0.01	<0.01	<0.01	1.2E-06
$C_{22}H_{42}H^+$	307.3381		CH	3.63	4952	0.87	<0.01	<0.01	<0.01	7.4E-07
$C_{22}H_{44}H^+$	309.3529		CH	3.64	4968	0.87	<0.01	<0.01	<0.01	6.2E-07
$C_{23}H_{34}H^+$	311.2743		CH	3.66	4983	0.39	<0.01	<0.01	<0.01	1.1E-06
$C_{23}H_{40}H^+$	317.3177	C_{23} Aromatics	CH	3.69	5029	0.39	<0.01	<0.01	<0.01	2.6E-06
$C_{22}H_{39}NH^+$	318.3197		CHN_1	3.74	5095	0.09	<0.01	<0.01	<0.01	1.3E-06
$C_{23}H_{42}H^+$	319.3353		CH	3.70	5044	0.39	<0.01	<0.01	<0.01	1.4E-06
$C_{23}H_{44}H^+$	321.3495		CH	3.71	5059	0.39	<0.01	<0.01	<0.01	1.4E-06
$C_{23}H_{46}H^+$	323.3669		CH	3.72	5074	0.39	<0.01	<0.01	<0.01	2.1E-06
$C_{24}H_{38}H^+$	327.3021		CH	3.74	5104	-0.10	0.02	<0.01	<0.01	2.4E-06
$C_{24}H_{40}H^+$	329.3222		CH	3.75	5119	-0.10	<0.01	<0.01	<0.01	1.4E-06
$C_{24}H_{46}H^+$	335.3631		CH	3.79	5163	-0.10	<0.01	<0.01	<0.01	7.9E-07
$C_{24}H_{48}H^+$	337.3817		CH	3.80	5178	-0.10	<0.01	<0.01	<0.01	1.4E-06
$C_{25}H_{40}H^+$	341.3263	Sesterterpenes	CH	3.82	5207	-0.58	<0.01	<0.01	<0.01	8.3E-07
$C_{25}H_{42}H^+$	343.3335		CH	3.83	5222	-0.58	<0.01	<0.01	<0.01	1.3E-06
$C_{25}H_{44}H^+$	345.3543	C_{25} Aromatics	CH	3.84	5237	-0.58	<0.01	<0.01	<0.01	1.1E-06
$C_{25}H_{46}H^+$	347.3662		CH	3.85	5251	-0.58	<0.01	<0.01	<0.01	6.9E-07

$C_{25}H_{48}H^+$	349.3822		CH	3.86	5266		-0.58	<0.01	<0.01	<0.01	6.8E-07
$C_{25}H_{50}H^+$	351.3968		CH	3.87	5280		-0.58	<0.01	<0.01	<0.01	8.6E-07
$C_{26}H_{48}H^+$	361.3798		CH	3.93	5352		-1.07	<0.01	<0.01	<0.01	3.3E-07
$C_{26}H_{52}H^+$	365.4128		CH	3.95	5380		-1.07	<0.01	<0.01	<0.01	3.6E-07
$C_{24}H_{38}O_4H^+$	391.2827	Bis(2-ethylhexyl) phthalate	CHO_4	3.79	5172	1	-1.88	<0.01	<0.01	<0.01	2.3E-06

* The specific isomers listed for each formula were not all confirmed by other methods where specific compound names are provided. Conversely, isomers or additional identifications were not always included, especially if insufficient evidence exists in either previous literature or in our measurements to posit them as potential candidates. Identifications were based on GC-EI-MS and GC-TOF observations, as well as existing tobacco smoke literature. Additionally, the relative ratios for SHS presented here are representative of sidestream smoking conditions, and the relative abundances of some compounds could potentially shift with higher mainstream smoke combustion temperatures, which could also influence relative concentrations in LLF. Glycerol, propylene glycol, and ethylene glycol are listed as potential IDs with past identifications in tobacco smoke, though there is significant expected fragmentation with PTR, so the reported concentrations may be lower limits and may also have contributions on these molecular formulas from other isomers and fragments.

† While observed in some trials, formaldehyde and methanol concentrations were not provided due to instrument configurations during the majority of the study, leading to a lack of observations and sensitivity information below *m/z* 42.

^ Two masses were assigned a formula identification of $C_{20}H_{30}H^+$ (expected m/z = 271.2419) because of a lack of other prominent formulas nearby. The m/z were far enough apart that they were not grouped together, but mass drift between experimental data files may have separated them.

Other notes:

- Henry's law constants are from Sander, 2015.[53] Saturation concentrations were calculated using the Li et al. parameterization.[22]

Table S4A. PM off-gassing concentrations, aged ≤1.5 hours, by carbon number and elemental composition, measured by GC-TOF [abund L^{-1}]

C#	CH	CHN_1	CHN_2	CHO_1	CHO_2	CHN_1O_1	CHN_2O_1
4		5.5E+02	4.0E+04	3.2E+04	1.6E+05	3.7E+05	5.0E+03
5		3.8E+04	8.4E+04	7.5E+04	2.9E+05	8.0E+05	1.2E+04
6	1.2E+03	4.0E+04	1.2E+05	2.8E+05	3.3E+05	7.4E+05	6.5E+04
7	2.3E+04	4.6E+04	9.9E+04	3.0E+05	2.2E+05	3.9E+05	5.3E+04
8	2.1E+04	1.6E+05	2.2E+05	3.8E+05	2.6E+05	2.3E+05	3.3E+04
9	1.9E+04	3.2E+05	3.1E+05	3.2E+05	2.3E+05	2.7E+05	5.1E+04
10	1.0E+05	2.4E+05	3.4E+06	3.3E+05	1.7E+05	1.4E+05	2.7E+05
11	6.7E+04	3.2E+05	2.4E+05	1.8E+05	1.6E+05	8.5E+04	8.4E+04
12	1.4E+05	2.4E+05	5.5E+04	2.7E+05	1.4E+05	2.8E+04	3.6E+04
13	2.8E+05	1.1E+05	9.0E+03	4.5E+05	2.0E+05	1.6E+04	4.4E+04
14	4.4E+05	3.1E+04	2.7E+03	1.8E+05	1.4E+05	4.7E+03	1.5E+04
15	8.8E+05	1.0E+04	1.1E+03	6.5E+04	1.6E+05	2.4E+03	9.0E+03
16	2.9E+05	5.9E+03	3.1E+02	2.4E+04	4.7E+04	2.5E+03	8.1E+03
17	2.0E+05	7.1E+03	9.8E+02	7.5E+03	1.6E+05	1.8E+03	2.9E+03
18	1.6E+05	6.7E+03	3.5E+02	2.1E+03	5.5E+04	1.7E+03	4.3E+03
19	1.6E+05	5.0E+03	3.5E+02	4.9E+02	3.5E+04	2.8E+03	2.3E+03
20	5.7E+05	4.9E+03	7.4E+02	9.2E+02	4.7E+04	2.1E+03	2.1E+03
21	3.9E+04	4.5E+03	5.5E+02	8.6E+01	1.1E+04	1.3E+03	1.4E+03
22	1.6E+04	2.5E+03	6.4E+02	1.5E-02	7.3E+03	6.2E+03	9.2E+02
23	1.7E+04	2.4E+03	5.6E+02	7.8E+02	9.3E+03	1.1E+03	7.7E+02
24	1.9E+04	1.8E+03	5.8E+02	3.8E+03	7.0E+03	6.2E+02	4.9E+02
25	3.4E+04	1.0E+03	5.0E+02	3.6E+03	6.5E+03	3.9E+02	1.6E+03
26	1.4E+04						
27	1.3E+04						
28	1.1E+04						
29	1.3E+04						
30	1.9E+04						

Table S4B. LLF off-gassing concentrations, aged ≤1 hours, by carbon number and elemental composition, measured by GC-TOF [abund L^{-1}]

C#	CH	CHN_1	CHN_2	CHO_1	CHO_2	CHN_1O_1	CHN_2O_1
4		1.1E+04	3.7E+03	2.3E+04	2.0E+04	1.5E+04	4.3E+02
5		3.4E+05	1.3E+04	2.0E+05	2.7E+05	2.0E+04	3.8E+03
6	1.8E+04	3.7E+05	2.7E+04	2.1E+05	1.3E+05	3.0E+04	5.2E+03
7	2.4E+04	4.8E+05	1.8E+04	2.6E+05	5.3E+04	1.9E+04	8.2E+03
8	2.5E+04	3.4E+05	2.1E+04	3.2E+05	5.1E+04	1.7E+04	1.2E+04
9	1.9E+04	3.0E+05	5.7E+03	2.2E+05	4.0E+04	3.4E+04	8.7E+03
10	8.2E+04	1.6E+05	2.3E+04	1.6E+05	4.1E+04	1.1E+04	8.5E+03
11	1.9E+04	8.3E+04	2.7E+03	6.5E+04	1.9E+04	4.8E+03	8.9E+03
12	1.8E+04	3.2E+04	6.1E+02	4.6E+04	1.7E+04	1.3E+03	6.9E+03
13	2.0E+04	1.3E+04	3.0E+02	4.6E+04	2.1E+04	7.9E+02	1.1E+03
14	7.1E+04	7.0E+03	3.9E+02	1.7E+04	2.3E+04	7.5E+02	1.2E+03
15	2.5E+05	4.4E+03	2.8E+02	6.1E+03	2.4E+04	1.7E+03	2.3E+03
16	2.0E+04	5.0E+03	2.2E+02	3.0E+03	5.2E+03	1.2E+03	5.7E+02
17	1.3E+04	3.2E+03	2.6E+02	1.5E+03	1.6E+04	1.1E+03	5.9E+02
18	1.4E+04	4.6E+03	2.2E+02	1.0E+03	6.5E+03	1.1E+03	4.7E+02
19	1.5E+04	2.7E+03	2.5E+02	2.9E+02	5.7E+03	1.3E+03	5.7E+02
20	7.0E+04	1.7E+03	3.4E+02	4.7E+02	6.3E+03	1.1E+03	6.8E+02
21	5.4E+03	1.8E+03	2.6E+02	3.9E+02	1.8E+03	9.6E+02	7.9E+02
22	3.0E+03	2.3E+03	1.9E+02	2.3E+02	1.9E+03	2.0E+03	3.5E+02
23	4.3E+03	7.6E+02	1.4E+02	3.8E+02	3.1E+03	3.4E+02	2.6E+02
24	7.4E+03	6.5E+02	8.6E+01	9.1E+02	2.3E+03	2.3E+02	1.5E+02
25	2.1E+04	4.7E+02	4.7E+01	7.8E+02	2.3E+03	1.7E+02	1.2E+02
26	5.3E+03						
27	5.6E+03						
28	3.9E+03						
29	5.6E+03						
30	1.1E+04						

Table S4C. Gas-phase secondhand smoke concentrations, by carbon number and elemental composition, measured by GC-TOF [abund L^{-1}]

C#	CH	CHN_1	CHN_2	CHO_1	CHO_2	CHN_1O_1	CHN_2O_1
4		4.2E+04	5.0E+05	4.4E+05	1.2E+06	3.9E+05	1.8E+04
5		2.9E+06	1.1E+06	3.5E+06	3.9E+06	1.0E+06	6.9E+04
6	3.5E+05	2.9E+06	1.7E+06	3.3E+06	2.9E+06	1.0E+06	1.5E+05
7	1.0E+06	3.5E+06	1.0E+06	3.6E+06	1.8E+06	6.9E+05	1.0E+05
8	1.5E+06	2.4E+06	9.5E+05	3.0E+06	1.3E+06	4.9E+05	9.5E+04
9	1.7E+06	2.4E+06	8.3E+05	2.6E+06	1.0E+06	4.4E+05	7.6E+04
10	2.9E+06	1.2E+06	7.3E+06	2.5E+06	7.6E+05	1.9E+05	3.6E+05
11	1.6E+06	6.5E+05	4.0E+05	9.7E+05	5.1E+05	1.2E+05	1.6E+05
12	1.1E+06	2.6E+05	7.4E+04	3.1E+05	3.4E+05	3.7E+04	5.5E+04
13	8.6E+05	1.0E+05	1.8E+04	1.6E+05	4.0E+05	2.4E+04	6.7E+04
14	7.2E+05	4.3E+04	7.8E+03	4.2E+04	3.0E+05	1.8E+04	3.4E+04
15	1.0E+06	2.9E+04	4.9E+03	1.7E+04	2.6E+05	2.0E+04	2.2E+04
16	2.7E+05	2.5E+04	6.0E+03	7.5E+03	2.9E+05	1.6E+04	1.3E+04
17	1.4E+05	1.5E+04	2.3E+03	3.9E+03	3.0E+05	1.7E+04	1.0E+04
18	1.2E+05	1.1E+04	2.6E+03	7.6E+03	8.7E+05	1.9E+04	8.7E+03
19	1.0E+05	1.3E+04	3.1E+03	1.3E+04	7.8E+04	2.7E+04	7.4E+03
20	3.7E+05	1.1E+04	5.1E+03	3.2E+04	8.6E+04	1.3E+04	8.6E+03
21	2.7E+04	1.1E+04	4.4E+03	1.3E+03	3.8E+04	9.9E+03	7.4E+03
22	1.8E+04	9.1E+03	5.4E+03	3.6E+03	3.2E+04	8.3E+04	5.9E+03
23	1.7E+04	1.1E+04	4.8E+03	3.0E+03	3.8E+04	7.9E+03	6.2E+03
24	2.9E+04	9.0E+03	3.7E+03	1.1E+04	3.2E+04	8.7E+03	4.1E+03
25	7.2E+04	7.9E+03	4.0E+03	8.2E+03	2.9E+04	5.1E+03	9.7E+03
26	2.3E+04						
27	6.0E+04						
28	8.9E+04						
29	1.8E+05						
30	5.3E+04						

Table S5A. Polycyclic aromatic compounds in PM off-gassing evaluated using offline PUF samples

	Sample Mass [pg/sample]			
Compound	LOQ	Sample 1	Sample 2	Sample 3
9-Fluorenone	26241	298260	275525	290516
2-Methyl-1,4-naphthoquinone	6266	147885	81872	83931
9,10-Anthraquinone	12729	57409	23044	41414
1,4-Naphthoquinone	2259	15569	13121	19279
Benzo[a]fluorenone	1580	9271	18642	26345
Benzo[b]fluorenone	1159	4100	9930	13088
9,10-Phenanthrenequinone	300	2270	4324	5144
Benzanthrone	1837	1825	4620	4893
Benz[a]anthracene-7,12-dione	849	481	250	<LOQ
1-Nitronaphthalene	376	278	<LOQ	*
2-Nitronaphthalene	361	270	<LOQ	<LOQ
2-Nitrofluorene	421	<LOQ	<LOQ	*
2-Nitrofluoranthene	593	<LOQ	<LOQ	<LOQ
1-Nitropyrene	143	<LOQ	16	<LOQ
9-Nitroanthracene	478	<LOQ	<LOQ	<LOQ
2-Nitro-9-fluorenone	155	ND	ND	ND
3-Nitrophenanthrene	275	ND	ND	ND
9-Nitrophenanthrene	75	ND	ND	ND
2-Nitropyrene	75	ND	ND	ND
6-Nitrochrysene	75	ND	ND	ND
3-Nitrobenzanthrone	300	ND	ND	ND
1,3-Dinitropyrene	150	ND	ND	ND
1,6-Dinitropyrene	300	ND	ND	ND
1,8-Dinitropyrene	300	ND	ND	ND
6-Nitrobenz[a]pyrene	300	ND	ND	ND

Values shown for Samples 1-3 are blank corrected.

ND - Not detected

* - No data/Not determined

As the values are blank subtracted, all listed values were present above the LOQ prior to blank subtraction. Sampled volumes varied between samples (19.4, 32.9, and 86.4 m^3 for samples 1-3, respectively), and PM loadings on the collected filter from the smoking chamber may have varied between samples with PM concentrations in the chamber. The flow rates used with the PUF collection setup (i.e., 17-30 LPM) and measurement method were much larger (~100x) than those in the main filter off-gassing setup, resulting in non-representative vertical transport velocities and a large diluting flow given that off-gassing would have likely been strongly limited in this PUF sampling setup by internal diffusion within PM, and potentially interfacial transport. Thus, the results are presented in pg/sample.

Table S5B. Polychlorinated biphenyls and dibenzo-dioxins/furans (PCBs, PCDD/Fs) evaluated in PUF filter samples

	Sample Mass [pg/sample]			
Compound	Sample 1	Sample 2	Sample 3	Blank
PCB 77	4.6	<328	6.4	4.4
PCB 81	<6.0	<230	<5.98	<1.36
PCB 105	14.4	<67.4	16.2	9.4
PCB 114	<6.96	<65.6	<6.96	<2.28
PCB 118	46.0	<74	52.4	34.0
PCB 123	<7.6	<66.2	<7.6	<2.42
PCB 126	<6.8	<394	<6.80	<4.88
PCB 156	5.2	<42.4	7.2	2.6
PCB 157	<2.94	<52.4	<4.34	<1.06
PCB 167	3.6	<37.6	<3.98	1.6
PCB 169	<3.94	<334	<6.36	<2.30
PCB 189	<1.25	<27.2	<1.48	<1.32
2,3,7,8-TCDD	<0.98	<1.64	<1.38	<0.97
1,2,3,7,8-PeCDD	<1.33	<1.26	<2.06	<0.90
1,2,3,4,7,8-HxCDD	<1.13	<1.13	<1.76	<1.13
1,2,3,6,7,8-HxCDD	<1.29	<1.29	<2.2	<1.29
1,2,3,7,8,9-HxCDD	<1.24	<1.24	<2.44	<1.24
1,2,3,4,6,7,8-HpCDD	<1.74	<3.42	<2.26	<0.88
OCDD	<2.76	<3.70	<1.42	1.52
2,3,7,8-TCDF	<0.81	<1.10	<0.75	<0.56
1,2,3,7,8-PeCDF	<0.68	<1.16	<0.68	<0.68
2,3,4,7,8-PeCDF	<0.33	<1.04	<0.52	<0.73
1,2,3,4,7,8-HxCDF	<0.73	<1.56	<0.74	<0.55
1,2,3,6,7,8-HxCDF	<0.64	<1.32	<0.92	<0.48
2,3,4,6,7,8-HxCDF	<0.72	<1.62	<1.01	<0.54
1,2,3,7,8,9-HxCDF	<1.02	<1.98	<1.24	<0.63
1,2,3,4,6,7,8-HpCDF	<0.94	<1.83	<1.03	<0.65
1,2,3,4,7,8,9-HpCDF	<0.96	<1.71	<0.83	<0.61
OCDF	<1.24	<2.2	<1.87	<1.24

Values have not been blank subtracted (blank values shown on right).
Upper limits are provided in many cases given limitations with extraction standards.

Table S6. Input parameters for multi-compartment modeling

Parameter (Unit)	Value	Description
c_{air} [cm^{-3}]		Concentration in inhaled breath
c_{lung} [cm^{-3}]		Concentration in lung gas phase
c_{LLF} [cm^{-3}]		Concentration in lung lining fluid
c_{blood} [cm^{-3}]		Concentration in blood
c_{tissue} [cm^{-3}]		Concentration in tissue
V_{FRC} [cm^3]	2500	Lung functional reserve capacity
V_{tidal} [cm^3]	750	Lung tidal volume
V_{lung} [cm^3]	$V_{FRC} + 0.5 \times V_{tidal}$	Lung average volume
V_{LLF} [cm^3]	20	LLF volume
V_{blood} [cm^3]	5000	Blood volume
V_{tissue} [cm^3]	20000	Tissue volume
t_{breath} [s]	5	Puff/breath duration
A_{LLF} [cm^2]	1.89×10^6	LLF surface area
α	0.5	Accommodation coefficient*
R [m^3 Pa K^{-1} mol^{-1}]	8.314	Gas constant
T [K]	310	Body temperature
p [bar]	1	Air pressure
M [g mol^{-1}]	see Table S3	Molar mass
W [cm s^{-1}]	$\sqrt{\frac{8 * R * T}{\pi * M}}$	Mean thermal velocity
H' [mol m^{-3} Pa^{-1}]	see Table S3	Henry's law coefficient
$K_{air,LLF}$	$H' \times R \times T$	Air-LLF partitioning coefficient
$K_{LLF,blood}$	1	LLF-blood partitioning coefficient
$K_{blood,tissue}$	1	Blood-tissue partitioning coefficient
$k_{LLF,blood}$ [min^{-1}]	1	LLF-blood transport coefficient
$k_{blood,tissue}$ [h^{-1}]	0.33	Blood-tissue transport coefficient

*Mass accommodation coefficient, i.e., fraction of airborne molecules that adsorb to a surface upon contact

Table S7. Compounds analyzed via Vocus PTR-TOF: average concentrations found in SHS, PM off-gassing, and LLF off-gassing samples compared between a sigmoidal and a piecewise sigmoidal/lognormal fit as described in Section S2.2 and S2.3

Molecular Formula	Ion *m/z*	Potential Compound IDs*	$Sens_{calc}$ [cps $ppbv^{-1}$]	$Sens_{calc}$ [cps $ppbv^{-1}$]	$Conc_{Smoke}$ [ppb]	$Conc_{Smoke}$ [ppb]	$Conc_{PM}$ [ppb]	$Conc_{PM}$ [ppb]	$Conc_{LLF}$ [ppb]	$Conc_{LLF}$ [ppb]
			Sigmoid	Piecewise	Sigmoid	Piecewise	Sigmoid	Piecewise	Sigmoid	Piecewise
CH_2OH^+	31.0163	Formaldehyde	19	19	†	†	†	†	†	†
CH_4OH^+	33.0322	Methanol	30	30	†	†	†	†	†	†
$C_3H_4H^+$	41.0376	Alkyl fragment, Isoprene fragment	428	428	1257.4	1257.2	20.8	20.8	51.9	51.9
$C_2H_3NH^+$	42.0329	Acetonitrile	1365	1365	1336.7	1337.0	1.3	1.3	280.1	280.2
$C_2H_2OH^+$	43.0170	Acetic acid fragment	1484	1484	566.3	566.4	46.9	46.9	24.8	24.8
$C_3H_6H^+$	43.0533	Propene, Alkyl fragment	774	774	311.5	311.4	4.1	4.1	17.5	17.4
$C_2H_5NH^+$	44.0488	Vinylamine	1201	1201	117.5	117.5	2.5	2.5	0.3	0.3
$C_2H_4OH^+$	45.0328	Acetaldehyde	2286	2286	1537.9	1537.8	15.1	15.1	370.1	370.0
CH_3NOH^+	46.0280	Formamide	3007	3007	17.0	17.0	2.4	2.4	2.1	2.1
$C_2H_7NH^+$	46.0643	Ethylmethylamine, Dimethylamine	2293	2293	21.7	21.7	1.4	1.4	0.2	0.2
$CH_2O_2H^+$	47.0120	Formic acid	1767	1767	6.4	6.4	1.3	1.3	0.3	0.3
$C_2H_6OH^+$	47.0484	Ethanol	2090	2090	27.6	27.6	0.8	0.8	1.8	1.8
$CH_4O(H_2O)H^+$	51.0435	Methanol-water adduct	2620	2620	102.6	102.5	0.4	0.4	3.8	3.8
$C_3H_3NH^+$	54.0334	Acrylonitrile	4742	4742	155.6	155.6	0.08	0.08	45.7	45.7
$C_3H_5NH^+$	56.0453	Propionitrile	5230	5230	163.6	163.6	1.7	1.7	23.5	23.5
$C_3H_4OH^+$	57.0332	Acrolein	4077	4077	1043.6	1043.6	8.1	8.1	9.2	9.2
$C_4H_8H^+$	57.0694	Butenes, Alkyl/Butanol/Hexanol fragment	2315	2315	424.8	424.9	7.1	7.1	18.6	18.6

$C_3H_7NH^+$	58.0644	Propenamine	2647	2647	127.3	127.3	1.2	1.2	0.2	0.2
$C_3H_6OH^+$	59.0490	Acetone	4101	4101	2877.2	2877.0	75.2	75.2	510.1	510.0
$C_2H_5NOH^+$	60.0438	Acetamide	4896	4896	73.9	73.9	12.3	12.3	10.1	10.1
$C_3H_9NH^+$	60.0802	C_3 amines	2671	2671	68.1	68.1	0.6	0.6	0.2	0.2
$C_2H_4O_2H^+$	61.0282	Acetic acid	2457	2457	2136.0	2136.1	227.5	227.5	49.7	49.7
$C_2H_6O_2H^+$	63.0436	Ethylene glycol	3079	3079	80.9	81.0	4.1	4.1	17.1	17.1
$CH_2O(H_2O)_2H^+$	67.0410	Formaldehyde-water Adduct	4144	4144	16.9	16.9	0.5	0.5	1.9	1.9
$C_5H_6H^+$	67.0538	1,3-Cyclopentadiene	2489	2489	218.6	218.6	2.1	2.1	4.6	4.6
$C_4H_5NH^+$	68.0492	Pyrrole	3414	3414	588.2	588.2	1.5	1.5	78.5	78.5
$C_4H_4OH^+$	69.0330	Furan	2392	2392	254.6	254.5	8.8	8.8	4.0	4.0
$C_5H_8H^+$	69.0695	Isoprene	2520	2520	1594.6	1594.6	3.2	3.2	22.8	22.8
$C_4H_7NH^+$	70.0651	Pyrroline	3414	3414	329.3	329.3	1.3	1.3	39.9	39.9
$C_3H_2O_2H^+$	71.0124	Propiolic acid	3104	3104	34.9	34.9	2.1	2.1	1.4	1.4
$C_4H_6OH^+$	71.0489	Methacrolein, MVK	4157	4157	571.1	571.2	5.7	5.7	48.4	48.4
$C_5H_{10}H^+$	71.0851	Pentenes, Cyclopentanes, Alkyl fragment	2551	2551	193.6	193.6	3.7	3.7	2.5	2.5
$C_3H_5NOH^+$	72.0440	Acrylamide	4966	4966	19.5	19.5	3.6	3.6	1.9	1.9
$C_4H_9NH^+$	72.0795	Pyrrolidine	3416	3416	43.2	43.2	1.0	1.0	0.05	0.05
$C_3H_4O_2H^+$	73.0280	Methylglyoxal, acrylic acid	3108	3108	71.0	71.0	18.1	18.1	1.4	1.4
$C_4H_8OH^+$	73.0644	2-Butanone, MEK	4163	4163	498.4	498.5	1.9	1.9	130.6	130.6
$C_3H_7NOH^+$	74.0595		4686	4686	32.0	32.0	6.2	6.2	1.9	1.9
$C_3H_6O_2H^+$	75.0440	C_3 ester, C_3 acid, hydroxyacetone,	3112	3112	1334.7	1334.8	17.4	17.4	32.2	32.2

		glycidol								
$C_3H_8O_2H^+$	77.0595	C_3 diols, Propylene glycol	3117	3117	151.7	151.7	12.8	12.8	12.3	12.3
$C_2H_6O_3H^+$	79.0388		3602	3602	86.7	86.7	8.2	8.2	2.4	2.4
$C_6H_6H^+$	79.0537	Benzene	2668	2668	181.9	181.9	1.4	1.4	3.4	3.4
$C_5H_5NH^+$	80.0494	Pyridine	3462	3462	498.9	498.9	9.2	9.2	39.1	39.1
$C_5H_4OH^+$	81.0333	2,4-Cyclopentadiene-1-one	4182	4182	208.6	208.6	8.0	8.0	1.4	1.4
$C_4H_4N_2H^+$	81.0437		4368	4368	12.7	12.7	0.2	0.2	0.3	0.3
$C_6H_8H^+$	81.0696	Hexatriene, Monoterpene fragment	2697	2697	462.9	462.9	5.7	5.7	10.0	10.0
$C_5H_7NH^+$	82.0651	Methylpyrrole	3441	3441	289.0	289.0	2.4	2.4	51.1	51.1
$C_5H_6OH^+$	83.0490	2-Methylfuran	4186	4186	469.6	469.6	3.4	3.4	8.3	8.3
$C_6H_{10}H^+$	83.0853	Hexenes, Monoterpene fragment, C_6 fragment (e.g., hexanal or hexenols)	2725	2725	243.0	243.0	2.4	2.4	4.6	4.6
$C_4H_5NOH^+$	84.0440	Methyloxazoles	4737	4737	10.2	10.2	1.1	1.1	1.3	1.3
$C_5H_9NH^+$	84.0808	Pentanenitrile	3448	3448	187.7	187.7	33.8	33.8	42.9	42.9
$C_4H_4O_2H^+$	85.0282	2-(3H)Furanone	3152	3152	263.3	263.4	8.8	8.8	1.2	1.2
$C_5H_8OH^+$	85.0646	Cyclopentanone	4190	4190	247.1	247.1	2.5	2.5	34.7	34.7
$C_6H_{12}H^+$	85.1009	Hexenes	2753	2753	101.0	101.0	1.8	1.8	0.8	0.8
$C_4H_7NOH^+$	86.0601	2-Pyrrolidinone	4747	4747	33.1	33.1	13.0	13.0	1.9	1.9
$C_5H_{11}NH^+$	86.0953	Piperidine	3457	3457	28.4	28.4	1.5	1.5	0.06	0.06
$C_4H_6O_2H^+$	87.0439	2,3-Butanedione, Butyrolactone	3164	3164	572.6	572.5	14.4	14.4	21.8	21.8
$C_5H_{10}OH^+$	87.0800	Pentanone, pentanal, and others	4193	4193	121.6	121.6	0.5	0.5	35.3	35.3

$C_4H_9NOH^+$	88.0752	C_4 amide	4756	4756	26.7	26.7	3.8	3.8	3.1	3.1
$C_3H_4O_3H^+$	89.0231	Pyruvic acid	3630	3630	16.1	16.1	2.1	2.1	0.8	0.8
$C_4H_8O_2H^+$	89.0595	Butanoic acid, ethyl acetate, C_4 esters	3176	3176	133.9	133.9	3.6	3.6	3.8	3.8
$C_2H_3NO_3H^+$	90.0183		3414	3414	2.8	2.8	0.8	0.8	0.4	0.4
$C_4H_{11}NOH^+$	90.0910	C_4 amine alcohol	4765	4765	13.9	13.9	5.6	5.6	0.1	0.1
$C_3H_6O_3H^+$	91.0383		3634	3634	8.8	8.8	1.5	1.5	1.3	1.3
$C_7H_6H^+$	91.0540	Monoterpene fragment, Cresol fragment	2835	2835	164.5	164.5	9.0	9.0	3.7	3.7
$C_3H_8O_3H^+$	93.0549	Glycerol	3638	3638	19.4	19.4	3.0	3.0	8.5	8.5
$C_7H_8H^+$	93.0694	Toluene	2862	2862	438.4	438.4	2.1	2.1	5.8	5.8
$C_6H_7NH^+$	94.0649	Methylpyridines	3520	3520	423.1	423.1	2.0	2.0	29.8	29.8
$C_6H_6OH^+$	95.0490	Phenol	4204	4204	274.5	274.5	46.6	46.6	4.1	4.1
$C_5H_6N_2H^+$	95.0606	Methylpyrazines, Methylpyrimidines	4400	4400	59.0	59.0	2.3	2.3	0.7	0.7
$C_7H_{10}H^+$	95.0853	Monoterpene fragment	2889	2889	271.1	271.1	4.4	4.4	5.8	5.8
$C_5H_5NOH^+$	96.0440	4-Pyridinol	4791	4791	10.2	10.2	4.4	4.4	1.2	1.2
$C_6H_9NH^+$	96.0804	C_2 Pyrroles	3507	3507	117.8	117.8	0.4	0.4	18.9	18.9
$C_5H_4O_2H^+$	97.0285	Furfural	3231	3231	846.3	846.3	4.5	4.5	22.6	22.6
$C_6H_8OH^+$	97.0644	2,5-Dimethylfuran	4206	4206	386.4	386.4	2.1	2.1	9.6	9.6
$C_5H_8N_2H^+$	97.0751	Pyrazine + C_2 or Imidazole + C_2	4403	4403	1.4	1.4	1.9	1.9	0.7	0.7
$C_7H_{12}H^+$	97.1010	Heptanal fragment, Methylcyclohexane ion	2915	2915	85.9	85.9	1.8	1.8	1.7	1.7
$C_5H_7NOH^+$	98.0597	Furfurylamine, Dimethyloxazoles	4799	4799	20.9	20.9	7.8	7.8	1.8	1.8
$C_6H_{11}NH^+$	98.0958	Isoamyl cyanide, 4-Methylpentanenitrile	3518	3518	59.6	59.6	0.3	0.3	14.7	14.7

$C_5H_6O_2H^+$	99.0439	Furfuryl alcohol	3246	3246	261.7	261.7	17.0	17.0	2.9	2.9
$C_6H_{10}OH^+$	99.0801	Cyclohexanone, Methylcyclopentanone	4208	4208	74.3	74.3	1.4	1.4	11.9	11.9
$C_7H_{14}H^+$	99.1165	Heptenes	2941	2941	8.2	8.2	1.0	1.0	0.3	0.3
$C_4H_5NO_2H^+$	100.0392		4807	4807	3.6	3.6	1.3	1.3	0.4	0.4
$C_5H_9NOH^+$	100.0757	Methylpyrrolidione	4807	4807	24.0	24.0	7.9	7.9	1.1	1.1
$C_4H_4O_3H^+$	101.0231	Succinic anhydride	3651	3651	13.7	13.7	2.2	2.2	0.9	0.9
$C_5H_8O_2H^+$	101.0597	Methyl methacrylate	3262	3262	146.1	146.1	9.3	9.3	8.2	8.2
$C_6H_{12}OH^+$	101.0955	Hexanals, hexanones	4210	4210	25.2	25.2	0.2	0.2	7.6	7.6
$C_5H_{11}NOH^+$	102.0911		4814	4814	25.3	25.3	4.2	4.2	4.5	4.5
$C_4H_6O_3H^+$	103.0389	Acetic anhydride	3654	3654	137.9	137.9	24.0	24.0	2.1	2.1
$C_5H_{10}O_2H^+$	103.0751	C_5 aldehydes, C_5 ketones, C_5 esters, C_5 acids	3277	3277	35.5	35.5	4.4	4.4	1.5	1.5
$C_7H_5NH^+$	104.0479	Benzonitrile	3555	3555	95.7	95.7	1.0	1.0	13.4	13.4
$C_6H_4N_2H^+$	105.0438	Pyridinecarbonitriles	4415	4415	52.7	52.7	1.6	1.6	0.3	0.3
$C_4H_8O_3H^+$	105.0540	4-Hydroxybutanoic acid	3657	3657	35.9	35.9	1.7	1.7	1.9	1.9
$C_8H_8H^+$	105.0696	Styrene	3018	3018	143.7	143.7	5.0	5.0	3.9	3.9
$C_7H_7NH^+$	106.0655	3-Ethenylpyridine	3567	3567	342.9	342.9	10.3	10.3	21.9	21.9
$C_7H_6OH^+$	107.0491	Benzaldehyde	4215	4215	82.4	82.4	2.6	2.6	8.1	8.1
$C_8H_{10}H^+$	107.0854	C_8 aromatics	3044	3044	298.4	298.4	2.2	2.2	4.5	4.5
$C_6H_5NOH^+$	108.0437	Pyridine aldehyde	4835	4835	17.8	17.8	3.6	3.6	1.4	1.4
$C_7H_9NH^+$	108.0807	C_7 Pyridine	3580	3580	172.6	172.6	1.5	1.5	14.8	14.8
$C_6H_4O_2H^+$	109.0282	Benzoquinones	3327	3327	54.6	54.6	6.5	6.5	3.6	3.6

$C_7H_8OH^+$	109.0642	Cresols and anisole	4217	4217	108.6	108.6	25.6	25.6	2.7	2.7
$C_6H_8N_2H^+$	109.0748	C_6 Pyrazines, Benzenediamines, Methylpyridinamines, C_6 Pyrimidines	4420	4420	50.8	50.8	3.2	3.2	0.6	0.6
$C_8H_{12}H^+$	109.1010		3069	3069	138.5	138.5	3.1	3.1	4.1	4.1
$C_6H_7NOH^+$	110.0594	Aminophenol	4842	4842	16.4	16.4	4.8	4.8	0.6	0.6
$C_7H_{11}NH^+$	110.0961	C_7 Pyrroles	3593	3593	51.1	51.1	0.3	0.3	7.6	7.6
$C_6H_6O_2H^+$	111.0441	5-Methylfurfural, 2-Acetylfuran, Catechols	3343	3343	291.1	291.1	5.3	5.3	6.9	6.9
$C_5H_6N_2OH^+$	111.0555	Methoxypyrazine	3531	3531	15.3	15.3	1.5	1.5	0.5	0.5
$C_7H_{10}OH^+$	111.0794	C_7 Furan	4218	4218	189.5	189.5	2.1	2.1	7.0	7.0
$C_8H_{14}H^+$	111.1168		3094	3094	40.6	40.6	1.7	1.7	1.0	1.0
$C_6H_9NOH^+$	112.0753		4848	4848	15.1	15.1	2.9	2.9	0.8	0.8
$C_5H_4O_3H^+$	113.0230	2,5-Furandione, 3-methyl-	3666	3666	24.7	24.7	2.5	2.5	0.4	0.4
$C_6H_8O_2H^+$	113.0596	2-hydroxy-3-methyl-2-cyclopenten-1-one	3360	3360	161.5	161.5	24.4	24.4	1.7	1.7
$C_5H_8N_2OH^+$	113.0731		3544	3544	8.9	8.9	1.1	1.1	0.1	0.1
$C_7H_{12}OH^+$	113.0955	Ethyl cyclopentanone	4220	4220	27.1	27.1	0.4	0.4	5.8	5.8
$C_8H_{16}H^+$	113.1323	Octene	3118	3118	4.9	4.9	0.9	0.9	0.3	0.3
$C_6H_{11}NOH^+$	114.0908	C_2 Pyrrolidinone, Acetylpyrrolidine	4854	4853	11.2	11.2	4.7	4.7	0.6	0.6
$C_5H_6O_3H^+$	115.0388	5-Hydroxymethyl-2[3H]-furanone	3669	3668	39.9	39.9	6.9	6.9	0.7	0.7
$C_6H_{10}O_2H^+$	115.0750	C_6 diketones, C_6 esters, C_6 acid	3378	3377	40.2	40.2	3.3	3.3	2.2	2.2
$C_6H_{13}NOH^+$	116.1071		4860	4857	18.0	18.0	3.5	3.5	4.3	4.3
$C_5H_8O_3H^+$	117.0552	1-(Acetyloxy)-2-	3673	3670	150.5	150.6	48.8	48.8	2.1	2.1

		propanone								
$C_6H_{12}O_2H^+$	117.0905	C_6 esters	3395	3392	15.2	15.2	5.0	5.0	0.9	0.9
$C_8H_7NH^+$	118.0645	Benzeneacetonitrile	3648	3644	69.4	69.5	19.5	19.5	8.2	8.2
$C_8H_6OH^+$	119.0474	Benzofuran	4230	4224	13.8	13.8	0.2	0.2	2.2	2.2
$C_7H_6N_2H^+$	119.0588		4430	4424	11.3	11.3	3.2	3.2	0.4	0.4
$C_5H_{10}O_3H^+$	119.0691		3678	3672	10.6	10.7	2.5	2.5	0.9	0.9
$C_9H_{10}H^+$	119.0850	Indane, Cyclopropylbenzene, α-Methylstyrene	3191	3186	85.0	85.2	3.3	3.3	2.4	2.4
$C_8H_9NH^+$	120.0806	Dihydropyridine or Methylethenylpyridine	3662	3655	34.0	34.1	5.4	5.4	3.7	3.7
$C_8H_8OH^+$	121.0637	Acetophenone and tolualdehydes	4235	4224	44.8	44.9	5.1	5.1	4.6	4.6
$C_7H_8N_2H^+$	121.0728		4432	4421	22.1	22.2	1.6	1.6	1.0	1.0
$C_9H_{12}H^+$	121.1010	C_9 Aromatics	3215	3207	141.1	141.5	1.9	1.9	2.5	2.5
$C_7H_7NOH^+$	122.0592		4876	4861	17.2	17.2	3.2	3.2	1.4	1.4
$C_8H_{11}NH^+$	122.0965	Pyridine + C_3	3676	3665	66.6	66.8	1.6	1.6	6.6	6.6
$C_7H_6O_2H^+$	123.0438	Benzoic acid	3448	3436	17.9	18.0	1.6	1.6	0.9	0.9
$C_6H_6N_2OH^+$	123.0558	Acetylpyrazine	3613	3600	10.9	11.0	1.3	1.3	0.4	0.4
$C_8H_{10}OH^+$	123.0797	C_8 Phenol, Methylanisole	4240	4225	62.4	62.6	16.1	16.2	2.7	2.7
$C_7H_{10}N_2H^+$	123.0920	C_7 Pyrazines	4434	4418	17.5	17.6	1.2	1.2	0.7	0.7
$C_9H_{14}H^+$	123.1168		3238	3227	106.9	107.3	2.0	2.0	2.2	2.3
$C_7H_9NOH^+$	124.0750		4881	4860	12.7	12.7	3.4	3.4	0.5	0.5
$C_8H_{13}NH^+$	124.1097		3691	3675	16.3	16.3	0.3	0.3	2.8	2.8
$C_6H_4O_3H^+$	125.0232	Hydroxybenzoquinone or	3694	3676	17.4	17.4	1.7	1.7	0.7	0.7

		Furandicarboxaldehyde								
$C_7H_8O_2H^+$	125.0589	Guaiacol	3466	3449	95.0	95.5	7.8	7.8	2.2	2.2
$C_6H_8N_2OH^+$	125.0702	Methoxymethylpyrazine	3627	3610	9.8	9.8	2.7	2.7	0.2	0.2
$C_8H_{12}OH^+$	125.0958		4245	4225	81.3	81.7	2.0	2.0	4.8	4.8
$C_9H_{16}H^+$	125.1324		3262	3246	20.0	20.1	1.0	1.0	0.4	0.4
$C_7H_{11}NOH^+$	126.0909		4885	4859	8.2	8.2	2.2	2.2	0.5	0.5
$C_6H_6O_3H^+$	127.0386	5-Hydroxymethyl, 2-furfural	3700	3677	35.9	36.1	11.9	12.0	1.5	1.5
$C_7H_{10}O_2H^+$	127.0750		3484	3462	50.2	50.5	10.4	10.5	0.7	0.7
$C_6H_{10}N_2OH^+$	127.0879		3641	3619	5.5	5.5	0.9	0.9	0.05	0.05
$C_8H_{14}OH^+$	127.1113	6-Methyl-5-hepten-2-one (6-MHO)	4251	4225	15.3	15.4	0.4	0.4	3.9	3.9
$C_9H_{18}H^+$	127.1480	Nonene	3285	3265	3.2	3.2	0.8	0.8	0.1	0.1
$C_{10}H_8H^+$	128.0597	Naphthalene (ionized)	3297	3274	9.5	9.6	2.0	2.0	1.2	1.2
$C_7H_{13}NOH^+$	128.1072		4890	4856	8.5	8.5	2.5	2.5	0.6	0.6
$C_6H_8O_3H^+$	129.0543		3706	3678	52.1	52.5	16.9	17.1	0.3	0.3
$C_{10}H_8H^+$	129.0683	Naphthalene	3308	3283	33.1	33.3	2.3	2.3	4.4	4.5
$C_9H_7NH^+$	130.0646	Quinoline/Isoquinoline	3734	3702	23.8	24.0	14.9	15.1	1.0	1.0
$C_7H_{15}NOH^+$	130.1234		4894	4852	2.4	2.4	0.7	0.8	0.3	0.3
$C_9H_6OH^+$	131.0492		4264	4224	11.9	12.0	1.7	1.8	0.1	0.1
$C_6H_{10}O_3H^+$	131.0695		3713	3678	30.6	30.9	8.0	8.1	0.6	0.6
$C_{10}H_{10}H^+$	131.0843		3331	3300	30.2	30.4	1.8	1.8	2.0	2.0
$C_9H_9NH^+$	132.0810	Skatole	3749	3710	45.9	46.4	16.8	17.0	5.6	5.7
$C_9H_8OH^+$	133.0644	Methylbenzofuran	4271	4223	26.0	26.3	3.5	3.6	2.1	2.1

$C_8H_8N_2H^+$	133.0771		4452	4402	22.9	23.1	10.4	10.5	0.7	0.8
$C_{10}H_{12}H^+$	133.1008	Ethylstyrene, Methylindanes	3354	3316	61.3	62.0	2.2	2.2	1.9	1.9
$C_8H_7NOH^+$	134.0598		4903	4842	7.0	7.1	1.8	1.8	0.5	0.5
$C_9H_{11}NH^+$	134.0947		3764	3717	18.7	18.9	3.7	3.7	2.3	2.3
$C_9H_{10}OH^+$	135.0803	Methyl acetophenone	4279	4221	29.7	30.1	4.1	4.2	3.1	3.1
$C_8H_{10}N_2H^+$	135.0962		4457	4398	7.6	7.7	1.9	2.0	0.4	0.4
$C_{10}H_{14}H^+$	135.1166	C_{10} Aromatics	3377	3332	90.9	92.2	3.7	3.7	1.9	1.9
$C_8H_9NOH^+$	136.0752		4907	4836	11.5	11.7	2.2	2.2	0.9	0.9
$C_9H_{13}NH^+$	136.1126		3778	3724	26.5	26.9	4.2	4.2	3.3	3.3
$C_8H_8O_2H^+$	137.0591		3574	3519	18.8	19.1	3.1	3.1	0.8	0.8
$C_7H_8N_2OH^+$	137.0711		3715	3657	7.7	7.9	1.5	1.6	0.3	0.3
$C_9H_{12}OH^+$	137.0957		4286	4220	31.9	32.4	7.3	7.4	1.9	1.9
$C_{10}H_{16}H^+$	137.1326	Monoterpenes	3400	3347	223.9	227.4	2.1	2.2	1.5	1.5
$C_8H_{11}NOH^+$	138.0930		4911	4829	6.9	7.0	2.2	2.3	0.2	0.2
$C_7H_6O_3H^+$	139.0386	Salicylic acid	3744	3678	6.5	6.6	1.4	1.4	0.3	0.3
$C_8H_{10}O_2H^+$	139.0747	Methylguaiacol	3592	3528	34.4	35.0	7.6	7.7	1.1	1.1
$C_7H_{10}N_2OH^+$	139.0866	Ethylmethoxypyrazine	3730	3663	5.5	5.6	2.2	2.3	0.1	0.1
$C_9H_{14}OH^+$	139.1105		4294	4218	36.1	36.8	1.9	1.9	4.0	4.1
$C_{10}H_{18}H^+$	139.1479	Monoterpenoids	3422	3361	14.5	14.7	0.5	0.5	0.2	0.2
$C_8H_{13}NOH^+$	140.1075		4914	4821	4.9	5.0	1.3	1.3	0.6	0.6
$C_7H_8O_3H^+$	141.0541		3753	3677	7.2	7.4	2.0	2.0	0.2	0.2
$C_8H_{12}O_2H^+$	141.0907		3610	3538	15.0	15.3	4.4	4.5	0.4	0.4
$C_7H_{12}N_2OH^+$	141.1043		3745	3669	2.4	2.4	0.7	0.7	0.07	0.07

$C_{10}H_{20}H^+$	141.1637	Decene	3444	3375	2.3	2.4	0.7	0.7	0.1	0.1
$C_8H_{15}NOH^+$	142.1230		4918	4813	2.9	3.0	0.9	0.9	0.2	0.2
$C_7H_{10}O_3H^+$	143.0690		3761	3676	8.4	8.6	3.6	3.7	0.10	0.10
$C_{11}H_{10}H^+$	143.0847	Methylnaphthalenes	3466	3388	31.8	32.5	5.0	5.1	4.9	5.0
$C_9H_{18}OH^+$	143.1430	Nonanal	4311	4214	3.5	3.5	0.3	0.3	0.4	0.5
$C_{10}H_9NH^+$	144.0804	Methylquinolines or Naphthylamine	3838	3747	6.5	6.7	5.3	5.5	0.6	0.6
$C_8H_{17}NOH^+$	144.1416		4921	4804	1.2	1.2	0.3	0.3	0.2	0.2
$C_6H_8O_4H^+$	145.0495	Triacetin fragment (-$C_3H_5O_2$), Levoglucosan fragment (-OH)	3806	3710	22.9	23.5	21.6	22.1	0.4	0.4
$C_{10}H_8OH^+$	145.0637	2-Ethenylbenzofuran	4320	4212	13.1	13.4	3.4	3.5	0.6	0.6
$C_9H_8N_2H^+$	145.0803		4488	4375	4.5	4.7	2.7	2.8	0.2	0.2
$C_{11}H_{12}H^+$	145.0992	Ethylindene	3488	3401	30.0	30.8	2.4	2.5	2.0	2.0
$C_{10}H_{11}NH^+$	146.0961	C_{10} Indole	3853	3751	16.0	16.4	4.6	4.8	2.3	2.4
$C_8H_6N_2OH^+$	147.0544		3790	3685	3.3	3.4	2.5	2.6	0.07	0.07
$C_{10}H_{10}OH^+$	147.0794	C_{10} Benzofuran	4329	4209	21.4	22.0	2.5	2.5	1.7	1.8
$C_9H_{10}N_2H^+$	147.0919	Myosmine	4495	4370	13.9	14.3	33.4	34.3	1.3	1.3
$C_{11}H_{14}H^+$	147.1153		3510	3412	26.6	27.3	1.5	1.5	0.8	0.8
$C_9H_9NOH^+$	148.0761		4928	4785	7.7	8.0	2.6	2.7	0.6	0.7
$C_{10}H_{13}NH^+$	148.1136		3868	3756	10.2	10.5	2.7	2.8	1.2	1.2
$C_8H_4O_3H^+$	149.0229	Phthalic anhydride	3788	3673	*0.4*	0.5	*0.09*	0.10		
$C_8H_8N_2OH^+$	149.0747		3805	3689	2.3	2.4	1.2	1.3	0.1	0.1
$C_{10}H_{12}OH^+$	149.0943	Estragole	4338	4206	12.9	13.3	3.7	3.8	1.2	1.3
$C_9H_{12}N_2H^+$	149.1067	Nornicotine	4503	4365	4.6	4.8	2.0	2.1	0.3	0.3

$C_{11}H_{16}H^+$	149.1321	C_{11} Aromatics	3532	3424	27.7	28.6	1.6	1.7	0.5	0.5
$C_9H_{11}NOH^+$	150.0920		4931	4774	7.8	8.0	3.0	3.1	0.7	0.7
$C_{10}H_{15}NH^+$	150.1286		3884	3759	13.1	13.5	1.4	1.4	2.0	2.1
$C_9H_{10}O_2H^+$	151.0743	Vinylguaiacol	3701	3578	15.4	15.9	7.2	7.5	0.5	0.5
$C_8H_{10}N_2OH^+$	151.0873		3820	3693	4.3	4.4	1.8	1.8	0.1	0.1
$C_{10}H_{14}OH^+$	151.1108	Carvone	4348	4203	20.9	21.6	4.1	4.3	2.0	2.0
$C_{11}H_{18}H^+$	151.1469		3553	3435	19.3	20.0	0.7	0.7	0.3	0.3
$C_9H_{13}NOH^+$	152.1094		4934	4763	4.1	4.2	1.7	1.7	0.2	0.2
$C_8H_8O_3H^+$	153.0544	Vanillin	3807	3670	4.1	4.3	2.1	2.2	0.2	0.2
$C_{12}H_8H^+$	153.0688	Acenaphthylene	3575	3445	2.0	2.1	1.2	1.2	0.4	0.4
$C_9H_{12}O_2H^+$	153.0901		3719	3584	12.6	13.1	4.6	4.8	0.5	0.5
$C_8H_{12}N_2OH^+$	153.1040		3836	3697	2.9	3.0	1.5	1.5	0.05	0.05
$C_{10}H_{16}OH^+$	153.1259	Camphor, Monoterpenoids	4357	4199	17.4	18.1	1.8	1.9	2.6	2.7
$C_{11}H_{20}H^+$	153.1632		3575	3445	1.8	1.9	0.3	0.3	0.05	0.06
$C_{11}H_7NH^+$	154.0649		3914	3766	1.5	1.6	1.6	1.6	0.1	0.1
$C_8H_{10}O_3H^+$	155.0687	Syringol	3817	3668	4.2	4.3	2.7	2.8	0.1	0.1
$C_{12}H_{10}H^+$	155.0841	Biphenyl and Acenaphthene	3596	3455	5.2	5.4	2.6	2.7	1.0	1.0
$C_{10}H_{18}OH^+$	155.1417	Cineole, Monoterpenoids	4367	4195	5.1	5.3	0.3	0.4	0.5	0.5
$C_{11}H_{22}H^+$	155.1794	Undecene	3596	3454	1.6	1.6	0.5	0.6	0.08	0.08
$C_{11}H_9NH^+$	156.0793		3929	3769	1.7	1.7	2.3	2.4	0.2	0.2
$C_{10}H_8N_2H^+$	157.0755	Dipyridyl	4534	4343	1.4	1.5	1.0	1.1	9.6	9.6
$C_{12}H_{12}H^+$	157.1010	C_{12} Naphthalenes	3617	3464	20.2	21.1	8.6	9.0	3.2	3.3

$C_{10}H_{20}OH^+$	157.1583	Decanal	4377	4192	2.8	2.9	0.3	0.3	0.3	0.3
$C_{11}H_{11}NH^+$	158.0969		3944	3771	3.2	3.3	3.5	3.6	0.3	0.3
$C_7H_{10}O_4H^+$	159.0656	Triacetin fragment	3870	3694	9.4	9.9	47.8	50.0	0.1	0.2
$C_{11}H_{10}OH^+$	159.0794		4387	4188	6.0	6.3	11.5	12.0	0.5	0.5
$C_{10}H_{10}N_2H^+$	159.0915	Nicotyrine	4543	4337	8.5	8.9	7.7	8.1	0.5	0.5
$C_{12}H_{14}H^+$	159.1144		3638	3473	19.8	20.8	4.5	4.7	1.2	1.3
$C_{11}H_{13}NH^+$	160.1141		3959	3773	6.2	6.5	3.0	3.1	0.8	0.8
$C_9H_8N_2OH^+$	161.0701		3897	3708	2.1	2.2	3.0	3.1	0.08	0.08
$C_{11}H_{12}OH^+$	161.0943		4397	4184	10.8	11.3	1.2	1.2	1.0	1.0
$C_{10}H_{12}N_2H^+$	161.1073	Anatabine, Anabaseine	4552	4331	17.3	18.2	33.9	35.6	0.4	0.4
$C_{12}H_{16}H^+$	161.1303		3659	3481	15.4	16.2	1.9	2.0	0.4	0.4
$C_{10}H_{14}N_2H^+$	162.0924	Nicotine ionized	4556	4328	4.5	4.7	2.3	2.5	0.4	0.5
$C_{10}H_{14}N_2H^+$	162.1138	Nicotine ionized	4556	4327	6.3	6.7	11.2	11.8	0.1	0.1
$C_{11}H_{15}NH^+$	162.1302		3975	3775	5.7	6.0	3.1	3.3	0.6	0.6
$C_{10}H_{14}N_2H^+$	163.1248	Nicotine	4561	4324	461.9	487.2	762.7	804.4	5.2	5.5
$C_{12}H_{18}H^+$	163.1620	C_{12} Aromatics	3680	3489	5.3	5.6	0.5	0.5	0.07	0.08
$C_{10}H_{14}N_2$ (^{13}C)H^+	164.1266	Nicotine (^{13}C)	4565	4321	44.9	47.4	87.9	92.9	0.5	0.5
$C_{11}H_{17}NH^+$	164.1416		3990	3776	8.9	9.4	7.4	7.8	1.0	1.0
$C_{10}H_{12}O_2H^+$	165.0896	Eugenol	3827	3617	6.0	6.3	3.2	3.3	0.3	0.4
$C_9H_{12}N_2OH^+$	165.0998		3928	3711	2.6	2.7	1.5	1.5	0.1	0.2
$C_{11}H_{16}OH^+$	165.1277		4419	4175	9.0	9.5	5.7	6.0	0.7	0.7
$C_{12}H_{20}H^+$	165.1633		3701	3496	5.4	5.7	0.3	0.3	0.1	0.1
$C_{10}H_{15}NOH^+$	166.1271		4954	4672	1.8	1.9	0.8	0.9	0.1	0.1

$C_{13}H_{10}H^+$	167.0842	Phenalene, Fluorene	3721	3504	1.5	1.6	1.5	1.6	0.3	0.3
$C_9H_{14}N_2OH^+$	167.1184		3943	3712	1.7	1.8	1.2	1.3	0.06	0.07
$C_{11}H_{18}OH^+$	167.1418		4429	4170	4.2	4.5	0.8	0.9	0.7	0.7
$C_{12}H_{22}H^+$	167.1788		3721	3503	0.8	0.9	0.2	0.2	0.04	0.04
$C_{12}H_9NH^+$	168.0806	Carbazole	4020	3779	0.6	0.7	0.8	0.9	0.1	0.1
$C_{13}H_{12}H^+$	169.0989	Methylbiphenyl	3742	3510	3.8	4.1	3.4	3.6	0.9	0.9
$C_{12}H_{24}H^+$	169.1950	Dodecene	3742	3510	1.3	1.4	0.4	0.5	0.09	0.1
$C_{12}H_{11}NH^+$	170.0958		4035	3779	1.2	1.3	1.7	1.8	0.2	0.2
$C_{13}H_{14}H^+$	171.1151	C_{13} Naphthalenes	3762	3516	8.4	9.0	6.9	7.4	1.4	1.5
$C_{12}H_{13}NH^+$	172.1153		4051	3779	2.7	2.8	2.8	3.0	0.4	0.4
$C_{11}H_{12}N_2H^+$	173.1060		4607	4291	1.8	1.9	2.6	2.8	0.2	0.2
$C_{13}H_{16}H^+$	173.1314		3782	3522	11.8	12.7	4.1	4.4	0.6	0.6
$C_{11}H_{11}NOH^+$	174.0934		4964	4614	1.0	1.0	1.1	1.2	0.1	0.1
$C_{12}H_{15}NH^+$	174.1316		4066	3779	2.9	3.1	1.6	1.7	0.3	0.3
$C_{10}H_{10}N_2OH^+$	175.0854		4004	3715	0.9	1.0	1.5	1.6	0.04	0.05
$C_7H_{14}N_2O_3H^+$	175.1092		4004	3715	5.1	5.5	3.0	3.2	0.4	0.4
$C_{12}H_{14}OH^+$	175.1111		4473	4150					*0.5*	*0.5*
$C_{13}H_{18}H^+$	175.1470		3802	3527	9.8	10.5	1.7	1.8	0.3	0.3
$C_{11}H_{13}NOH^+$	176.1104		4966	4599	2.0	2.2	1.5	1.6	0.2	0.2
$C_{12}H_{17}NH^+$	176.1459		4081	3779	1.9	2.1	1.0	1.1	0.2	0.2
$C_{10}H_{12}N_2OH^+$	177.1014	Cotinine	4020	3715	1.6	1.7	2.9	3.2	0.10	0.1
$C_{12}H_{16}OH^+$	177.1238		4484	4144	3.0	3.3	1.6	1.8	0.4	0.4
$C_{11}H_{16}N_2H^+$	177.1372		4627	4276	1.8	1.9	1.6	1.7	0.2	0.2

$C_{13}H_{20}H^+$	177.1629	C_{13} Aromatics	3822	3532	7.9	8.5	1.3	1.4	0.4	0.4
$C_{10}H_{14}N_2OH^+$	179.1170	Hydroxynicotine	4035	3715	1.5	1.7	0.7	0.8	0.4	0.4
$C_{12}H_{18}OH^+$	179.1413		4496	4139	2.4	2.7	1.2	1.3	0.3	0.3
$C_{13}H_{22}H^+$	179.1789		3842	3537	3.1	3.4	0.4	0.4	0.09	0.10
$C_{11}H_{16}O_2H^+$	181.1221		3970	3640	1.7	1.8	1.1	1.2	0.1	0.2
$C_{10}H_{16}N_2OH^+$	181.1335		4050	3714	1.6	1.8	2.3	2.5	0.05	0.05
$C_{12}H_{20}OH^+$	181.1554		4507	4133	1.7	1.8	0.6	0.7	0.3	0.3
$C_{13}H_{24}H^+$	181.1945		3862	3541	0.5	0.6	0.1	0.2	0.02	0.03
$C_{13}H_{11}NH^+$	182.0954	Methylcarbazole	4127	3777	0.2	0.3	0.4	0.5	0.05	0.06
$C_{13}H_{10}OH^+$	183.0787	Benzophenone	4519	4128	0.6	0.6	0.7	0.8	0.1	0.1
$C_{10}H_{14}O_3H^+$	183.0993		3966	3622	0.6	0.7	0.5	0.5	0.04	0.04
$C_{14}H_{14}H^+$	183.1157	Dimethylbiphenyls	3882	3546	2.1	2.3	2.9	3.2	0.5	0.6
$C_{13}H_{26}H^+$	183.2105		3882	3545	1.1	1.2	0.3	0.3	0.06	0.06
$C_{13}H_{13}NH^+$	184.1122		4142	3775	0.6	0.7	1.0	1.1	0.1	0.2
$C_{14}H_{16}H^+$	185.1308	Naphthalene + C_4	3901	3549	3.8	4.1	3.5	3.9	0.5	0.5
$C_{13}H_{15}NH^+$	186.1305		4157	3774	1.2	1.3	1.3	1.4	0.2	0.2
$C_{13}H_{14}OH^+$	187.1085		4542	4115	1.2	1.4	1.2	1.3	0.1	0.2
$C_{14}H_{18}H^+$	187.1464		3921	3552	5.2	5.7	2.7	2.9	0.3	0.3
$C_{13}H_{17}NH^+$	188.1490		4172	3772	1.3	1.5	0.9	1.0	0.1	0.1
$C_{13}H_{16}OH^+$	189.1249		4553	4109	1.8	2.0	1.5	1.6	0.2	0.2
$C_{14}H_{20}H^+$	189.1623		3940	3555	6.1	6.8	1.7	1.9	0.2	0.2
$C_{13}H_{19}NH^+$	190.1648		4187	3770	1.3	1.5	0.6	0.6	0.08	0.09
$C_{10}H_{14}N_2$ $(^+N_2)H^+$	191.1400	Nicotine-nitrogen adduct	4171	3748	4.5	5.0	4.1	4.6	0.4	0.4

$C_{13}H_{18}OH^+$	191.1458		4565	4102	1.6	1.8	2.0	2.2	0.2	0.2
$C_{14}H_{22}H^+$	191.1776	C_{14} Aromatics	3960	3558	7.9	8.8	1.3	1.4	0.2	0.2
$C_{13}H_{21}NH^+$	192.1805		4202	3768	1.6	1.8	0.4	0.4	0.06	0.07
$C_{13}H_{20}OH^+$	193.1574		4577	4095	2.2	2.4	1.2	1.3	0.3	0.4
$C_{14}H_{24}H^+$	193.1926		3979	3560	2.2	2.5	0.3	0.3	0.05	0.05
$C_{13}H_{22}OH^+$	195.1734	Solanone	4589	4089	3.2	3.5	1.2	1.3	0.6	0.7
$C_{14}H_{26}H^+$	195.2089		3998	3562	0.4	0.4	0.1	0.2	0.03	0.03
$C_{14}H_{12}OH^+$	197.0961		4601	4083	0.3	0.3	0.4	0.5	0.06	0.07
$C_{12}H_{20}O_2H^+$	197.1559	Geranyl acetate	4110	3646	0.4	0.4	0.4	0.4	0.02	0.03
$C_{14}H_{28}H^+$	197.2260	Tetradecene	4017	3564	0.9	1.1	0.3	0.3	0.05	0.06
$C_{14}H_{15}NH^+$	198.1300		4247	3760	0.3	0.4	0.5	0.5	0.06	0.07
$C_{15}H_{18}H^+$	199.1464	Naphthalene + C_5	4036	3566	1.5	1.7	1.6	1.8	0.2	0.2
$C_{14}H_{17}NH^+$	200.1468		4262	3757	0.5	0.6	0.6	0.6	0.07	0.08
$C_{14}H_{16}OH^+$	201.1283		4625	4068	0.7	0.8	0.8	0.9	0.09	0.1
$C_{15}H_{20}H^+$	201.1621		4055	3567	3.0	3.4	2.0	2.3	0.2	0.2
$C_{13}H_{14}O_2H^+$	203.1047		4161	3645	0.7	0.8	0.8	1.0	0.04	0.04
$C_{14}H_{18}OH^+$	203.1424		4637	4061	0.9	1.1	0.9	1.1	0.1	0.1
$C_{15}H_{22}H^+$	203.1785		4074	3568	6.7	7.7	2.7	3.1	0.2	0.3
$C_{13}H_{16}O_2H^+$	205.1228		4179	3644	0.5	0.6	0.5	0.5	0.05	0.06
$C_{14}H_{20}OH^+$	205.1585		4649	4054	1.3	1.5	1.1	1.3	0.2	0.2
$C_{15}H_{24}H^+$	205.1941	Sesquiterpenes and C_{15} Aromatics	4092	3568	13.7	15.7	3.5	4.0	0.2	0.2
$C_{13}H_{18}O_2H^+$	207.1382		4196	3643	0.7	0.8	0.6	0.7	0.06	0.07
$C_{14}H_{22}OH^+$	207.1729		4661	4046	1.3	1.5	0.9	1.1	0.3	0.3

$C_{15}H_{26}H^+$	207.2085		4111	3569	3.0	3.5	0.8	0.9	0.06	0.07
$C_{10}H_{13}N_3O_2H^+$	208.1059	Nicotine-derived nitrosamine ketone	5457	4728	0.05	0.06	0.06	0.06	<0.01	<0.01
$C_{13}H_{20}O_2H^+$	209.1528		4213	3641	1.2	1.4	1.0	1.2	0.1	0.1
$C_{14}H_{24}OH^+$	209.1861		4673	4039	0.5	0.5	0.3	0.3	0.06	0.07
$C_{15}H_{28}H^+$	209.2252		4129	3569	0.3	0.3	0.1	0.2	0.02	0.02
$C_{12}H_{19}NO_2H^+$	210.1471		5052	4357	0.8	1.0	0.5	0.6	0.1	0.1
$C_{11}H_{18}N_2O_2H^+$	211.1442		4278	3681	0.4	0.5	0.5	0.6	0.08	0.09
$C_{13}H_{22}O_2H^+$	211.1667		4230	3640	0.5	0.6	0.4	0.5	0.06	0.07
$C_{15}H_{30}H^+$	211.2403	Pentadecene	4148	3569	0.7	0.8	0.4	0.4	0.03	0.04
$C_{11}H_{20}N_2O_2H^+$	213.1601		4293	3678	0.6	0.7	0.6	0.7	0.07	0.08
$C_{16}H_{20}H^+$	213.1654	Naphthalene + C_6	4166	3569	0.2	0.2	0.2	0.2	0.03	0.03
$C_{16}H_{22}H^+$	215.1783		4184	3568	1.0	1.2	0.9	1.1	0.08	0.09
$C_{14}H_{16}O_2H^+$	217.1244		4280	3634	0.3	0.4	0.5	0.5	0.02	0.02
$C_{15}H_{20}OH^+$	217.1579		4722	4009	0.6	0.7	0.6	0.8	0.10	0.1
$C_{16}H_{24}H^+$	217.1931		4203	3568	1.5	1.8	0.9	1.1	0.08	0.09
$C_{15}H_{22}OH^+$	219.1730		4734	4001	0.9	1.1	0.9	1.0	0.2	0.2
$C_{16}H_{26}H^+$	219.2085	C_{16} Aromatics	4221	3567	1.5	1.8	0.8	0.9	0.09	0.1
$C_{14}H_{20}O_2H^+$	221.1536		4314	3629	0.3	0.4	0.2	0.3	0.04	0.04
$C_{15}H_{24}OH^+$	221.1915	Sesquiterpenoids	4747	3993	0.7	0.9	0.7	0.8	0.2	0.2
$C_{16}H_{28}H^+$	221.2227		4239	3566	0.4	0.5	0.2	0.3	0.03	0.03
$C_{14}H_{22}O_2H^+$	223.1690		4331	3627	0.2	0.3	0.2	0.3	0.03	0.04
$C_{15}H_{26}OH^+$	223.2026	Sesquiterpenoids	4759	3985	0.3	0.4	0.2	0.3	0.05	0.06
$C_{16}H_{30}H^+$	223.2423		4257	3564	0.1	0.2	0.1	0.2	0.01	0.02

$C_{17}H_{20}H^+$	225.1617		4275	3563	0.2	0.2	0.2	0.3	0.03	0.04
$C_{15}H_{28}OH^+$	225.2183		4771	3977	0.2	0.3	0.1	0.1	0.03	0.03
$C_{16}H_{32}H^+$	225.2563	Hexadecenes	4275	3563	0.3	0.4	0.3	0.3	0.05	0.06
$C_{12}H_{22}N_2O_2H^+$	227.1724		4397	3648	0.3	0.3	0.3	0.3	0.04	0.04
$C_{17}H_{22}H^+$	227.1818	Naphthalene + C_7	4292	3562	0.2	0.2	0.2	0.2	0.02	0.03
$C_{15}H_{30}OH^+$	227.2359	C_{15} Carbonyls	4784	3969	0.2	0.2	0.09	0.1	0.04	0.05
$C_{12}H_{24}N_2O_2H^+$	229.1923		4310	3560	0.5	0.6	0.5	0.6	0.05	0.06
$C_{14}H_{28}O_2H^+$	229.2136		4380	3618	0.2	0.2	0.1	0.1	0.02	0.03
$C_{16}H_{22}OH^+$	231.1744		4808	3953	0.2	0.2	0.2	0.2	0.03	0.03
$C_{17}H_{26}H^+$	231.2087		4328	3558	0.5	0.6	0.4	0.5	0.05	0.06
$C_{15}H_{20}O_2H^+$	233.1534		4413	3612	0.2	0.2	0.2	0.2	0.02	0.03
$C_{16}H_{24}OH^+$	233.1892		4821	3945	0.2	0.2	0.2	0.2	0.04	0.05
$C_{17}H_{28}H^+$	233.2247	C_{17} Aromatics	4345	3555	0.4	0.4	0.3	0.4	0.03	0.04
$C_{15}H_{22}O_2H^+$	235.1671		4430	3608	0.4	0.5	0.3	0.3	0.07	0.09
$C_{17}H_{30}H^+$	235.2426		4363	3553	0.05	0.06	0.06	0.08	<0.01	<0.01
$C_{17}H_{32}H^+$	237.2561		4380	3550	0.05	0.07	0.07	0.09	<0.01	<0.01
$C_{16}H_{30}OH^+$	239.2349	Hexadecanoic acid fragment	4858	3919	0.06	0.07	0.04	0.05	0.01	0.01
$C_{17}H_{34}H^+$	239.2714	Heptadecenes	4398	3547	0.07	0.09	0.2	0.2	0.02	0.02
$C_{18}H_{24}H^+$	241.1925	C_{18} Naphthalene	4415	3545	0.2	0.2	0.2	0.3	0.03	0.04
$C_{18}H_{26}H^+$	243.2090		4432	3542	0.3	0.4	0.3	0.4	0.04	0.05
$C_{15}H_{30}O_2H^+$	243.2300		4495	3592	0.10	0.1	0.07	0.09	0.02	0.02
$C_{17}H_{24}OH^+$	245.1898		4895	3894	0.06	0.07	0.06	0.07	0.01	0.02
$C_{18}H_{28}H^+$	245.2245		4449	3539	0.3	0.4	0.3	0.4	0.03	0.04

$C_{15}H_{32}O_2H^+$	245.2457		4511	3588	0.1	0.1	0.07	0.09	0.02	0.02
$C_{17}H_{26}OH^+$	247.2051		4908	3885	0.06	0.08	0.06	0.07	0.01	0.02
$C_{18}H_{30}H^+$	247.2410	C_{18} Aromatics	4467	3536	0.2	0.3	0.2	0.2	0.02	0.03
$C_{18}H_{32}H^+$	249.2558		4484	3532	0.06	0.07	0.05	0.07	<0.01	<0.01
$C_{18}H_{34}H^+$	251.2737		4501	3528	0.02	0.02	0.02	0.02	<0.01	<0.01
$C_{18}H_{36}H^+$	253.2879	Octadecenes	4517	3525	0.05	0.07	0.08	0.1	0.02	0.02
$C_{19}H_{26}H^+$	255.2080	Naphthalene + C_9	4534	3522	0.1	0.1	0.1	0.2	0.02	0.03
$C_{19}H_{28}H^+$	257.2241		4551	3518	0.2	0.2	0.2	0.3	0.03	0.04
$C_{19}H_{30}H^+$	259.2396		4568	3514	0.3	0.3	0.3	0.4	0.04	0.05
$C_{18}H_{28}OH^+$	261.2194	Linolenic acid fragment	4995	3824	0.04	0.05	0.04	0.05	<0.01	<0.01
$C_{19}H_{32}H^+$	261.2555	C_{19} Aromatics	4584	3509	0.1	0.2	0.1	0.2	0.02	0.03
$C_{19}H_{34}H^+$	263.2719		4601	3505	0.02	0.03	0.02	0.02	<0.01	<0.01
$C_{19}H_{36}H^+$	265.2857		4618	3501	0.02	0.02	0.02	0.02	<0.01	<0.01
$C_{19}H_{38}H^+$	267.3046	Nonadecenes	4634	3496	0.08	0.1	0.1	0.2	0.02	0.02
$C_{20}H_{28}H^+$	269.2245	Naphthalene + C_{10}	4651	3492	0.2	0.2	0.2	0.2	0.03	0.04
$C_{20}H_{30}H^+$	271.2400		4667	3487	0.6	0.8	0.7	1.0	0.1	0.1
$C_{20}H_{30}H^+$	271.2486		4667	3487	0.3	0.4	0.3	0.5	0.06	0.08
$C_{20}H_{32}H^+$	273.2553	Diterpenes	4683	3483	0.4	0.5	0.4	0.5	0.06	0.08
$C_{20}H_{34}H^+$	275.2734	C_{20} Aromatics	4699	3478	0.07	0.09	0.07	0.10	<0.01	0.01
$C_{20}H_{36}H^+$	277.2900		4716	3473	0.01	0.02	<0.01	0.01	<0.01	<0.01
$C_{16}H_{22}O_4H^+$	279.1581	Dibutyl phthalate	4547	3333	0.09	0.1	0.03	0.03	0.01	0.02
$C_{20}H_{38}H^+$	279.3049	Neophytadiene	4732	3467	0.03	0.04	0.08	0.1	0.01	0.01
$C_{20}H_{40}H^+$	281.3227	Eicosenes	4748	3462	0.01	0.02	0.01	0.02	<0.01	<0.01

$C_{22}H_{18}H^+$	283.1490		4764	3459	0.07	0.09	0.01	0.02	<0.01	<0.01
$C_{19}H_{38}OH^+$	283.2975		5132	3724	0.03	0.03	0.02	0.03	<0.01	<0.01
$C_{21}H_{38}H^+$	291.3030		4828	3436	<0.01	<0.01	<0.01	<0.01	<0.01	<0.01
$C_{21}H_{40}H^+$	293.3154		4843	3430	<0.01	0.01	<0.01	<0.01	<0.01	<0.01
$C_{22}H_{30}H^+$	295.2399		4859	3425	<0.01	<0.01	<0.01	<0.01	<0.01	<0.01
$C_{21}H_{42}H^+$	295.3299		4859	3425	0.01	0.02	<0.01	<0.01	<0.01	<0.01
$C_{22}H_{38}H^+$	303.3021	C_{22} Aromatics	4921	3402	0.03	0.04	<0.01	<0.01	<0.01	<0.01
$C_{22}H_{40}H^+$	305.3169		4937	3396	<0.01	<0.01	<0.01	<0.01	<0.01	<0.01
$C_{22}H_{42}H^+$	307.3381		4952	3390	<0.01	<0.01	<0.01	<0.01	<0.01	<0.01
$C_{22}H_{44}H^+$	309.3529		4968	3384	<0.01	<0.01	<0.01	<0.01	<0.01	<0.01
$C_{23}H_{34}H^+$	311.2743		4983	3378	<0.01	<0.01	<0.01	<0.01	<0.01	<0.01
$C_{23}H_{40}H^+$	317.3177	C_{23} Aromatics	5029	3359	<0.01	0.01	<0.01	<0.01	<0.01	<0.01
$C_{22}H_{39}NH^+$	318.3197		5095	3395	<0.01	<0.01	<0.01	<0.01	<0.01	<0.01
$C_{23}H_{42}H^+$	319.3353		5044	3353	<0.01	0.01	<0.01	<0.01	<0.01	<0.01
$C_{23}H_{44}H^+$	321.3495		5059	3347	<0.01	0.01	<0.01	<0.01	<0.01	<0.01
$C_{23}H_{46}H^+$	323.3669		5074	3340	<0.01	0.01	<0.01	<0.01	<0.01	<0.01
$C_{24}H_{38}H^+$	327.3021		5104	3328	0.02	0.03	<0.01	<0.01	<0.01	<0.01
$C_{24}H_{40}H^+$	329.3222		5119	3321	<0.01	<0.01	<0.01	<0.01	<0.01	<0.01
$C_{24}H_{46}H^+$	335.3631		5163	3302	<0.01	<0.01	<0.01	<0.01	<0.01	<0.01
$C_{24}H_{48}H^+$	337.3817		5178	3295	<0.01	0.01	<0.01	<0.01	<0.01	<0.01
$C_{25}H_{40}H^+$	341.3263	Sesterterpenes	5207	3282	<0.01	<0.01	<0.01	<0.01	<0.01	<0.01
$C_{25}H_{42}H^+$	343.3335		5222	3275	<0.01	<0.01	<0.01	<0.01	<0.01	<0.01
$C_{25}H_{44}H^+$	345.3543	C_{25} Aromatics	5237	3268	<0.01	<0.01	<0.01	<0.01	<0.01	<0.01

$C_{25}H_{46}H^+$	347.3662		5251	3262	<0.01	<0.01	<0.01	<0.01	<0.01	<0.01
$C_{25}H_{48}H^+$	349.3822		5266	3255	<0.01	<0.01	<0.01	<0.01	<0.01	<0.01
$C_{25}H_{50}H^+$	351.3968		5280	3248	<0.01	<0.01	<0.01	<0.01	<0.01	<0.01
$C_{26}H_{48}H^+$	361.3798		5352	3214	<0.01	<0.01	<0.01	<0.01	<0.01	<0.01
$C_{26}H_{52}H^+$	365.4128		5380	3200	<0.01	<0.01	<0.01	<0.01	<0.01	<0.01
$C_{24}H_{38}O_4H^+$	391.2827	Bis(2-ethylhexyl) phthalate	5172	2892	<0.01	0.01	<0.01	<0.01	<0.01	<0.01

* The specific isomers listed for each formula were not all confirmed by other methods where specific compound names are provided. Conversely, isomers or additional identifications were not always included, especially if insufficient evidence exists in either previous literature or in our measurements to posit them as potential candidates. Identifications were based on GC-EI-MS and GC-TOF observations, as well as existing tobacco smoke literature. Additionally, the relative ratios for SHS presented here are representative of sidestream smoking conditions, and the relative abundances of some compounds could potentially shift with higher mainstream smoke combustion temperatures, which could also influence relative concentrations in LLF. Glycerol, propylene glycol, and ethylene glycol are listed as potential IDs with past identifications in tobacco smoke, though there is significant expected fragmentation with PTR, so the reported concentrations may be lower limits and may also have contributions on these molecular formulas from other isomers and fragments.

† While observed in some trials, formaldehyde and methanol concentrations were not provided due to instrument configurations during the majority of the study, leading to a lack of observations and sensitivity information below *m/z* 42.

^ Two masses were assigned a formula identification of $C_{20}H_{30}H^+$ (expected m/z = 271.2419) because of a lack of other prominent formulas nearby. The m/z were far enough apart that they were not grouped together, but mass drift between experimental data files may have separated them.

Other notes:

- Henry's law constants are from Sander, 2015.[53] Saturation concentrations were calculated using the Li et al. parameterization.[22]